CAL/APT Goal LLPRS – Rigid Phase III:

Concrete Test Section 516CT Report

Report Prepared for

CALIFORNIA DEPARTMENT OF TRANSPORTATION

By

Jeffery R. Roesler, Louw du Plessis, David Hung, David Bush, John T. Harvey

April 1999
Pavement Research Center
Institute of Transportation Studies
University of California at Berkeley

Technical Report Documentation Page

1. Report No.	2. Government Accession No.	3. Recipient's Catalog No.
FHWA/CA/OR-99/03		

4. Title and Subtitle	5. Report Date
CAL/APT Goal LLPRS--Rigid Phase III: Concrete Test Section 516CT Report	6. Performing Organization Code

7. Authors	8. Performing Organization Report No.
Jeffery R. Roesler, Louw du Plessis, David Hung, John T. Harvey	

9. Performing Organization Name and Address	10. Work Unit No.
California Department of Transportation New Technology and Research, MS-83 P.O. Box 942873 Sacramento, CA 94273-0001	11. Contract or Grant No.

12. Sponsoring Agency Name and Address	13. Type of Report and Period Covered
California Department of Transportation Sacramento, CA 95819	14. Sponsoring Agency Code

15. Supplementary Notes

This project was performed in cooperation with the U.S. Department of Transportation, Federal Highway Administration.

16. Abstract

In order to evaluate the future performance of rehabilitated concrete pavements, a Heavy Vehicle Simulator (HVS) was used to test a Portland Cement Concrete pavement section constructed at the University of California at Berkeley. The main goals of this accelerated pavement testing were to familiarize the staff with concrete pavement construction, install instrumentation in the slabs, develop a rigid pavement testing procedure using the HVS, and monitor the in-situ instrumentation with loading. All the information and experience gained from this testing was used later for instrumentation and HVS testing of six fast setting hydraulic cement concrete (FSHCC) test sections located in Palmdale, CA.

A test plan was designed to provide concrete pavement testing and analysis research regarding the LLPRS-Rigid design options being considered by Caltrans. The objectives of this test plan were 1) to evaluate the adequacy of structural design options (tied concrete shoulders, doweled joints, and widened truck lanes) being considered by Caltrans, primarily with respect to joint distress, fatigue cracking, and corner cracking; 2) to assess the durability of concrete slabs made with cements meeting the requirements for early ability to place traffic upon them and to develop methods to screen new materials for durability; and 3) to measure the effects of construction and mix design variables on the durability and structural performance of concrete pavements.

17. Key Words	18. Distribution Statement
fast-setting hydraulic cement concrete, portland cement concrete, accelerated pavement testing, rigid pavement, instrumentation	No restrictions. This document is available to the public through the National Technical Information Service, Springfield, VA 22161

19. Security Classif. (of this report)	20. Security Classif. (of this page)	21. No. of Pages	22. Price
Unclassified	Unclassified	140	

Form DOT F 1700.7 (8-72)

TABLE OF CONTENTS

LIST OF TABLES

LIST OF FIGURES

1.0 INTRODUCTION

Over the past 50 years, only several full-scale concrete pavements have been tested, e.g., the AASHO Road Test, Mn/ROAD, and the various US Army Corps of Engineers tests (1). These full-scale test pavements have resulted in essential information for further improvement in pavement design procedures. They have also raised many questions that need to be answered with future road tests. The use of accelerated pavement testing equipment enables full-scale concrete pavements to be constructed and tested more cheaply than road tests. Caltrans currently owns two heavy vehicle simulators (HVS), which have been used to load asphalt concrete pavements at the University of California at Berkeley. The HVS allows for continuous load testing in a controlled environment and the potential for reduced variability in materials and testing.

In order to evaluate the future performance of rehabilitated concrete pavements, the second HVS was used to test an accelerated Portland Cement Concrete pavement section constructed at the University of California-Berkeley. The main goals of this accelerated pavement testing was to familiarize the staff with concrete pavement construction, install instrumentation in the slabs, develop a rigid pavement testing procedure using the HVS, and monitor the in-situ instrumentation with loading. All the information and experience gained from this testing would be needed later for instrumentation and HVS testing of six fast setting hydraulic cement concrete (FSHCC) test sections located in Palmdale, CA.

1.1 Background of LLPRS

The California Department of Transportation (Caltrans) Long-Life Pavement Rehabilitation Strategies (LLPRS) Task Force was commissioned in April, 1997. The

product Caltrans has identified for the LLPRS Task Force to develop is Long Life Pavement Rehabilitation guidelines and specifications for implementation on projects in the 1998/99 fiscal year. The focus of the LLPRS Task Force has been rigid pavement strategies. A separate task force has more recently been established for flexible pavement strategies, called the Asphalt Concrete Long-Life (AC Long-Life) Task Force.

The University of California at Berkeley (UCB) and its subcontractors, Dynatest, Inc., the Roads and Transport Technology Division of the CSIR, and Symplectic Engineering Corporation, Inc. are investigating for Caltrans the viability of various LLPRS options that have been proposed.

1.2 Objectives

1.2.1 LLPRS Objectives

In recent years Caltrans engineers and policy makers have felt that existing methods of rigid pavement maintenance and rehabilitation may not be optimum from a benefit/cost or lifecycle cost standpoint. Caltrans is also becoming more concerned with increasingly severe traffic management problems. The costs of applying lane closures in urban areas is very large compared to the actual costs of materials and placement. Additionally, there is increased need for maintenance forces to be in the roadway, elevating costs and safety concerns. The costs to Caltrans clients, the traveling public, are increasing due to the increasing frequency of lane closures, which cause delays and additional vehicle operating costs from deteriorating ride quality.

A need to develop lane replacement strategies that will not require long-term closures associated with the use of PCC (Portland Cement Concrete), and that will

provide longer lives than the current assumed design life of 20 years for PCC pavements, was identified. The Caltrans LLPRS-Rigid committee has developed strategies for rehabilitation of concrete pavements that are intended to meet the following objectives:

1. Provide 30+ years of service life,
2. Require minimal maintenance, although zero maintenance is not a stated objective,
3. Have sufficient production to rehabilitate or reconstruct about 6 lane-kilometers within a construction window of 67 hours (10 a.m. Friday to 5 a.m. Monday).

1.2.2 Contract Team Research Objectives

The objective of the contract work is to develop as much information as possible to estimate whether the Long Life Pavement Rehabilitation Strategies for Rigid Pavements (LLPRS-Rigid) will meet the objectives stated in 1.2.1.

A test plan was designed to provide concrete pavement testing and analysis research regarding the LLPRS-Rigid design options being considered by Caltrans. (2) The objectives of this test plan were the following:

- To evaluate the adequacy of structural design options (tied concrete shoulders, doweled joints, and widened truck lanes) being considered by Caltrans at this time primarily with respect to joint distress, fatigue cracking, and corner cracking,

- To assess the durability of concrete slabs made with cements meeting the requirements for early ability to place traffic upon them and to develop methods to screen new materials for durability, and
- To measure the effects of construction and mix design variables on the durability and structural performance of concrete pavements.

In order to achieve these objectives, three types of investigation are being performed:

1. Computer modeling and design analysis, including use of existing mechanistic-empirical design methods and estimation of critical stresses and strains within the pavement structure under environmental and traffic loading for comparison with failure criteria;
2. Laboratory testing of the strength, fatigue properties, and durability of concrete materials that will be considered for use in the LLPRS pavements; and
3. Verification of failure mechanisms, performance of several pavement design features, and mechanistic-empirical pavement design validation under traffic and environmental loading by means of accelerated pavement testing using the Heavy Vehicle Simulator (HVS) on test sections constructed in the field.

The first milestone in the research project was the preparation of a set of reports identifying essential issues that may affect the success of the proposed rehabilitation strategies. These reports can be found in References 18, 19 and 20.

1.3 Overview of this Report

During this report, feedback is given on CAL/APT Goal LLPRS—Rigid Phase III program currently underway at the Pavement Research Center (PRC) at the University of California, Berkeley Richmond Field Station (RFS). It is divided into three main sections:

- Construction and instrumentation details of the full-scale concrete slab constructed at RFS,
- HVS test program and pavement response results, and
- The verification of the concrete performance through an analytical based computer model.

In order to prepare HVS2 for the full-scale evaluation of concrete pavements in the field, a preliminary study was undertaken at the PRC. This study included the evaluation of various types of instruments, methods of data recording, and the logistics involved with placing concrete around sensitive instrumentation. After the slab was cast, the HVS was utilized to evaluate performance of the various instruments as well as the performance of the slab under accelerated trafficking.

The three main headings listed above are further subdivided into the following:

- analysis of the base course,
- description of the concrete slab and construction details,
- description of the various instruments and the complete instrumentation plan,
- the HVS testing plan, data collection schedules and loading details,
- test results gathered from the various instruments and data collection systems,

- analysis of the results, and
- significant findings and conclusions.

2.0 CONCRETE SLAB GEOMETRY AND MATERIALS

2.1 Test Site Location

A Portland Cement Concrete (PCC) test slab with an accelerator ($CaCl_2$) was constructed between Building 280A and Building 280B at the University of California at Berkeley Richmond Field Station (RFS). Due to the limited area inside Building 280 caused by the testing of an asphalt concrete test section by HVS1, the concrete test slab was placed outside.

2.2 Pavement Geometry

The intention of the test slab was to simulate a section of rigid pavement similar to that of the California highway system, in particular, the proposed field test site on State Route 14 in Palmdale, California. Due to limited space at the RFS site, the dimensions of the overall test slab measured 3.66 m wide by 23.5 m long with a design thickness of 200 mm, as shown in Figure 1. The joint spacing was similar to the joint spacing proposed for the field test site on State Route 14, Palmdale. Like most of the existing Caltrans rigid pavements, the test slab did not have doweled joints and there were no lanes adjacent to the test slab. The only shoulder was the existing asphalt concrete pavement adjacent to the concrete test section.

2.3 Pavement Materials

2.3.1 Subgrade

The subgrade did not require any preparation work by the contractor. Prior to construction of the test site, Dynamic Cone Penetrometer (DCP) tests were performed on the in-situ subgrade. Six DCP tests were completed along the centerline of the test section approximately one every 2.5 m. The DCP results were correlated to other pertinent soil properties and are summarized in Table 1.

Table 1 Results of DCP Investigation of Subgrade Soil.

Sample Number	Average Elastic Moduli (MPa)	Ranges of Elastic Moduli (MPa)	CBR (percent)	R-Value (PCA, 1984)
1	43	23-81	8	39
2	38	20-71	7	34
3	37	20-70	7	34
4	51	27-96	10	46
5	39	21-73	7	34
6	30	16-56	5	24
Average	**40**		**7**	**35**
Standard Deviation	**7**		**2**	**7**

2.3.2 Base Materials

The Class 2 aggregate base with 19 mm maximum size aggregate was imported from Syar Lake Herman Plant. Initial compaction was performed by a Bobcat 753 with pneumatic tires, while final compaction was completed by a Wacker Vibraplate compactor to a design thickness of 150 mm. Because the test section was initially for the purpose of practice, compaction methodologies and monitoring (quality control) did not follow any specifications.

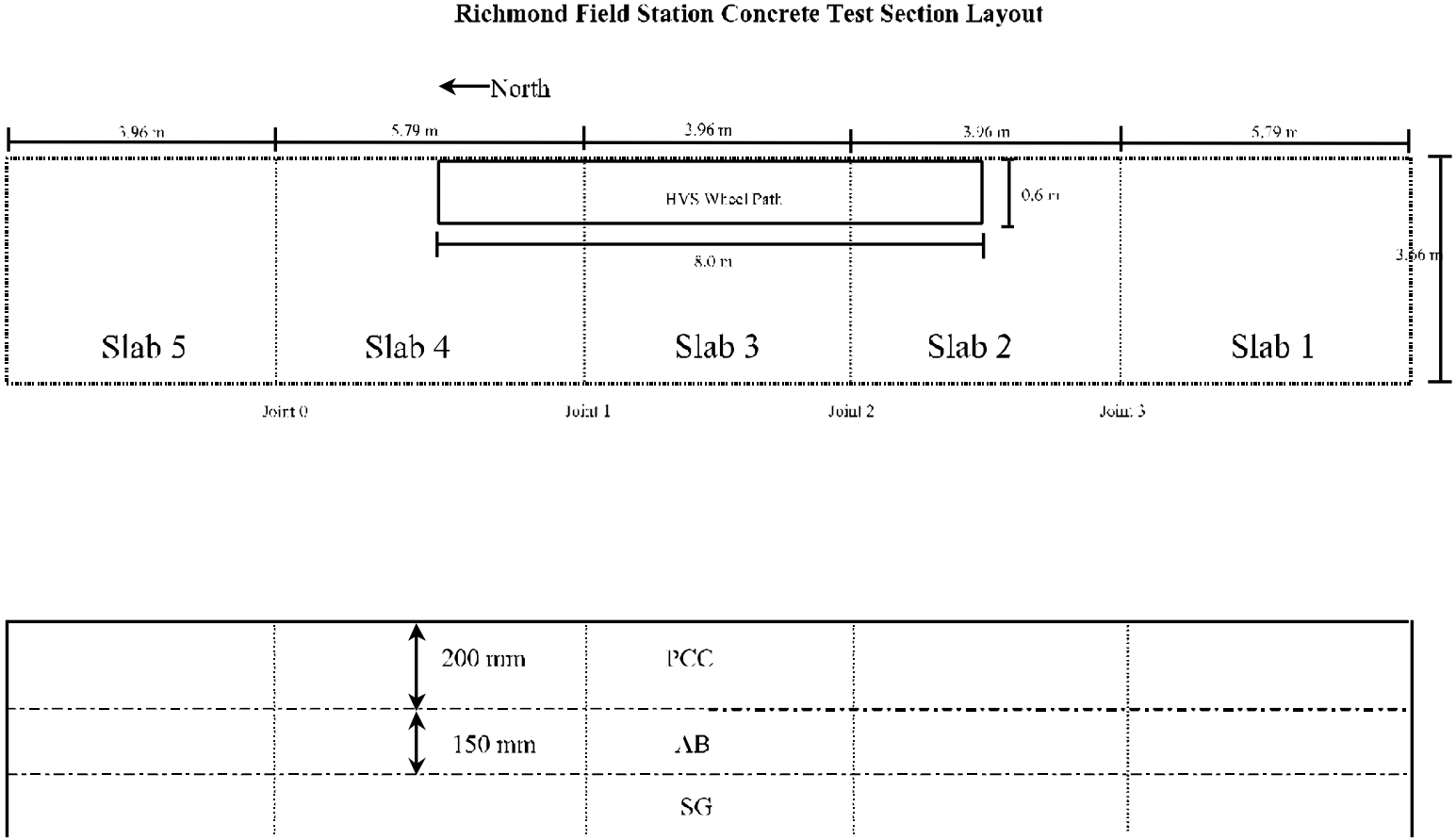

Figure 1. PCC test section dimensions and joint spacing.

2.3.3 Concrete Materials

The PCC mix was produced at Sugar City Building Materials Company in Pinole, California. The mix consisted of Type II cement, Radum 38 mm to 19 mm coarse aggregate, Radum gravel 25 mm to 6.4 mm, and Radum top sand. Table 2 contains the concrete mix design supplied to the PRC by Sugar City Building Materials.

Table 2 Concrete Mix Design.

Material	SSD Weights (kg)	Specific Gravity
Cement Type II	298	3.15
Water (liters)	125	1.00
Radum 38.1 mm × 19.1 mm	401	2.68
Radum gravel 25.4 mm × No. 4	544	2.68
Radum Top Sand	494	2.68
Air 1 Percent	-	-
Water/Cement Ratio	0.42	-

The mix also included two percent calcium chloride by weight as a set accelerator to compensate for the effect of cool temperatures on the day of construction and to accelerate the strength gain of the concrete. The concrete slab test section was placed on December 23, 1997.

UCB personnel took concrete from the last truck for making 152 mm × 305 mm cylinders and 152 mm × 152 mm × 533 mm beam samples for laboratory testing. The cylinders were used for determining the compressive strength of the concrete (ASTM C 39), while the beams were used to determine the flexural strength of the concrete. Cylinder samples were tested by Caltrans personnel, while beam samples were tested by both UCB and Caltrans. The flexural strength tests used two different loading methods. Caltrans used center point loading with 152 mm × 152 mm × 914 mm beams (CT 523),

while UCB used third-point loading (ASTM C 78). Concrete test results are shown in Tables 3 and 4.

Table 3 Concrete Compressive Strength Test Results.

Sample #	Age (days)	Compressive Strength (MPa)
1	7	38.9
2	7	38.7
3	28	51.6
4	28	50.8
5	90	57.5
6	90	55.4

Table 4 Concrete Flexural Strength Test Results.

Sample Number	Age (days)	Flexural Strength (MPa)
1*	7	3.7
2*	7	4.2
3	14	4.5
4	21	4.6
5*	28	5.7
6	98	5.9

* indicates beams tested by Caltrans using center-point loading

2.4 Deflection Analysis Using the Falling Weight Deflectometer (FWD)

On January 6, 1998, nondestructive load-deflection tests were performed on the PCC test slab at the University of California at Berkeley (UCB) Richmond Field Station (RFS). The purpose of this analysis was to determine the pavement's load carrying capacity and calculate the pavement layer stiffnesses.

The Dynatest Model 8082 Heavy Weight Deflectometer (HWD) Test System was used to generate the load-deflection data. The HWD generates a transient, impulse-type load of 25-30 millisecond duration at any desired (peak) load level between 27 kN and 245 kN (6,000 and 55,000 lbf.), thereby approximating the effect of a 48-80 km/hr. (30–50 mph) moving wheel load. For this project, test loads ranged from 36 kN to 156 kN

(8,000 to 35,000 lbf.) and were normalized at 40, 89, and 133kN (9, 20, and 30 kip). Different load ranges were used to determine if any nonlinearity existed in the subgrade.

The HWD-generated load deflection data was analyzed using the Dynatest ELMOD computer program. ELMOD is an acronym for Evaluation of Layer Moduli and Overlay Design, and the program is used primarily for AC and CRCP pavement types. The ELMOD program backcalculates the mechanistic material properties of a semi-infinite pavement system (that is, the elastic moduli or "E"-values of each structural layer in the pavement) using the Odemark-Boussinesq transformed section approach. The ELCON program is for backcalculation of concrete pavements and provides joint and edge analysis capabilities using Westergaard's equations for evaluating jointed PCC pavements. For the purposes of this analysis, ELCON was primarily used. All HWD data presented are 14 day test results.

2.4.1 Analysis Approach

Table 5 outlines the FWD test pattern used on the RFS PCC test slab.

Table 5 FWD Test Pattern Used on the RFS PCC Test Slab.

Row	Test Path Location	Approximate Length, m (ft.)
A	1.03 m from East Edge	23.5 (77)
B	1.83 m from East Edge	23.5 (77)
C	2.62 m from East Edge	23.5 (77)

The stationing for this project was carried out in units of meters. The starting point (0) on the test slab is located at the northern end, with stationing increasing southward. Testing was performed at intervals varying from approximately 0.5 m to 3 m.

Layer thickness information provided by UCB personnel was used in the analyses, as shown in Table 6.

Table 6 Layer Thicknesses Used for FWD Analysis.

RFS PCC Test Slab		Layer Thickness, mm (in.)		
Rows	Location, m (ft.)	PCC	BASE	SUBGRADE
A, B, & C	0–23.5 (0–77)	200 (8)	150 (6)	~ ∞

The HWD data summarized below includes all rows that were tested. However, emphasis should be placed on the center row (Row B), where the theoretical rigid pavement model assumptions are closest to being satisfied. Due to the edge effects in Rows A and C, Westergaard analyses are only an approximation unless edge and infinite slab correction factors are made.

2.4.2 Deflections

Normalized center deflections for a 40, 89, and 133 kN (9,000; 20,000; and 30,000 lbf.) wheel load are plotted in Figures 2 through 4 for the test slab. The deflections are summarized in Table 7.

Figures 2 through 4 and Table 7 show that the measured deflections for all rows are somewhat variable, but consistent with measured deflections of typical Portland Cement Concrete (PCC) slabs. Longitudinal variations in deflection response appear

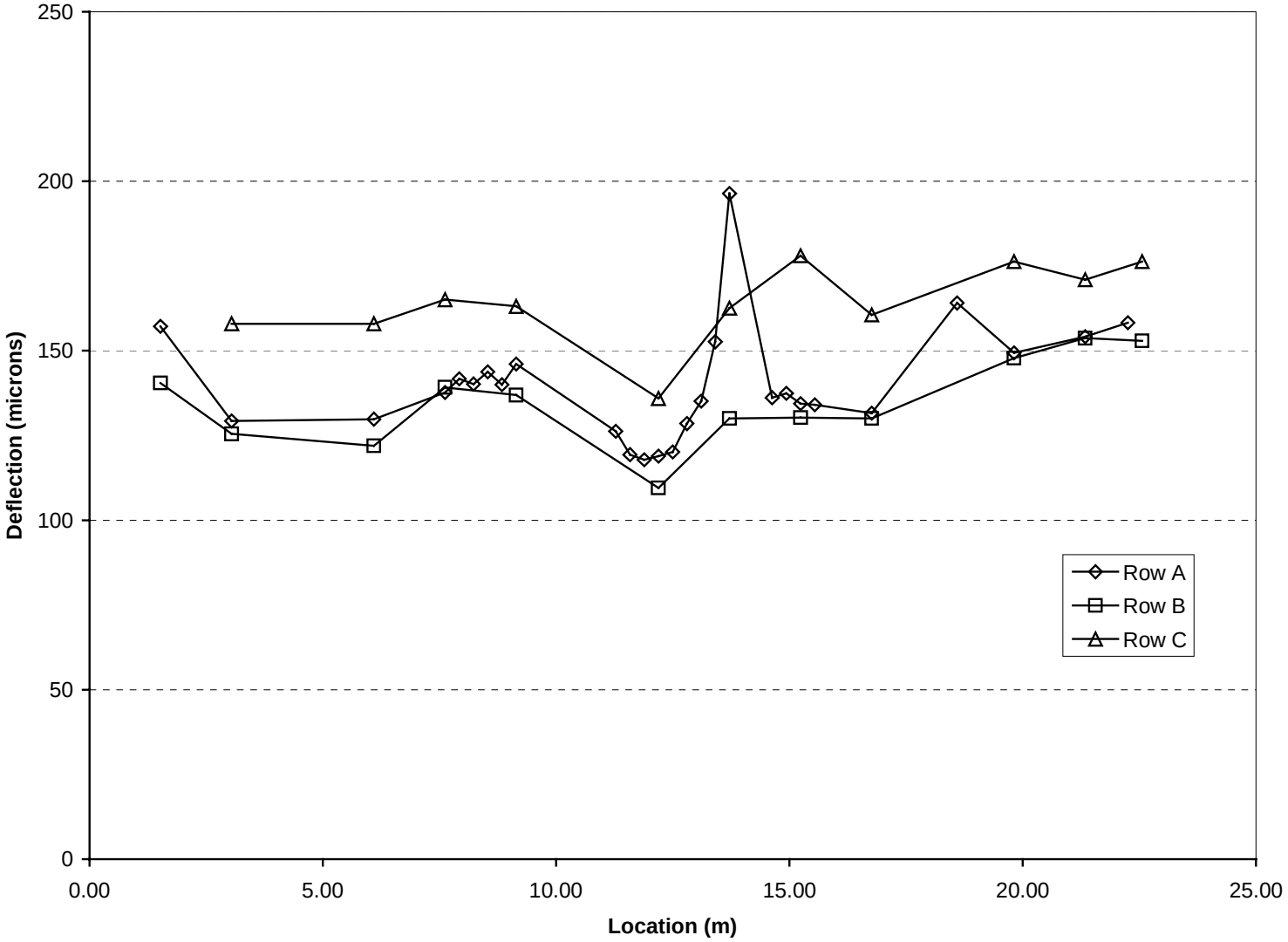

Figure 2. RFS PCC test slab - 40kN deflections.

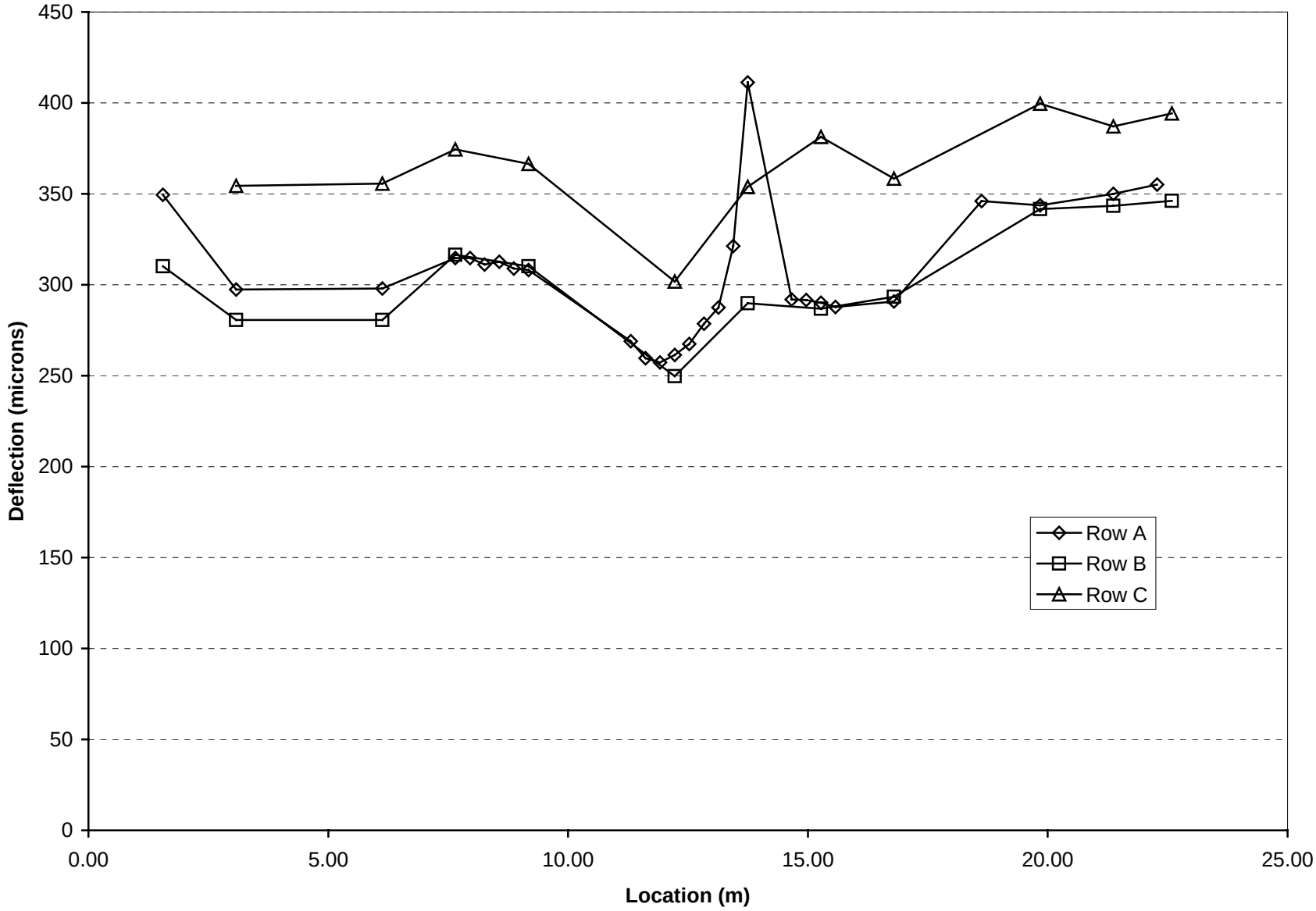

Figure 3. RFS PCC test slab - 89 kN deflections.

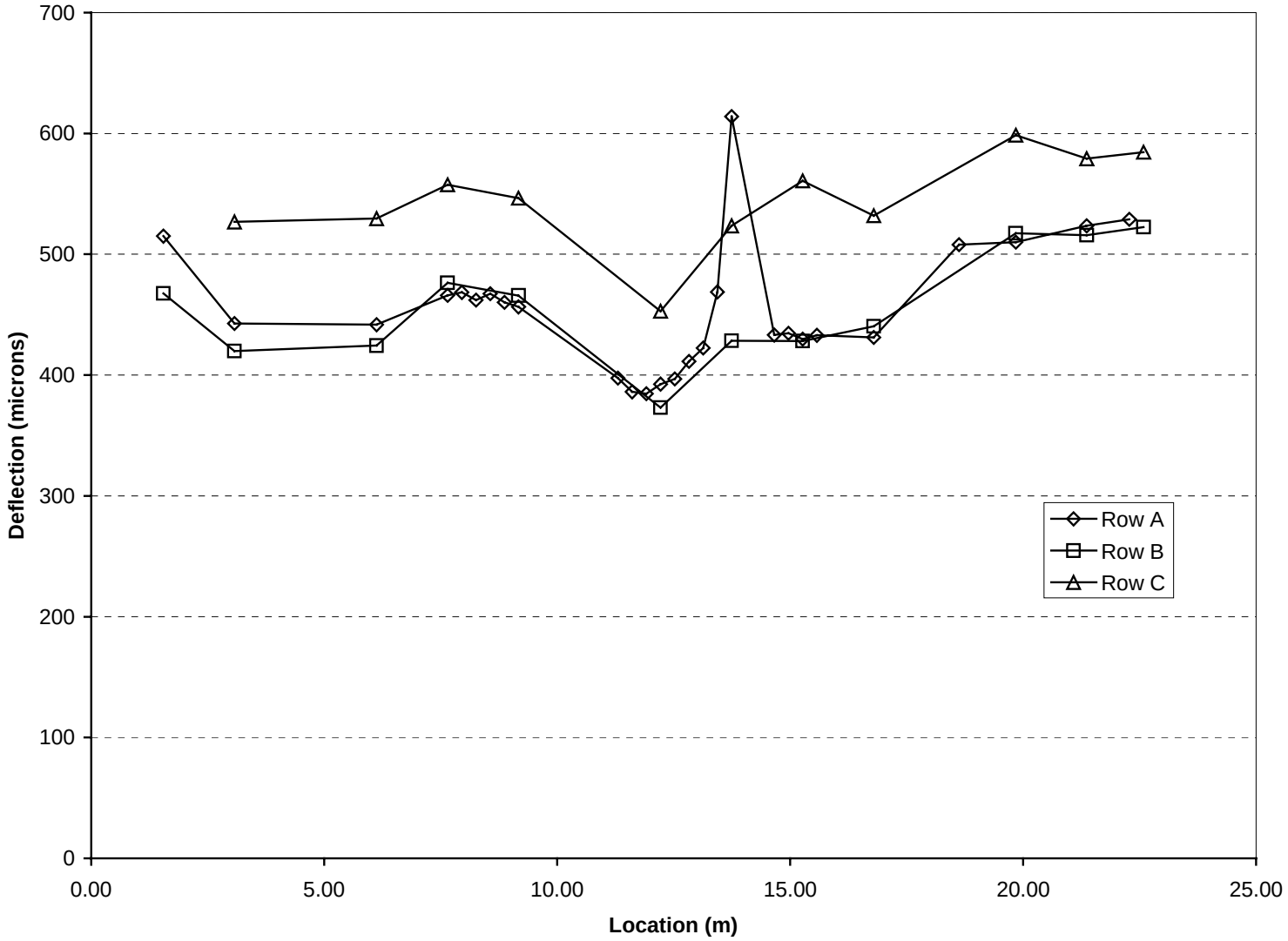

Figure 4. RFS PCC test slab - 133 kN deflections.

Table 7 Summary of the HWD Deflections on Section 516CT.

RFS PCC Test Slab		Normalized Deflections, mmx10^3 (mils) (1)		
Row	Test Load, kN (kip)	Average	Standard Deviation	84th Percentile
A				
	40 (9)	147 (5.81)	28 (1.10)	175 (6.90)
	89 (20)	320 (12.60)	52 (2.04)	372 (14.64)
	133 (30)	475 (18.70)	77 (3.01)	551 (21.71)
B				
	40 (9)	144 (5.68)	23 (0.89)	167 (6.57)
	89 (20)	323 (12.71)	47 (1.84)	370 (14.55)
	133 (30)	484 (19.05)	69 (2.72)	553 (21.77)
C				
	40 (9)	179 (7.07)	29 (1.16)	209 (8.23)
	89 (20)	395 (15.57)	58 (2.27)	453 (17.84)
	133 (30)	587 (23.11)	83 (3.26)	670 (26.37)

(1) High deflections were observed at the following locations:

Row A: 1.5 m, 9.45 m, 9.75 m, 13.7 m, 18.6 m, and 21.3 m.
Row B: 1.5 m, 15.2 m, and 19.8 m.
Row C: 1.5 m, 6.1 m, 12.2 m, 15.2 m, and 21.3m.

to be fairly consistent across rows A, B, and C. Locations where relatively large deflections were recorded are omitted in the following analyses to reduce the influence of outlying data. The outlying data appear to be in the vicinity of the slab joints, which may explain the increase in the measured deflection.

2.4.3 Pavement Layer Elastic Moduli

PCC and subgrade elastic moduli were backcalculated for each deflection basin using ELCON. The base moduli were fixed at 206 MPa (30 ksi) for all rows. This value was assumed based on the material descriptions and dynamic cone penetrometer (DCP) testing provided by UCB personnel. PCC elastic moduli are plotted for the test section in Figures 5 through 7 and are consistent at all load levels, averaging approximately 30,000 MPa (4,400 ksi). The HWD results were consistent with laboratory test data calculated

from compressive strength data taken on the day of placement. Using the ACI relationship

$$E_{pcc} = 57{,}000 \times (f'_c)^{0.5}$$

the 7-day and 28-day modulus was 29,496 MPa (4,277 ksi) and 33,862 MPa (4,910 ksi) respectively. Increased variation of moduli was observed near joint locations, consistent with the deflection data.

Backcalculated subgrade moduli for the test slab are shown in Figures 8 through 10. Inspection of these figures shows generally consistent subgrade response, with average moduli varying from approximately 100 MPa (14 ksi, corresponding R-value of approximately 23) to approximately 130 MPa (19 ksi, corresponding R-value of approximately 32). These values are fairly consistent with the subgrade moduli calculated for other pavement sections located at Richmond Field Station (3). PCC and subgrade elastic moduli and estimated subgrade R-values calculated from the deflection data are summarized in Tables 8 and 9.

The average HWD correlated R-value of 30 in Table 9 was similar to DCP correlated R-values of 35 in Table 1.

2.5 Joint Evaluation

The PCC joint evaluation analyses provide information in terms of calculated modulus of subgrade reaction (k) at the joint, ratio of k at joint to k at center (indication

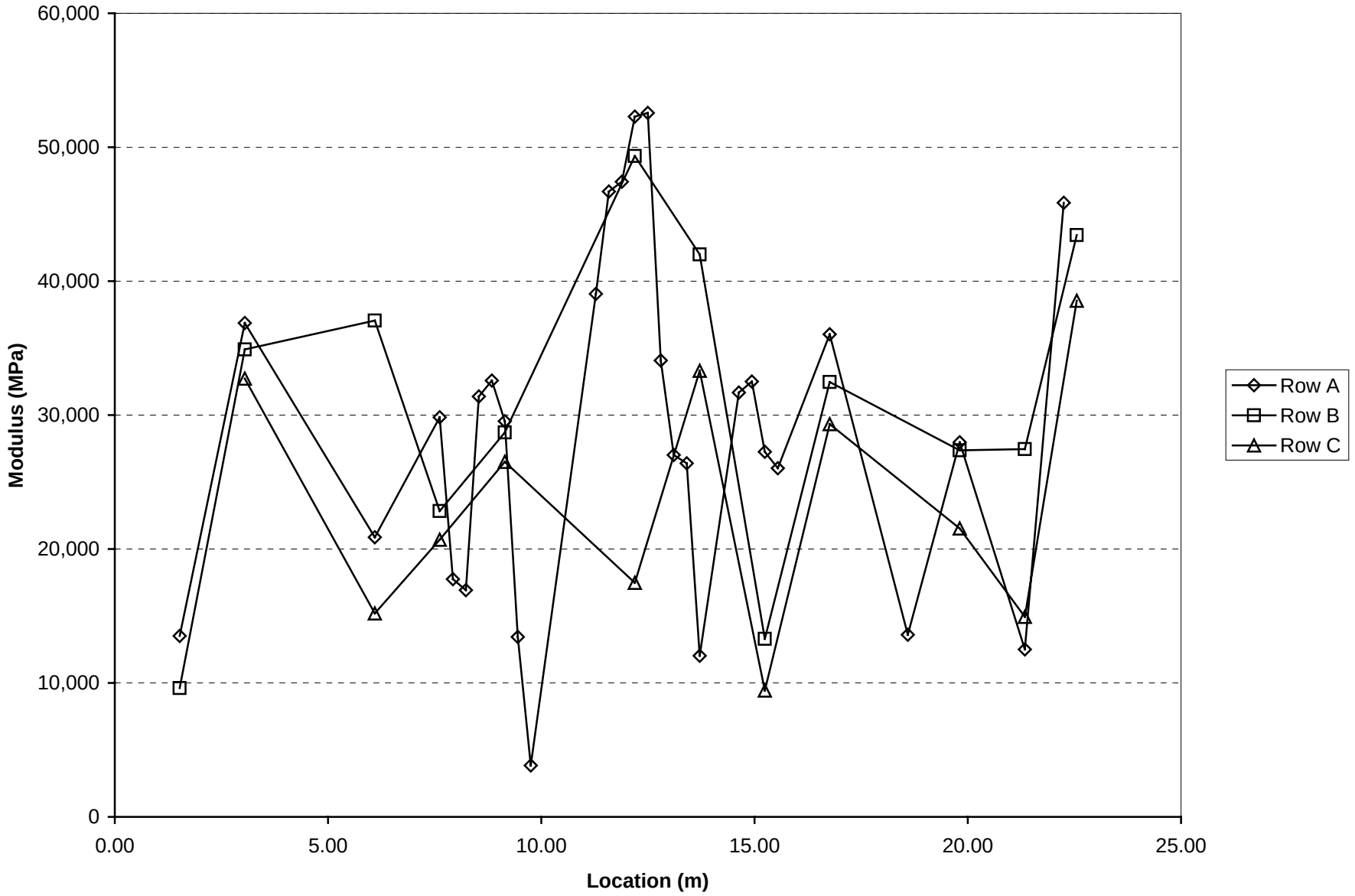

Figure 5. RFS PCC test slab - PCC moduli (40kN).

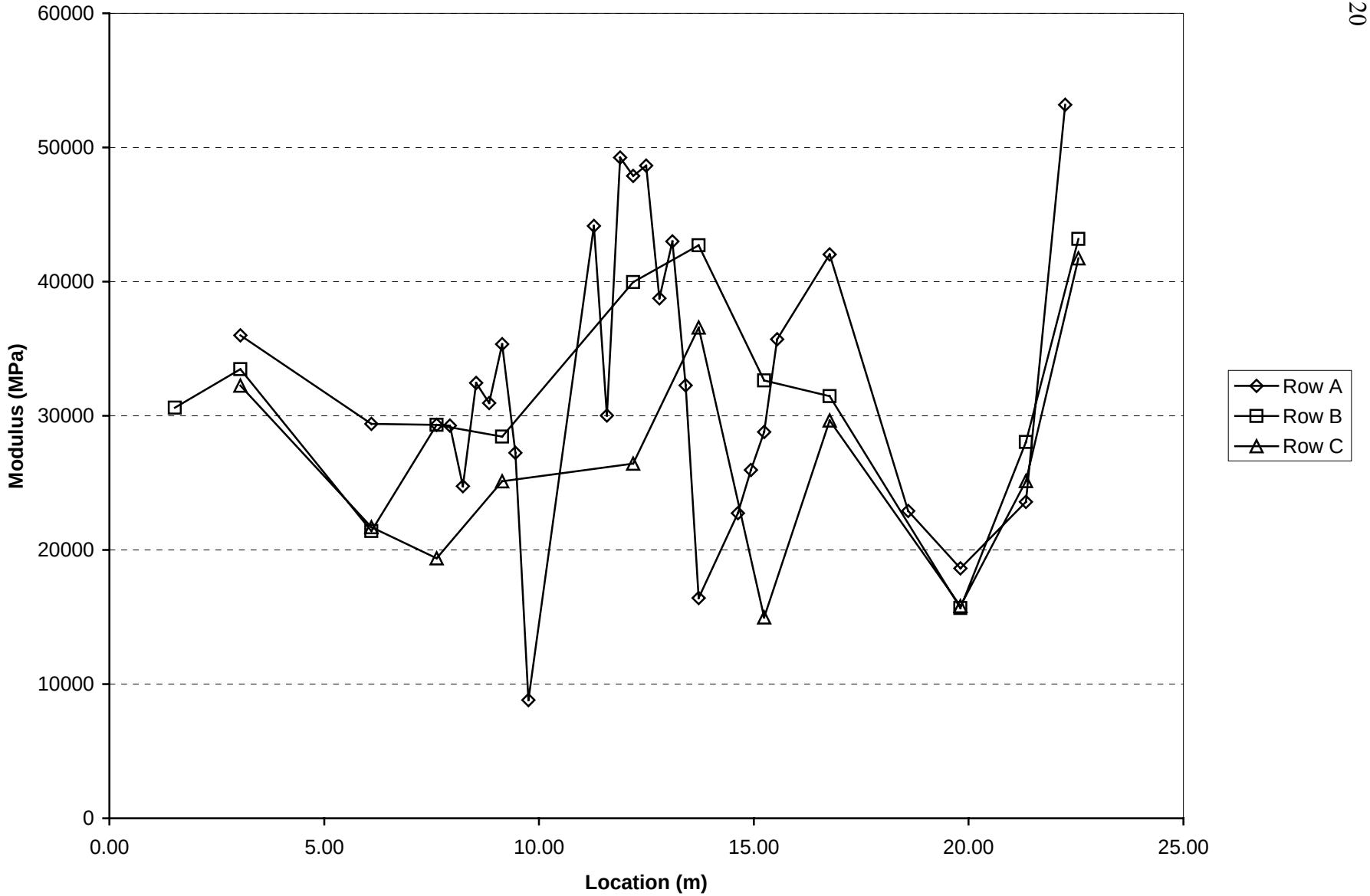

Figure 6. RFS PCC test slab - PCC moduli (89 kN).

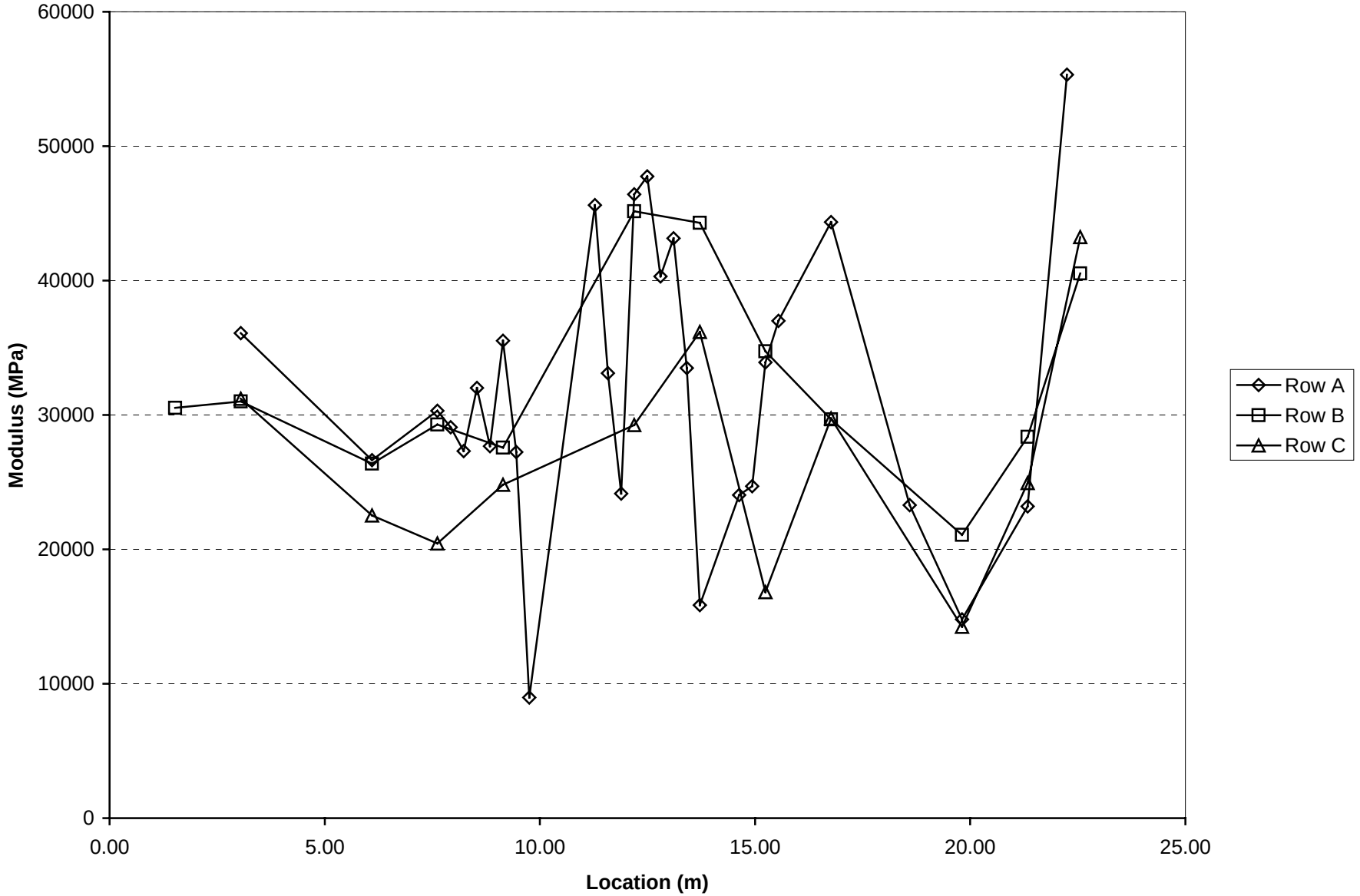

Figure 7. RFS PCC test slab - PCC moduli (133 kN).

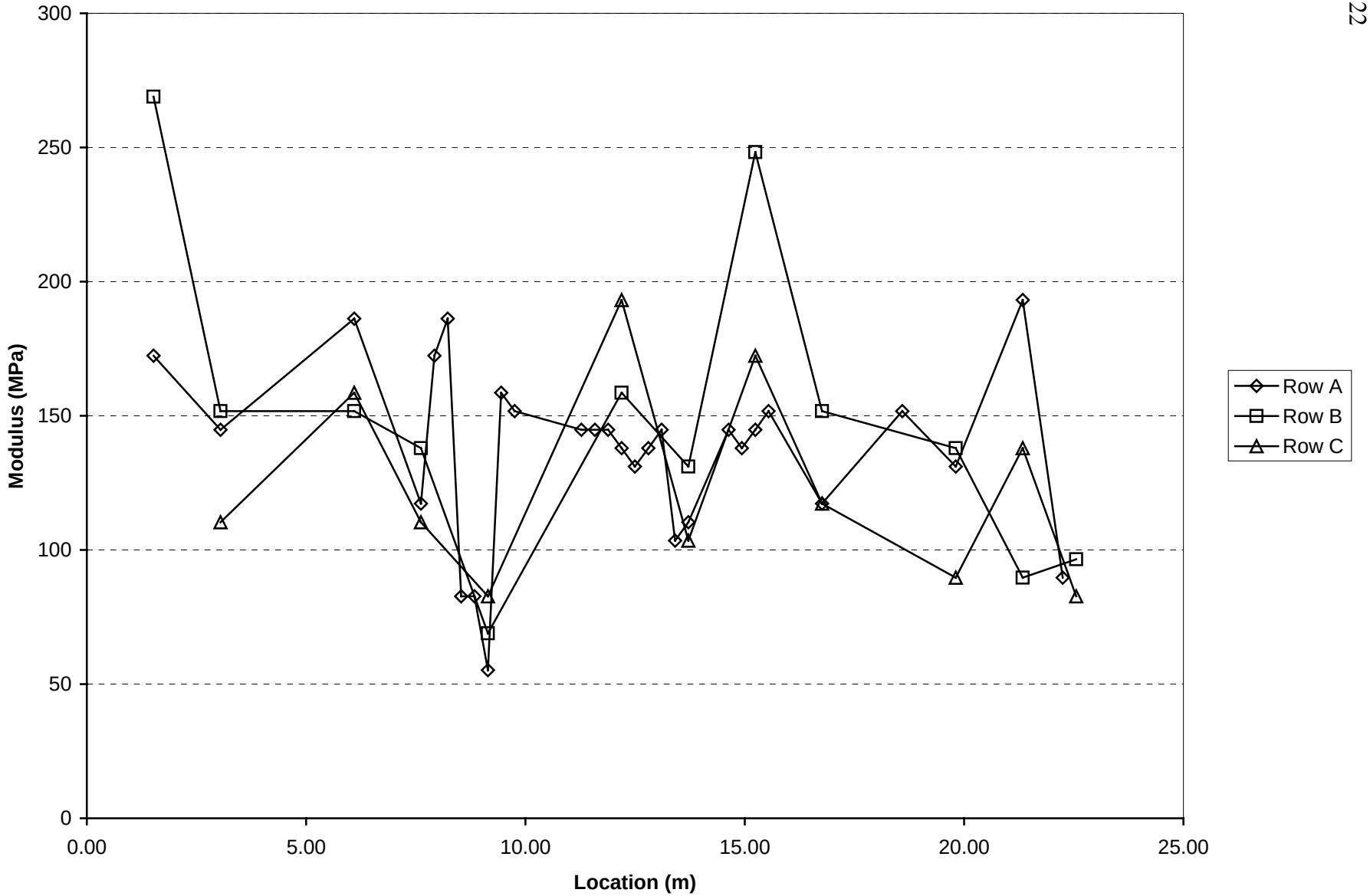

Figure 8. RFS PCC test slab - subgrade moduli (40 kN).

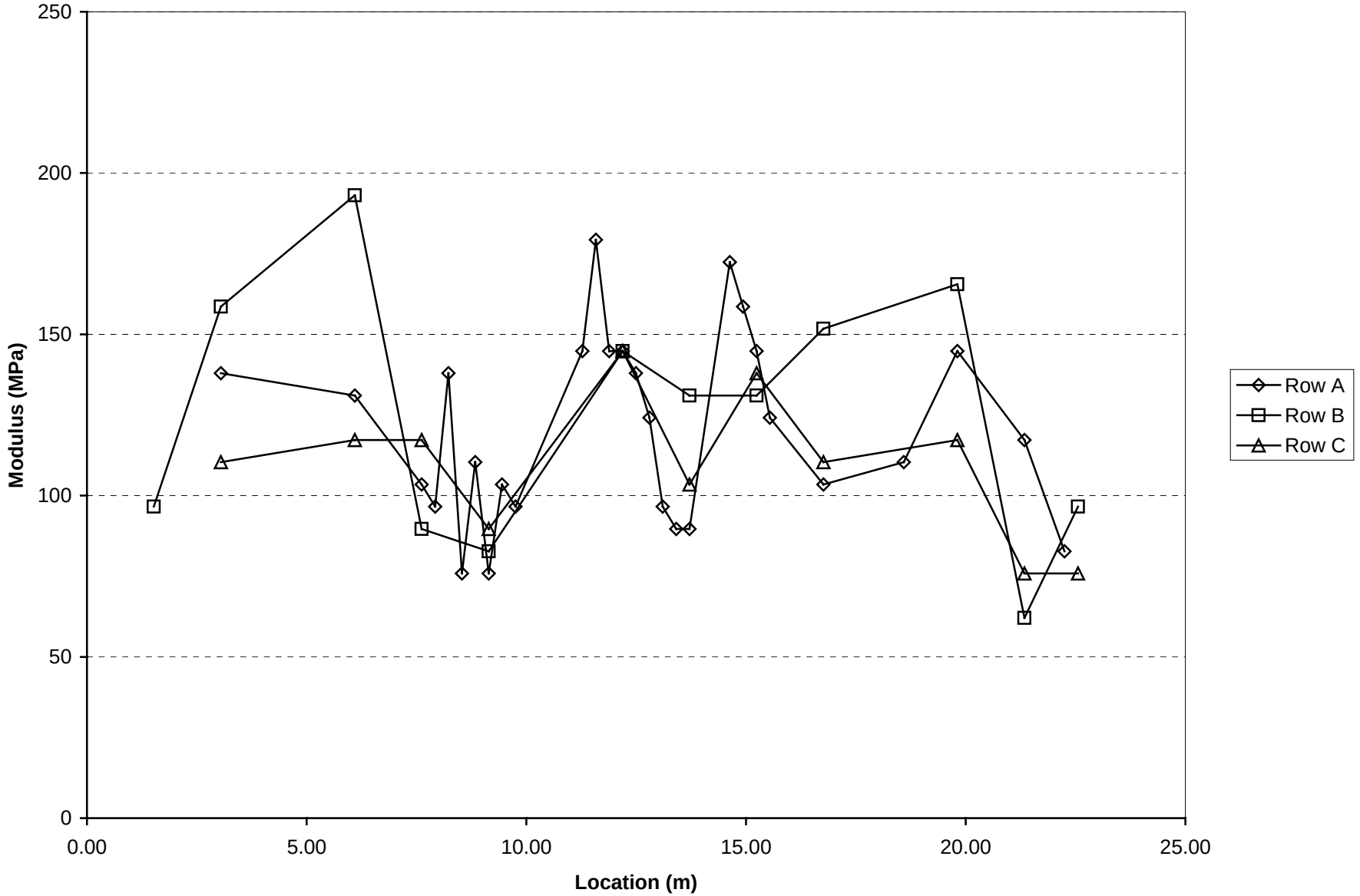

Figure 9. RFS PCC test slab - subgrade modulus (89 kN).

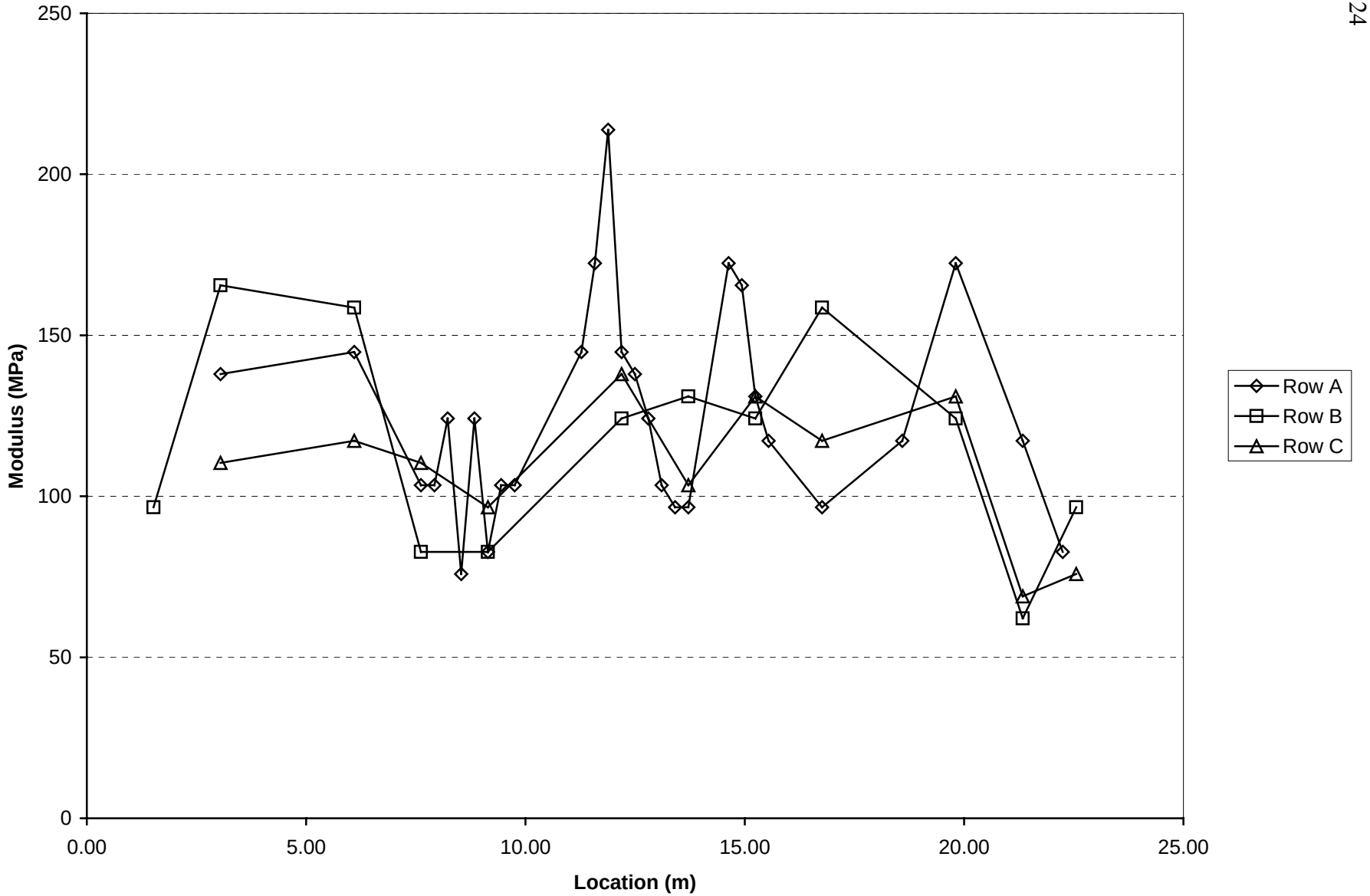

Figure 10. RFS PCC test slab - subgrade moduli (133 kN).

Table 8 PCC Elastic Moduli.

RFS PCC Test Slab		PCC MODULUS, GPa (ksi) [1]		
Row	Test Load, kN (kip)	Average	Standard Deviation	84th Percentile
A	40 (9)	28.9 (4,188)	12.8 (1,855)	16.1 (2,333)
	89 (20)	32.0 (4,645)	10.7 (1,547)	21.4 (3,099)
	133 (30)	31.5 (4,569)	10.7 (1,549)	20.8 (3,020)
B	40 (9)	30.7 (4,452)	11.8 (1,712)	18.9 (2,740)
	89 (20)	31.4 (4,554)	8.1 (1,172)	23.3 (3,382)
	133 (30)	32.4 (4,695)	7.4 (1,073)	25.0 (3,622)
C	40 (9)	23.6 (3,423)	9.2 (1,328)	14.4 (2,096)
	89 (20)	26.2 (3,806)	8.4 (1,214)	17.9 (2,593)
	133 (30)	26.7 (3,867)	8.5 (1,227)	18.2 (2,640)

(1) Relatively large moduli values were calculated at the following locations and were not used to calculate the summary results:

Row A – 1.5 m, 9.45 m, 9.75 m, 13.7 m, 18.6 m, and 21.3 m.
Row B – 1.5 m, 15.2 m, and 19.8 m.
Row C – 1.5 m, 6.1 m, 12.2 m, 15.2 m, and 21.3 m.

Table 9 Subgrade Elastic Moduli and Estimated Subgrade R-Values.

RFS PCC Test Slab		Subgrade Modulus, MPa (ksi) [1]			Calculated R-values [2]	
					TAI [3]	
Row	Test Load, kN (kip)	Average	Standard Deviation	84th Percentile	Average	84th Percentile
A	40 (9)	137 (20)	32 (5)	104 (15)	34	25
	89 (20)	121 (17)	28 (4)	93 (13)	29	21
	133 (30)	125 (18)	32 (5)	93 (13)	30	21
B	40 (9)	149 (22)	58 (8)	91 (13)	38	21
	89 (20)	125 (18)	40 (6)	86 (12)	30	20
	133 (30)	117 (17)	34 (5)	84 (12)	29	20
C	40 (9)	124 (18)	37 (5)	86 (12)	30	20
	89 (20)	109 (16)	22 (3)	87 (13)	27	21
	133 (30)	109 (16)	22 (3)	87 (13)	27	21

(1) Relatively large moduli values were calculated at the following locations and were not used to calculate the summary results:

Row A – 1.5 m, 9.45 m, 9.75 m, 13.7 m, 18.6 m, and 21.3 m.
Row B – 1.5 m, 15.2 m, and 19.8 m.
Row C – 1.5 m, 6.1 m, 12.2 m, 15.2 m, and 21.3 m.

(2) These values are consistent with measured R-values of similar soil and location conducted in Goal 1 testing.

(3) The Asphalt Institute (TAI) relationship is E_{sg} (psi) = 1155 + (555 × R-value).

of joint support condition), and joint load transfer efficiency (LTE). Joint evaluation analyses are highly dependent on the time of day the HWD test was performed due to temperature effects. The joint evaluation results are summarized in Table 10 (joints are numbered from 0 to 3 with numbering starting at the north end – see Figure 1).

Table 10 Joint Evaluation Results.

RFS PCC Test Slab		**Average Values of Joint Response**		
Joint	Test Load, kN (kip)	k_{joint}, MPa/m (pci)	k_{center}, MPa/m (pci)	LTE (percent)
0	40 (9)	58.5 (217)	53.2 (197)	99
	89 (20)	57.5 (213)	52.3 (194)	99
	133 (30)	58.2 (216)	54.9 (203)	99
1	40 (9)	44.3 (164)	27.9 (103)	90
	89 (20)	47.0 (174)	32.4 (120)	90
	133 (30)	48.8 (181)	35.1 (130)	90
2	40 (9)	53.3 (197)	51.3 (189)	97
	89 (20)	52.3 (194)	41.8 (155)	97
	133 (30)	54.4 (202)	43.5 (162)	96
3	40 (9)	38.6 (143)	49.5 (183)	98
	89 (20)	38.2 (142)	44.9 (167)	97
	133 (30)	39.0 (144)	44.8 (166)	97

The deflection transfer efficiency across all joints was greater than 90 percent, which is typical of a newly constructed pavement. The k-value of the subgrade varied from 30 to 55 MPa/m. The variation in k-value was high, however, doubling the k-value only changes the bending stress in the concrete slab by less than two percent.

3.0 INSTRUMENTATION AND DATA ACQUISITION

A variety of instruments were used in the practice test slab at RFS to measure pavement temperatures, strains, and deflections. All instruments were connected to one of two types of data acquisition system for signal conditioning and data storage.

3.1 Introduction

All instruments used can be grouped as either dynamic or online gages. Dynamic gages were connected to the HVS data acquisition system and required the trafficking of the HVS test wheel to trigger data collection. Dynatest PAST-2PCC, Tokyo Sokki PMR-60-6L, Crack Activity Meter (CAM), and Road Surface Deflectometer (RSD) are examples of dynamic gages. The profilometer also used the HVS data acquisition system, but did not require the test wheel to trigger the data collection.

Online gages were connected to the Campbell Scientific CR10X datalogger, which collected data automatically at specified time intervals. Thermocouples and Carlson A-8 strain meters were the two types of online sensors.

3.1.1 Data Acquisition Systems

Two separate data acquisition systems were used to collect data. The first was the HVS data acquisition unit developed by CSIR. The system consisted of a 16-channel analog to digital (A/D) board inside of a standard personal computer. Connected to the A/D board were two racks: one for dynamic strain gages and the other for the CAM, RSD, and profilometer. Each rack contained cards specific to a particular instrument. Up to 16 separate instruments could be used at one time. This data acquisition system allowed for collection of data under dynamic loading, which was achieved with a clock

connected to the motion of the HVS wheel. As the test wheel moved toward an instrument, the clock triggered the first data point and the acquisition system continued to record data until the wheel stopped moving or a maximum of 256 clock points was reached. Dynamic data collection was performed manually at specific repetition intervals per the test plan. Figure 11 shows the dynamic data acquisition schematic.

The second type of data acquisition system used was the Campbell Scientific CR10X. This system automatically collected temperature and environmental strain data every half-hour. This system consisted of a datalogger, multiplexers, battery pack, and a water-resistant enclosure to protect the components from the environment. The CR10X datalogger is a wiring panel providing terminals for connecting analog inputs, excitation outputs, digital I/O ports, and power to the system from a 12-volt battery pack. Multiplexers allow for additional analog input channels, such as thermocouples and Carlson A-8 strain gages. Downloading of data was performed once a week with a portable laptop via the 9-pin serial I/O port. All data acquisition software to operate the CR10X was supplied by Campbell Scientific. Figure 12 shows the CR10X layout.

3.1.2 Instrument Types and Descriptions

3.1.2.1 Thermocouples

Thermocouple wires were installed in the pavement to measure surface and in-

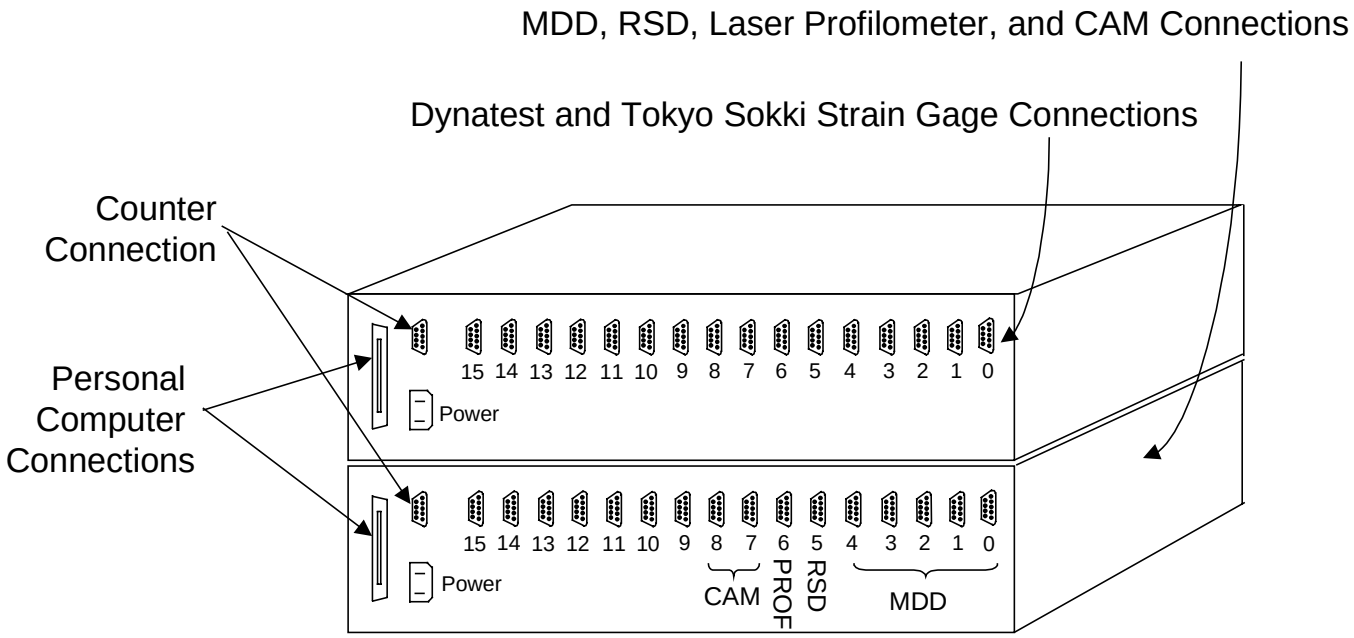

Figure 11. Dynamic data acquisition layout.

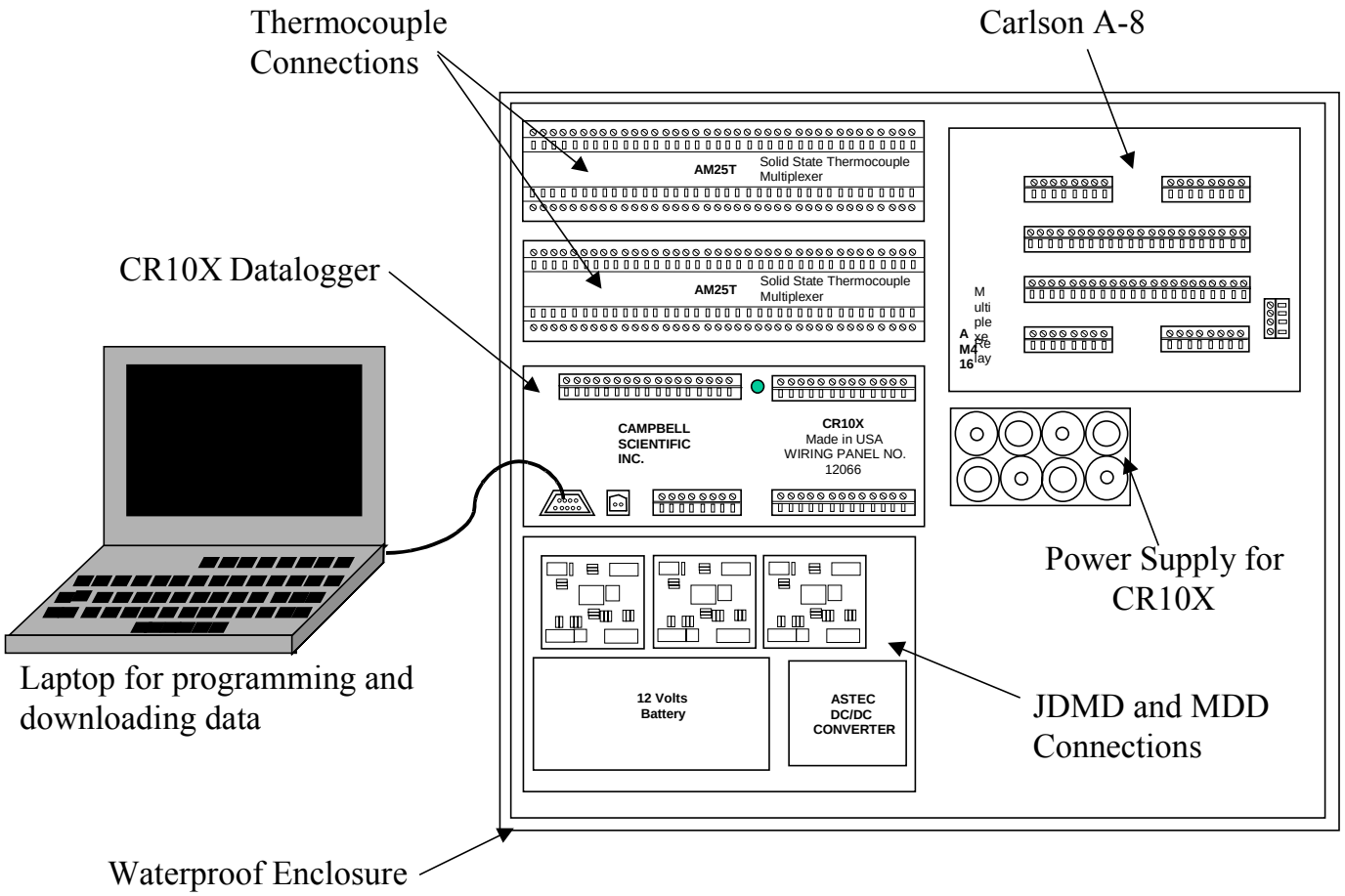

Figure 12. CR10X data acquisition layout.

depth concrete temperatures. Type K (nickel-chromium and nickel-aluminum leads) and Number 24 American Wire Gage thermocouple wires were used. The thermocouple wires are manufactured by Omega Technologies Company and have a maximum temperature capacity of 200°C. The ends of the thermocouple leads were soldered together in pairs to create the thermocouples. The soldered ends were then placed at various depths in the concrete pavement. A total of five thermocouples were used at each location with the wires taped to a 225 mm long by 7 mm diameter wooden dowel. The first thermocouple wire was placed at the surface of the concrete and the other four thermocouples were placed every 50 mm, with the bottom gage at 200 mm as shown in Figure 13.

For support, 25 mm of the dowel was driven into the aggregate base. Four sets of thermocouple wires were installed in the test slab. Figure 14 shows the location of the thermocouple sets in the concrete test section. Concrete temperature data was collected automatically by the CR10X every half- hour. During HVS testing, air temperatures were collected manually using an Omega HH-80 Series handheld digital thermometer readout.

3.1.2.2 Dynamic Strain Gages

Two types of dynamic strain gages were installed in the test slab to measure dynamic horizontal strains in the concrete.

3.1.2.2.1 Dynatest strain gages.

The first type of dynamic strain gage discussed is the Dynatest PAST-2PCC provided by Dynatest Consulting, Inc, of Ojai, California. This instrument consists of an electrical resistance strain gage embedded within a strip of glass-fiber reinforced epoxy, with transverse steel anchors at each end to form an H-shape as shown in Figure 15. Operation of the gages required a full bridge completion. This was achieved by assembling ¾ bridge modules. The ¾ bridge modules consisted of three 120-ohm resistors and one balancing resistor soldered on a 15 mm by 30 mm circuit board. The assembly was connected to the lead ends of the gage. Another 4-wire conductor with shield was connected from the bridge module to the HVS data acquisition system. Two Dynatest gages were placed 38 mm from the bottom of the concrete slab as shown in Figure 14. Dynamic bending strain data was collected manually with the HVS data acquisition system.

3.1.2.2.2 Tokyo Sokki strain gages

The second type of dynamic strain gage was the Tokyo Sokki PMR-60-6L, manufactured by Tokyo Sokki Kenkyujo Co., Ltd. Much like the Dynatest gage, these instruments measure bending strains in the concrete. The instrument consists of a strain gage to which 2 m of 24 gauge lead wire are attached. The strain gage and lead wire are hermetically sealed between thin resin plates, which waterproofed the instrument. The PMR-60-6L model contains three gages, making it a three-element rosette as shown in

Fig **thermocouple wires**

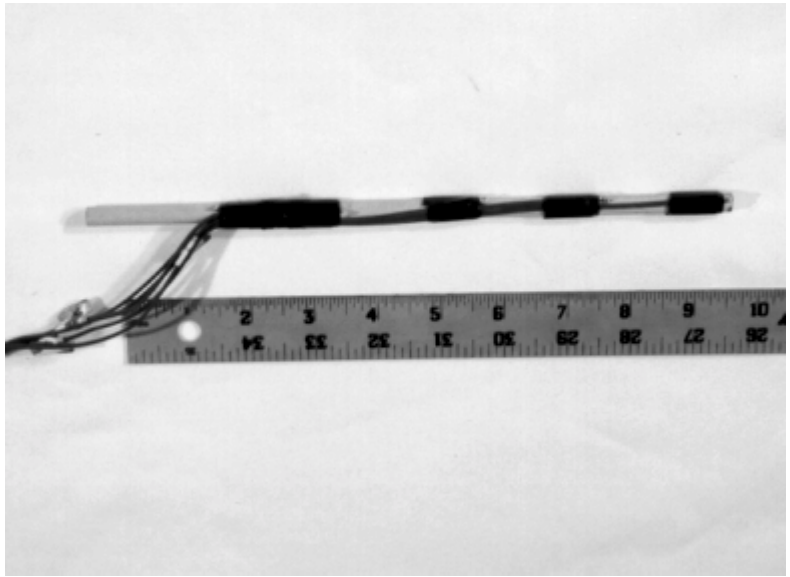

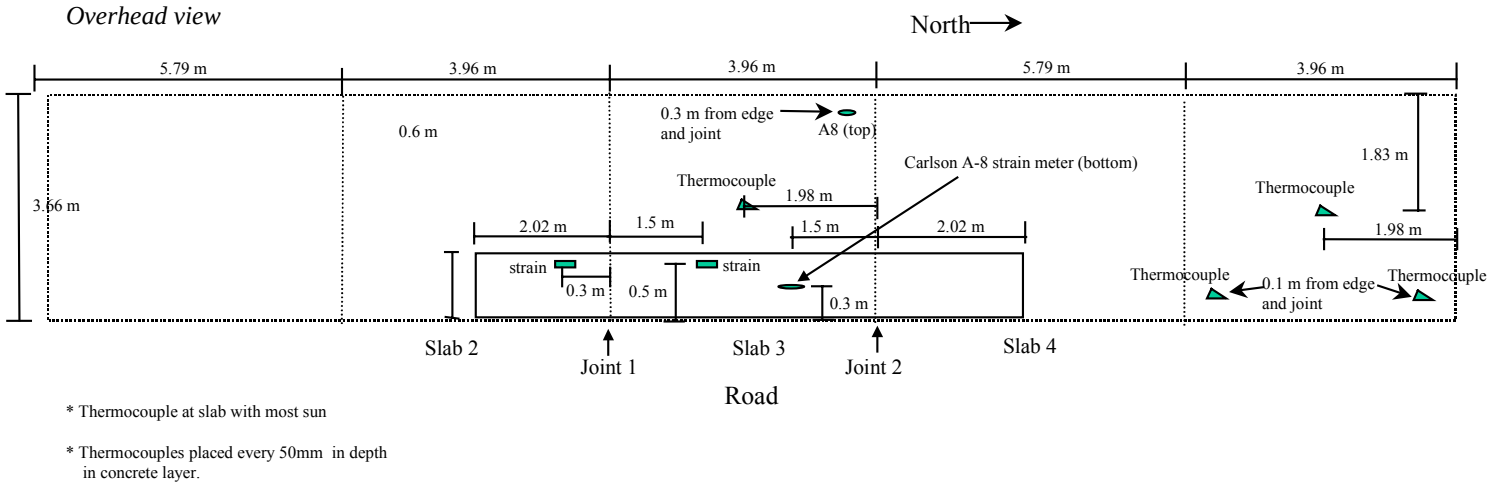

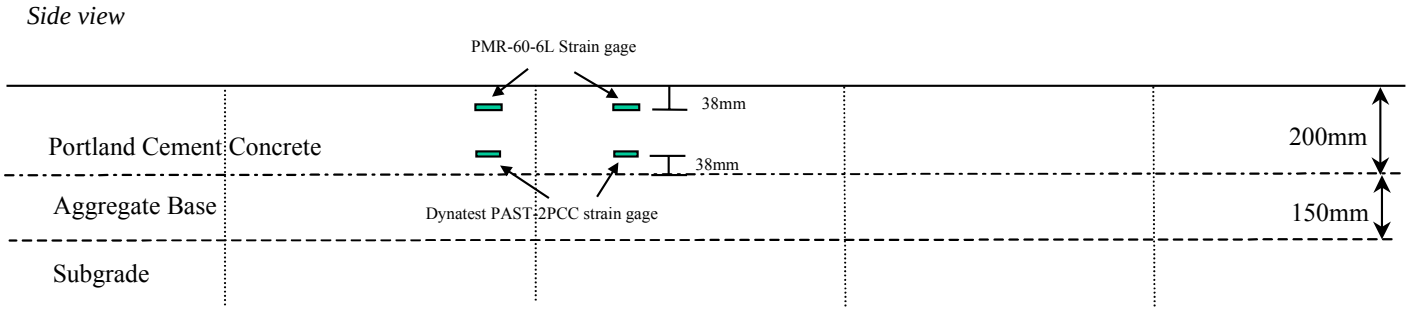

Figure 14. Location of gages on Section 516 CT.

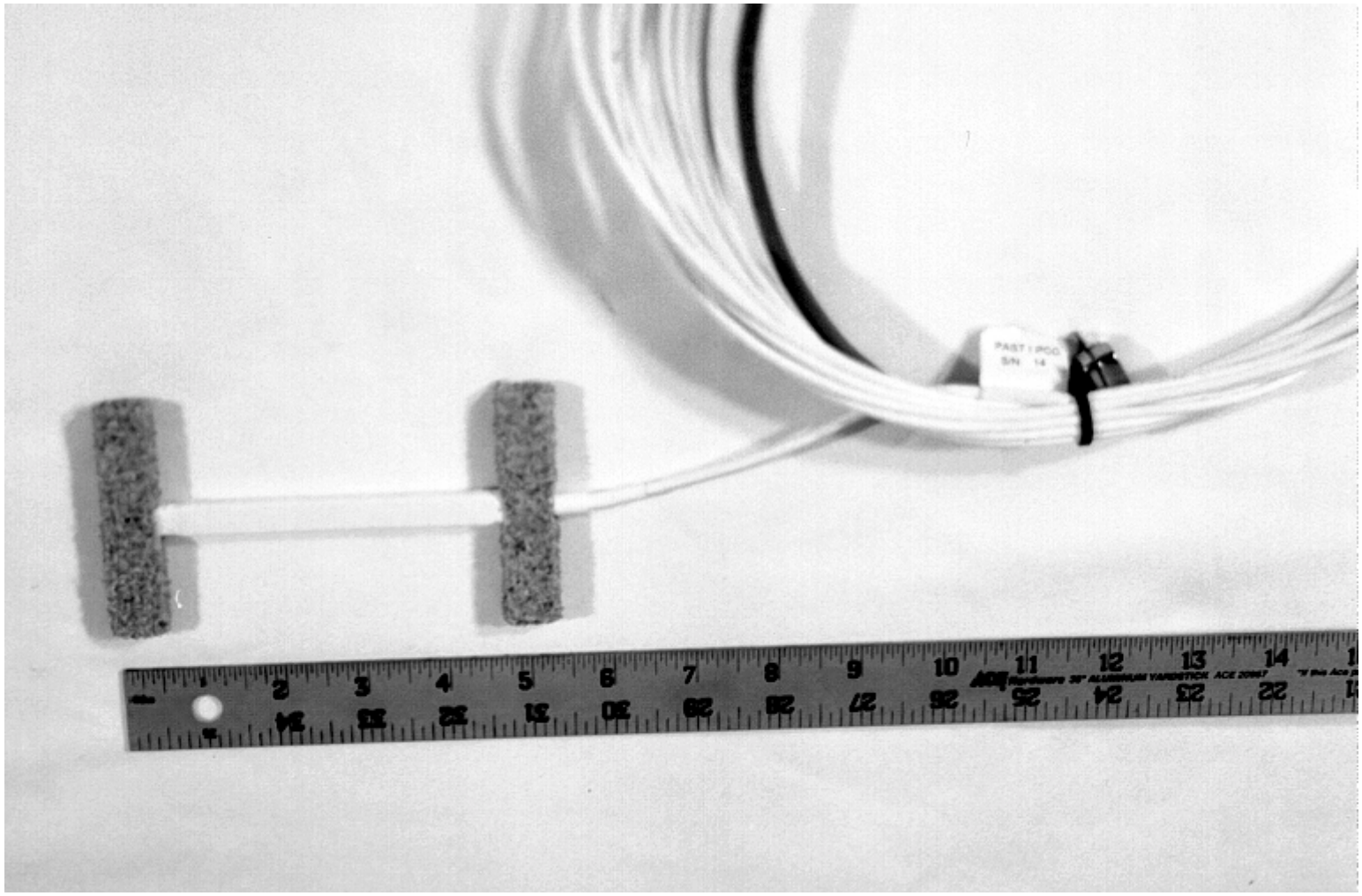

Figure 15. Dynatest PAST-2PCC strain gage.

Figure 16. Each gage required a ¾ bridge module for completion. A four-conductor cable with shield was used to connect the bridge module to the HVS data acquisition system. Two Tokyo Sokki PMR-60-6L gages were placed 38 mm from the top of the concrete slab at the same location as the Dynatest gages. Figure 14 shows the layout of the PMR gages in the concrete test section. Bending strain data was collected manually with the HVS data acquisition system.

3.1.2.3 Carlson A-8 strain meters

The Carlson A-8 strain meters, manufactured by RST Instruments, Inc., were the third type of strain gage embedded in the concrete. The gage was tubular and contained two coils of highly elastic steel wire. One coil increases in length and electrical resistance when strained, while the other decreases in length when unloaded or compressed. A picture of this gage is shown in Figure 17. This type of gage responds to changes in dimension of the concrete due to load stress, creep, shrinkage, temperature change, and moisture change. Completion resistors were required for the Carlson A-8 strain meters. Campbell Scientific supplied the bridge completion modules for the A-8 strain meters. One Carlson A-8 strain meter was installed 38 mm from the top of the concrete and the other 38 mm from the bottom of the concrete as shown in Figure 14. The Carlson A-8 strain meters were online sensors and were connected to the Campbell Scientific CR10X datalogger.

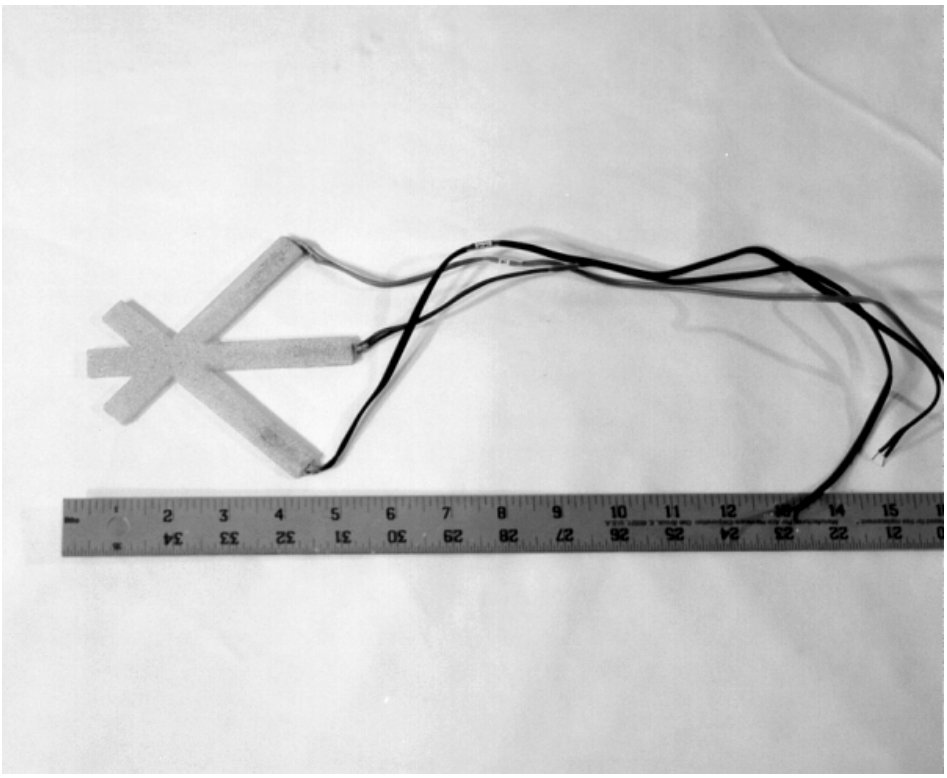

Figure 16. Tokyo Sokki PMR-60-6L strain gage.

Figure 17. Carlson A-8 strain meter.

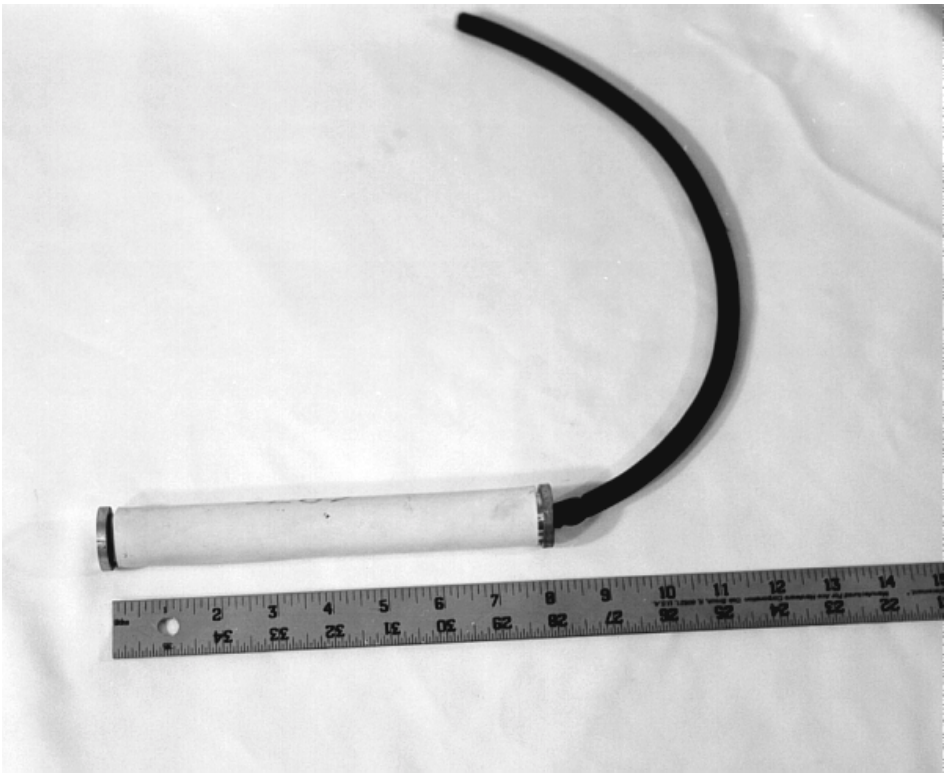

3.1.2.4 Crack Activity Meter (CAM)

The CAM was developed by CSIR to measure the horizontal and vertical movement of a surface crack as the HVS wheel passes near the crack. This device consists of a horizontal Linear Variable Displacement Transducer (LVDT) and a vertical LVDT, both of which are mounted on a frame as shown in Figure 18. The CAM was epoxied to the pavement on one side of the crack with the horizontal LVDT aligned perpendicular to the crack line. On the other side of the crack, targets for the LVDT heads were epoxied to the pavement as references for measuring displacement. During HVS testing, the CAM was placed across the concrete joints and one of the failure cracks. Data was collected manually using the HVS data acquisition system.

3.1.2.5 Road Surface Deflectometer (RSD)

The RSD was developed by CSIR to measure surface deflection under a loaded wheel. The RSD is a modified Benkelman beam with two reference feet at one end and the measuring point at the other, as shown in Figure 19. An LVDT is located between these two points. The RSD is 3 m long and thin enough for the dual tires to straddle the measuring point and move towards the LVDT, thus capturing the pavement deflection data.

RSD measurements were initially taken at five points, with the length of the RSD in the direction of wheel traffic. However, plots of the results varied too much because of the effect of slab movement on the RSD reference feet. Later data collection involved moving the RSD perpendicular to the direction of wheel traffic. This method allowed the

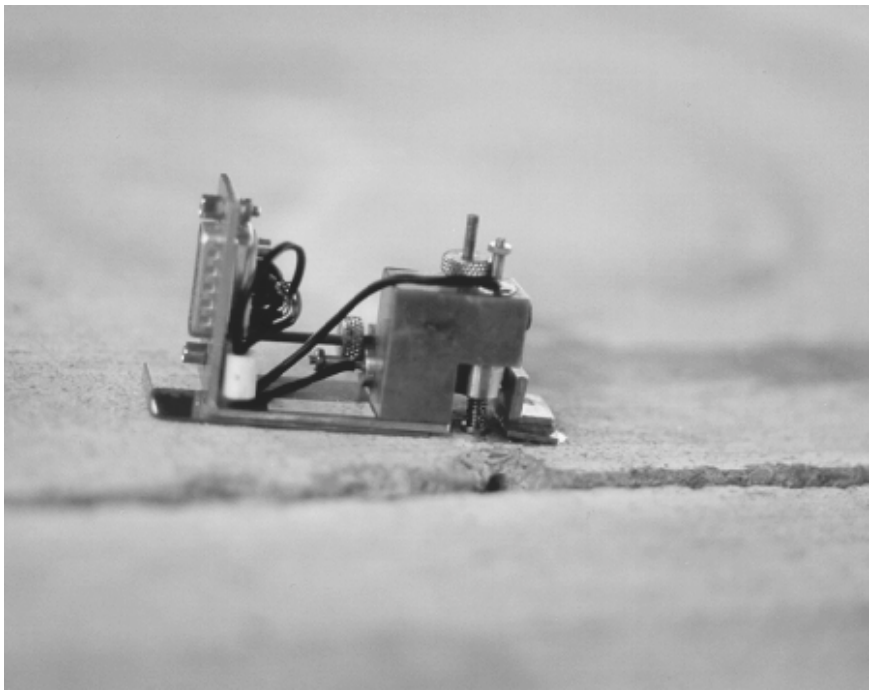

Figure 18a. Crack Activity Meter (CAM) side view.

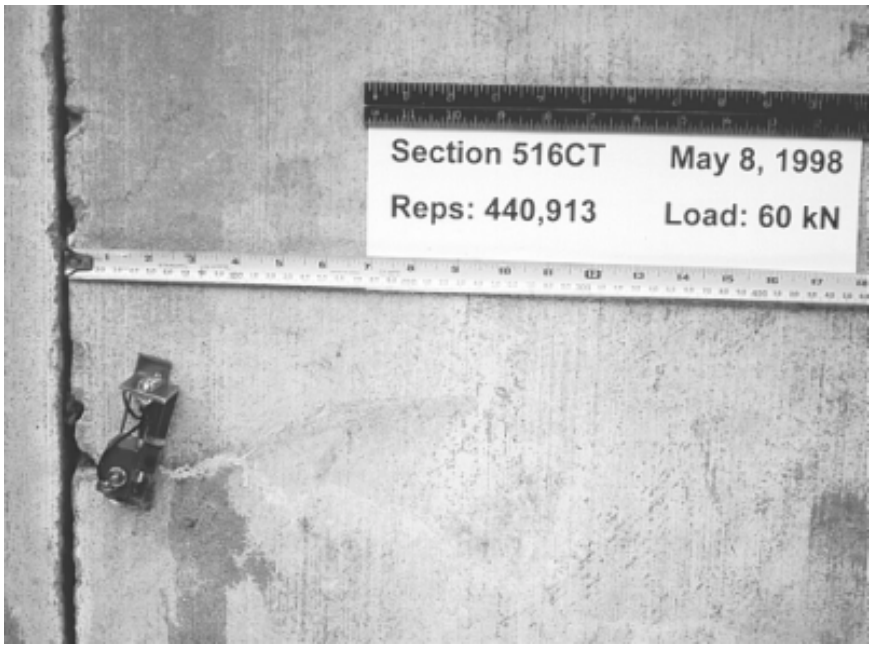

Figure 18b. Crack Activity Meter (CAM) overhead view.

Figure 19. Road Surface Deflectometer.

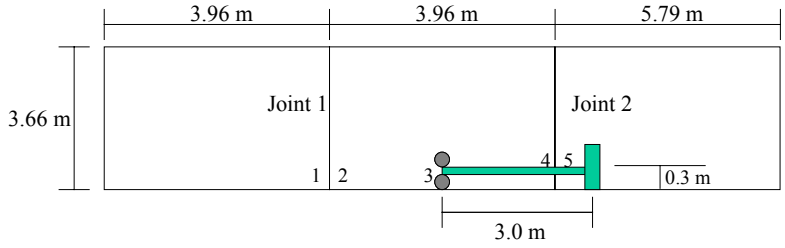

Figure 20a. RSD oriented parallel to the wheelpath.

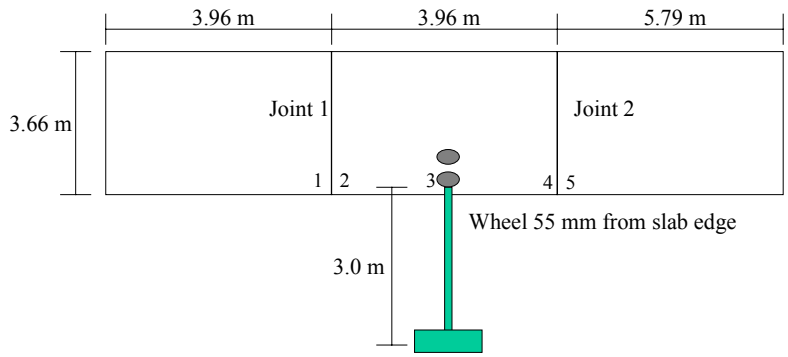

Figure 20b. RSD Oriented perpendicular to the wheelpath.

reference feet to be placed off the concrete test section where a stable reference point could be obtained. Figures 20a and 20b show the two orientations of the RSD used during HVS testing. RSD data collection was done manually using the HVS data acquisition system.

3.1.2.6 Laser profilometer

The laser profilometer was used to measure the surface profile of the test pavement. The laser device moves along a 3-m long frame, measuring the distance between the laser head and the pavement surface at 9-mm intervals to generate the surface profile of the pavement. This device was used in attempt to capture the longitudinal profile of the pavement. However, because the frame was not able to span the entire length of the trafficked area, and due to the slab movement from daily

temperature changes, this device was found to be inadequate for determining surface roughness.

3.1.2.7 Weather station

A Davis weather station was temporarily installed near the test slab to measure air temperature, rainfall, relative humidity, wind speed and direction, and solar radiation. This weather station will eventually be used to collect localized weather data at the Palmdale test sections.

4.0 CONSTRUCTION

The original intent behind constructing the PCC test slab was to allow the UCB Contract Team to familiarize themselves with the placement of instruments and their protection boxes, survivability of the instruments in the concrete, concrete construction procedures, and full-scale operation of HVS2. This exercise gave the team an opportunity to learn and make necessary changes in the test plan instrumentation and data collection before constructing and operating the Palmdale test sections.

Construction of the concrete test slab was completed by Scott Johnson Contractor of Point Richmond, California. Before the placement of PCC, the contractor excavated the existing material to a depth of 356 mm. This involved removing approximately 50 mm of existing asphalt concrete and 306 mm of aggregate subbase until the subgrade was reached. After the removal of the existing material, side forms were placed. Approximately 50 tons of Class 2 aggregate base was then placed and compacted to an average thickness of 150 mm.

One day prior to concrete construction, instruments were placed on the aggregate base. This involved locating all gages within the test section and attaching the gages on their corresponding installation cradles to achieve the correct height and orientation as shown in Figure 21. The cables from the gages were buried in small trenches in the aggregate base. The trenches and cables were then backfilled with sand to ensure they wouldn't be crushed by any large aggregates. The ends of all cables terminated at one location outside the PCC test section where they could be connected to the data collection systems.

The strain gages were protected by sheet metal boxes as a way to prevent the forces of the fresh concrete from moving or damaging the gages, as shown in Figure 22.

Welded to the sides of the boxes were metal spikes, which were driven into the aggregate base to prevent the boxes from moving under the forces of the fresh concrete. The sheet metal boxes surrounded each set of gages with enough room inside the box for a 25-mm diameter hand-held vibrator to be used to consolidate the concrete around the gages. Sheet metal boxes were not necessary for thermocouples because they were attached to dowels embedded in the aggregate base, as explained in section 3.1.2.1. The final step before concrete construction involved checking gage resistance against laboratory measured resistance with a multimeter. This check ensured that the gages were functioning properly prior to placement of concrete.

The PCC test section was cast on December 23, 1997. The air temperature during the concrete slab construction averaged 15°C. Three and one half loads of concrete (a total of 18.7 m^3 [24.5 $yd.^3$]) were transported in concrete mixer trucks from Sugar City Building Materials Co. in Point Richmond, CA, to the RFS. The concrete was placed on the north end of the test section first.

Concrete from the first truck appeared to have low workability while the mix was coming out of the chute and as a result, the operator added water into the drum to improve the workability. The concrete was shoveled into the sheet metal boxes and carefully placed around the gages. When the concrete filled the sheet metal boxes, the hand-held vibrator was used to consolidate the concrete inside and around the box. Each steel box remained in place around the gages until the concrete covered the entire box, with the expectation that the boxes would be removed just prior to finishing the concrete

Figure 21a. Carlson A-8 strain meter on its cradle to maintain gage height and orientation during concrete placement.

Figure 21b. Tokyo Sokki PMR-60-6L (top) and Dynatest PAST-2PCC (bottom) on cradle to maintain gage height and orientation during concrete placement.

Figure 22. Sheet metal boxes are used to protect strain gages from flow of fresh concrete.

surface. However, the first load of concrete soon began to loose its workability, and the second mixer truck did not arrive immediately after the first truck. There was concern that the concrete would harden to the point where the sheet metal boxes could not be pulled out, so the boxes were removed prematurely.

When the second and third loads of concrete arrived, water was again added. The fourth mixer truck brought a half load to finish the test section. The pavement surface was struck off using a 51 mm × 102 mm (2 in. × 4 in.) piece of wood after each mixer placed the concrete. The concrete was consolidated with a rolling tamper. Final finish was done by a float. After the PCC was set, the forms were stripped and the surface was sprayed with water for several days. Concrete beams for flexural strength testing and cylinders for compressive strength testing were sampled from the fourth truck only.

The joints were spaced according to the joint spacing at the field test slabs at the Palmdale test site. The joint spacing of the RFS test section is shown in Figure 1. The contractor used a concrete saw to cut a 45 mm deep groove at all joint locations.

A final resistance check was done to all strain gages installed in the pavement after the final set of the concrete. This check ensured that the embedded gages were not damaged during concrete placement. HVS2 was moved onto the test section on March 2, 1998 and the first HVS repetition and data collection was completed on March 16, 1998.

5.0 TEST OBJECTIVES OF THE HVS CONCRETE TESTING AT RFS

This chapter details the test objectives of the HVS concrete testing at the Richmond Field Station (RFS). The HVS test plan is presented and the pavement response data taken from the instrumentation is summarized. A brief description of the measured parameters is also included. The complete pavement analyses of the response data is presented in Chapter 8.

5.1 HVS2 Test Objectives

The primary objective of HVS2 was to evaluate the behavior of in-service concrete pavement structures on State Route 14 near Palmdale, California, as detailed in the Test Plan for CAL/APT Goal LLPRS—Rigid Phase III. (2) The concrete slab construction at the Richmond Field Station was originally built with the purpose of familiarizing the Pavement Research Center personnel with concrete slab construction, installing gages, monitoring embedded gages, and any loading problems encountered with HVS2. Because the Palmdale construction project was delayed due to weather and concrete materials questions, the scope of the RFS concrete slab testing was widened to include repetitive loading of the slabs until failure occurred.

The initial objectives were:

- To place concrete with high early strength with a low slump on a full-scale test section
- To determine whether constructing a full scale concrete pavement section would influence the serviceability of the sensitive in-place instrumentation

- To establish HVS testing protocols for rigid pavements in preparation for HVS testing near Palmdale
- To load the concrete test section until failure, and
- To compare the results of the HVS test with existing mechanistic rigid pavement techniques.

After the test section construction, the initial HVS trial slab test objectives were expanded. HVS test section 516CT can be summarized as the fatigue evaluation of a 200-mm jointed plain Portland Cement Concrete (PCC) pavement with calcium chloride under the influence of bidirectional accelerated wheel loads and ambient environmental conditions.

The original instrumentation plan and data collection schedule did not address the completion of a fatigue evaluation of the practice test pavement, however important knowledge was gained from the fatigue loading of section 516CT. During this HVS test, some data collection procedures were changed in an attempt to acquire consistent data. Although some of the collected data was not of sufficient quality to analyze, the behavior of the test section in terms of temperature and wheel loading were quantified along with the appearance of pavement distresses.

6.0 HVS TEST PROGRAM

HVS2 began testing section 516CT on 16 March 1998. The HVS test program included monitoring and reporting the repetitive loading parameters such as the applied wheel load, tire pressures, and number of repetitions, and environmental variables such as air and pavement in-depth temperature.

6.1 Loading Plan

HVS trafficking was performed in the channelized traffic mode, meaning all passes of the test wheel were in the same wheel path with no lateral wander. In order to increase the bending stresses in the pavement, edge loading was used, i.e., the outer dual tire wheel traveled on the edge of the test slab. This method of loading was used to accelerate the concrete fatigue damage process.

The flexural strength or modulus of rupture (M_R) of the concrete was 5.86 MPa. To accelerate the concrete fatigue damage, the applied dual tire load was set at 60 kN. This load produced a maximum edge stress (σ) of 2.5 MPa. The load stress ratio (σ/M_R) of the slab was 0.43 excluding any curling effects.

The HVS load (60 kN) was kept constant for the duration of the test. The HVS was only run for 14 hours per day (7:00 to 21:00) to eliminate potential noise problems with local residents. The HVS production rate for the 14 hour per day loading trafficking schedule was approximately 9,500 repetitions/day. This included down time for regular maintenance and for data collection.

6.2 Data Collection Schedule

Part of the data recording schedule is detailed in Table 11 with the exception of the Crack Activity Meter (CAM), which was used only after the first crack appeared.

6.2.1 Weather data

Weather data was automatically recorded using a Davis weather station. The weather data collected was air temperature, atmospheric pressure, wind speed, wind direction, and rainfall. Data was collected every hour resulting in 24 readings per day. The weather station was not in use for the entire duration of the HVS test.

6.2.2 Online measurements

Two Carlson A-8 strain gages were embedded in the concrete section during construction. Thermocouples were also embedded at four locations in the section to record concrete temperatures at the surface, 50 mm, 150 mm, and 200 mm below the surface. The CR10X data acquisition system was used to acquire data from the online devices. Online measurements were automatically recorded every 30 minutes resulting in 48 per day throughout the entire HVS test. One A-8 strain gage was placed near the bottom of the middle slab, and the other placed near the surface, close to the edge. For the exact placements of the various sensors see Figure 14.

6.2.3 Dynamic measurements

Several pavement response measurement devices along with strain gages were used:

- the Road Surface Deflectometer (RSD),

- the Crack Activity Meter (CAM), and
- two types of strain gages, the Dynatest model PAST - 2PCC and the Tokyo Sokki PMR-60-6L.

Data was acquired from the dynamic gages while the HVS was trafficking. The schedule for dynamic data acquisition is shown in Table 11.

6.2.4 Visual pavement surveys

The concrete surface was visually inspected daily. Any irregularities such as joint faulting, pumping, or edge and corner cracks were recorded. Due to the high water table surrounding the test site, regular measurements of the water table depth relative to the bottom surface of the slab were also recorded.

6.3 Concrete Pavement Failure Mechanisms

The objective of test 516CT was to evaluate the fatigue performance of the PCC slab under repetitive loading. Fatigue cracking can manifest itself as transverse or longitudinal cracking. Because edge loading was used in this test, only transverse fatigue cracking was expected. Other failure modes included in the regular monitoring plan were corner cracking and excessive joint faulting. Joint faulting was not expected to occur because faulting is a unidirectional loading phenomena. Caltrans pavement failure criteria were not utilized in the evaluation of this test because they require roughness measurements and third stage cracking (slab broken up into 3 or more pieces).

Table 11 Data Collection Schedule for HVS Test 516CT.

Tire pressure: 690kPa/100psi				**traffic load: 60 kN**				
Tire type: radial				**Temperature control range: ambient**				
Repetitions	Load (kN)	Longitudinal Profilometer Slab Edge	Transverse Profilometer Points 0-16	RSD Points 1 - 5 (kN)	Acquire All Channels Dynamic Gages	Download CR10X Data (1)	Check CR10X Batteries	Crack Monitoring (2,3)
10	60	Yes	No	60	Yes	Yes	Yes	
2.5k	60	Yes	No	60	Yes			Yes
10k	60	Yes	No	60	Yes			Yes
15k	60	Yes	No	60	Yes	Yes	Yes	Yes
39k	60	Yes	No	60	Yes			Yes
69k	60	Yes	No	60	Yes	Yes	Yes	Yes
83k	60	Yes	No	60	Yes		Yes	Yes
103k	60	Yes	No	60	Yes	Yes	Yes	Yes
117k	60	Yes	No	60	Yes		Yes	Yes
125k	60	Yes	No	60	Yes	Yes	Yes	Yes
137k	60	Yes	No	60	Yes		Yes	Yes
152k	60	Yes	No	60	Yes	Yes	Yes	Yes
170k	60	Yes	No	60	Yes		Yes	Yes
189k	60	Yes	No	60	Yes	Yes	Yes	Yes
203k	60	Yes	No	60	Yes		Yes	Yes
223k	60	Yes	No	60	Yes	Yes	Yes	Yes
256k	60	Yes	No	60	Yes		Yes	Yes
295k	60	Yes	No	60	Yes	Yes	Yes	Yes
321k	60	Yes	No	60	Yes		Yes	Yes
402k	60	Yes	No	60	Yes	Yes	Yes	Yes
439k	60	Yes	No	60	Yes		Yes	Yes
476k	60	Yes	No	60	Yes	Yes	Yes	Yes
512k	60	Yes	No	60	Yes	Yes	Yes	Yes

General Notes:

a. Test is performed without controlling moisture contents of materials

b. Air temperature measurements should be taken every two hours throughout the entire test

c. Record time and date of any cracks visually spotted on the concrete surface

Specific Notes:

(1) Portable Computer

(2) Location and length of all surface cracks

(3) Photograph cracks on surface (35mm camera)

(4) Perform with a straight edge ruler

7.0 RESULTS

7.1 Online Strain Measurements

Online strain data (Carlson A-8 gages) was recorded beginning on February 27, 1998. An example of the output can be seen in Figure 23, which represents the Carlson A-8 gage strain response for a 72-hour period between February 28, 1998 and March 2, 1998. Compressive strains are negative values while tensile strains are positive. A strain measurement of +20με approximately equals 551 kPa (80 psi) tensile stress. In addition to strain, the Carlson gages record pavement temperature. The advantage of this dual role for the Carlson gages is that both temperature and strains are recorded at exactly the same location. The daily strain variation can be attributed to daily air temperature variation. The difference in pavement temperature between the A-8 gage located near the corner of the slab close to the pavement surface and the gage located in the middle of the slab near the pavement bottom is also shown in Figure 23. The strain measurements closely follow the temperature fluctuation.

The initial strain measurements prior to concrete placement were not recorded. Typically, changes in strain over time are relative to the initial strain state of the pavement. Knowing the initial strain state of the pavement would have allowed for the calculation of the internal stress state of the pavement during diurnal temperature changes. Without this reference point for the data, it was difficult to analyze the data properly. However, it was possible to determine the daily changes in the pavement strain as the HVS test progressed.

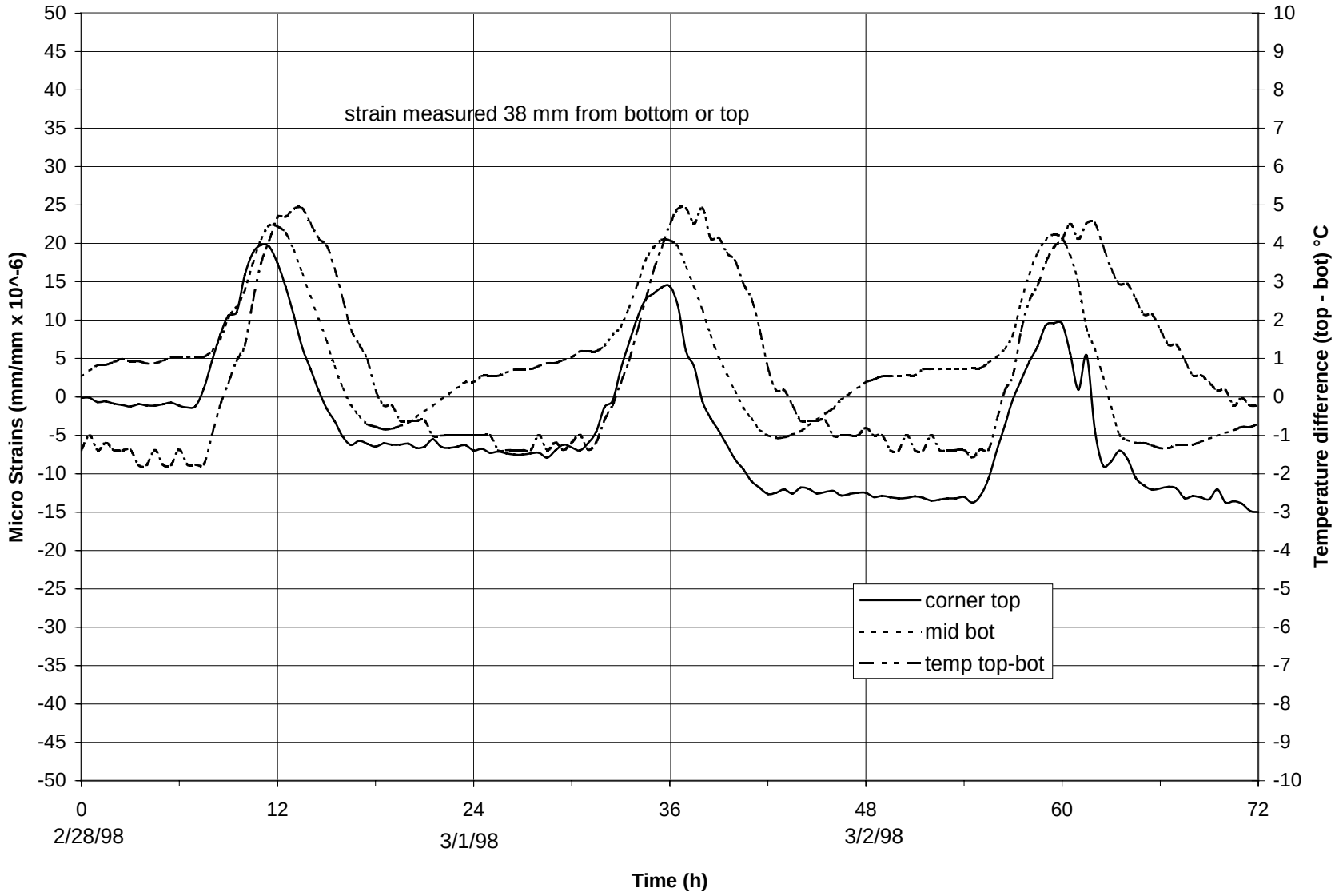

Figure 23. Carlson A-8 gage strain response for the period of February 28, 1998 to March 2, 1998.

The Carlson A-8 strain response for the 72-hour time period (April 27-29, 1998) is shown in Figure 24. Note the significant change in top versus bottom strains compared to the 72-hour period of February 28 to March 2, 1998 shown in Figure 23. The corner region near the pavement surface went into compression (negative values), whereas the middle of the slab near the pavement bottom stayed in the same strain state as at the beginning of the test. This change in strain at the corner top of the slab indicated shrinkage strains were occurring.

The measured strain in the slab was less sensitive to daily variations in temperature than to the long-term shrinkage of the slab. The difference in temperature-induced strains between 24:00 and 12:00 was approximately 20 microstrain in Figures 23 and 24. However, after two months (Figure 24), the corner top gage measured residual strains of approximately -90 microstrain. This shrinkage-induced strain corresponds to a tensile stress at the center of the slab of approximately 2.48 MPa (360 psi). This shrinkage stress is not correct because creep characteristics of the concrete were not accounted for. The overall strain fluctuations demonstrated shrinkage has to be taken into account if the slab is restrained, however creep effects must also be considered.

7.2 Dynamic Measurements

The elastic pavement responses under a 60 kN wheel load were recorded at regular intervals for the duration of the test. The results of the dynamic measurements are presented in the following sections.

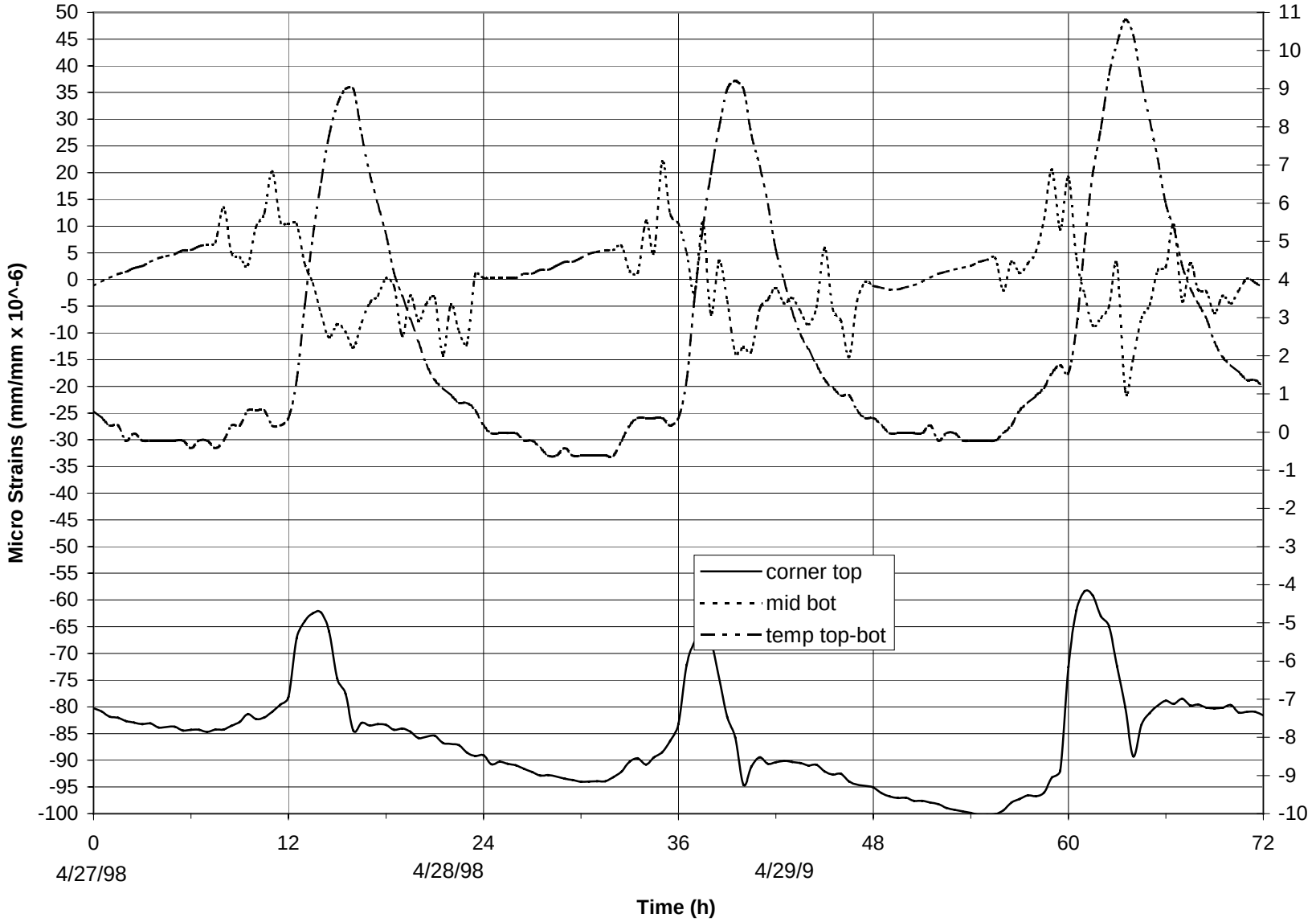

Figure 24. Carlson A-8 gage strain response for the period of April 27, 1998 to April 29, 1998.

7.2.1 Road Surface Deflectometer (RSD) results

RSD measurements were taken at five locations. RSD deflections were elastic deflections only and did not include any permanent deflections due to loss of support or microcracking. Figures 20a and 20b show the locations of each RSD measurement. All measurements were taken between the wheels. Originally, the beam of the RSD was placed parallel to the direction of travel and it was situated between the HVS wheels as had been done for flexible pavement measurement. This method was used for 325,000 load applications, after which the recording method was changed to place the beam perpendicular to the direction of travel (Figure 20). This second method was preferred because the reference feet of the RSD were off the concrete slab being trafficked, thereby eliminating any extraneous readings caused by having the reference feet on the same slab as the HVS wheel.

Figure 25 represents the RSD results from the 60 kN wheel load at all five locations. The deflections at the corner of the adjacent slabs (measuring points 1 and 5) were higher than the deflections at the corner of the middle slab. This was probably a result of the RSD reference feet not being far enough away from the wheel load influence area. The deflection at the mid-span edge (point 3) was the lowest and likely the most accurate. Deflection values ranged from 250 to 750 microns at the beginning of the test, to between 800 and 1550 microns after 325,000 repetitions.

Given that the deflections of a concrete slab are very dependent on the temperature differential through the slab thickness, the responses should be presented with the temperature at the time the deflection measurements were taken. This is shown in Figure 26, where air temperature (right hand axis) is plotted together with the

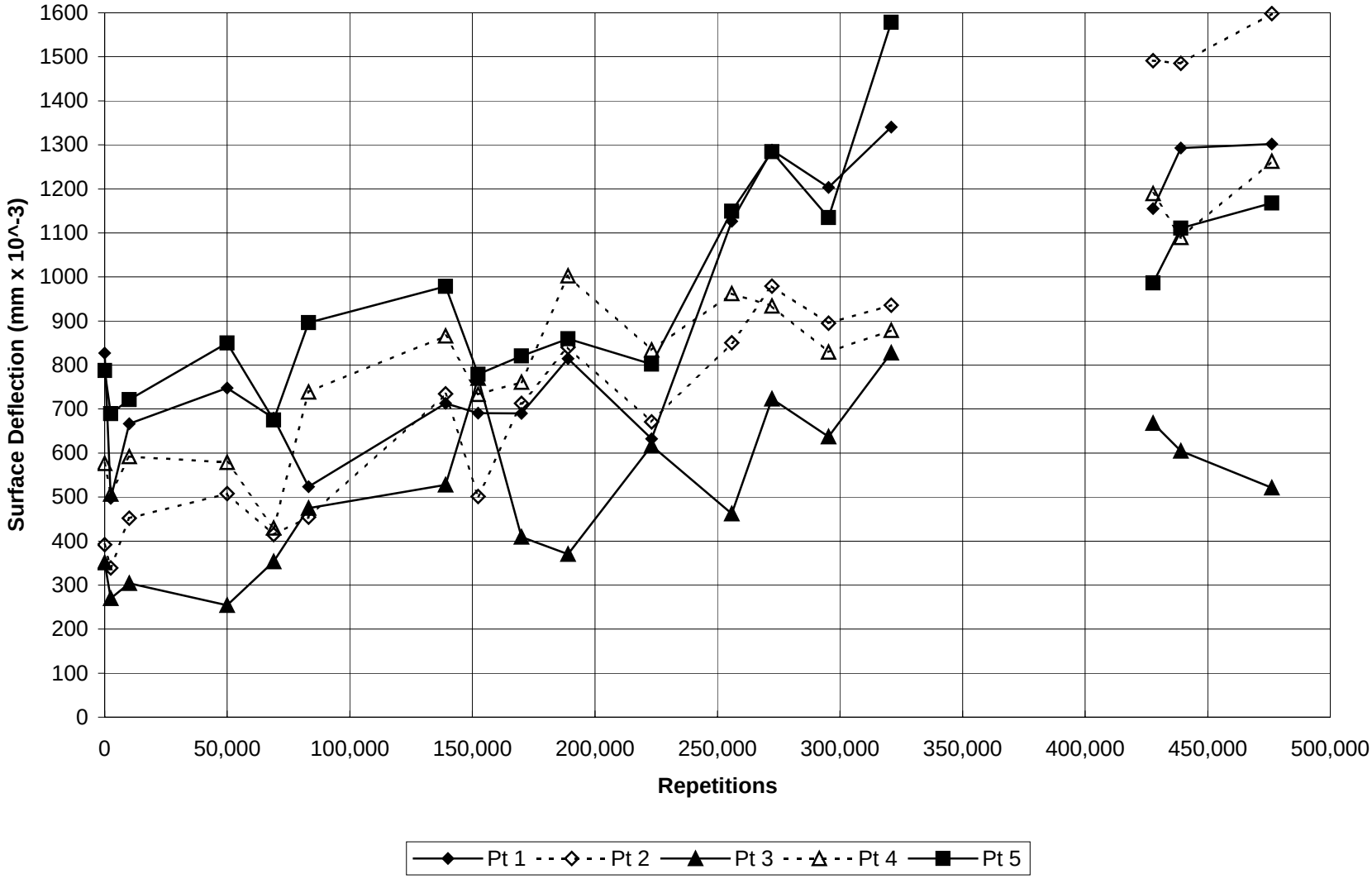

Figure 25. RSD results from 60kN wheel load at all five RSD measurement locations.

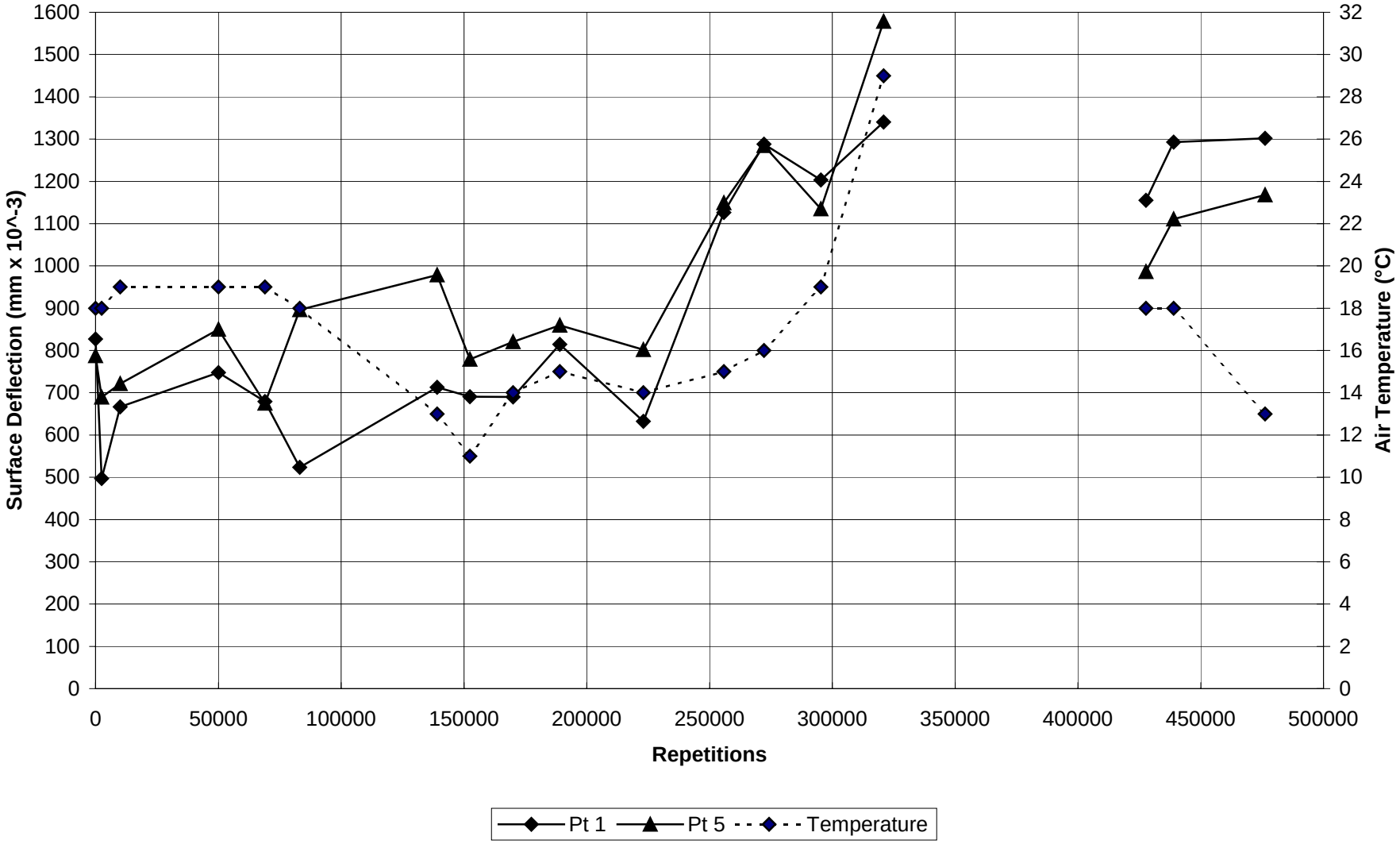

Figure 26. RSD deflections for Points 1 and 5 plotted with temperature.

deflections at points 1 and 5 for the same period.

At 350,000 load applications, the method of recording RSD measurements was changed as explained in section 3.1.2.6. The results of new RSD measurements can be seen in Figures 25 and 26. The new readings were taken at 427,709; 439,022; and 476,207 load applications. The new RSD methodology did not have enough points to draw any conclusions.

7.2.2 Dynamic strain gage results

Four strain gages were embedded in the concrete slab at various locations. Two Dynatest strain gages were placed 38 mm from the bottom of the slab while two Tokyo Sokki gages were placed 38 mm from the top of the slab. One of each gage was placed near a joint and one of each gage was placed near the slab edge. For the exact gage placement, see Figure 14.

To simplify the reporting of results, the strain gages were numbered as indicated in Table 12 (the numbers correspond to the data acquisition channel number).

All dynamic strain data are graphically presented in Figures 27 to 34. Two strain readings are presented from each strain sensor: the maximum tensile strain (positive) and the maximum compressive strain (negative). These strains were measured while the HVS wheel load (60 kN) was moving along the slab edge. Because strain gages are affected by temperature, the air temperature at time of data collection was included in all graphs and should be read from the vertical right hand axis. All dynamic strains were elastic strains and the strain results did not include the effects of permanent strain.

Table 12 Numbering System For Strain Gages.

Number	Gage	Location	Orientation

Dynatest 2	Dynatest PAST-2PCC	Bottom of pavement near middle slab edge		Parallel to travel
Dynatest 15	Dynatest PAST-2PCC	Bottom of pavement near adjacent slab joint		Parallel to travel
PMR 12 Black	Tokyo Sokki PMR-60-6L	Top of pavement near middle slab edge	Arm 1 of rosette	Parallel to travel
PMR 12 Blue			Arm 2 of rosette	45° to travel
PMR 12 Red			Arm 3 of rosette	Perpendicular to travel
PMR 25 Black	Tokyo Sokki PMR-60-6L	Top of pavement near adjacent slab joint:	Arm 1 of rosette	Parallel to travel
PMR 25 Blue			Arm 2 of rosette	45° to travel
PMR 25 Red			Arm 3 of rosette	Perpendicular to travel

Figure 27 shows the maximum tensile strain at the middle slab edge was approximately 35 microstrain throughout the test. The maximum tensile strain was measured 38 mm from the bottom of the slab, and so the actual maximum tensile strain was probably 60 percent higher or 56 microstrain (strain extrapolation to the bottom of the slab). The minimum distance between all gages and any interface was equivalent to the maximum size aggregate (38 mm). Figure 28 shows a similar trend to Figure 27, but the signs are reversed because the gage was located near the top surface of the slab. Figures 29 and 30 show the strain gages located perpendicular to the edge and at a 45-degree angle to the edge. Both gages have a lower strain level because the maximum bending strain for this loading position is parallel to the edge.

At approximately 440,000 repetitions, the maximum compressive strain began to decrease, as shown in Figure 30. At this time, a corner crack began forming near the

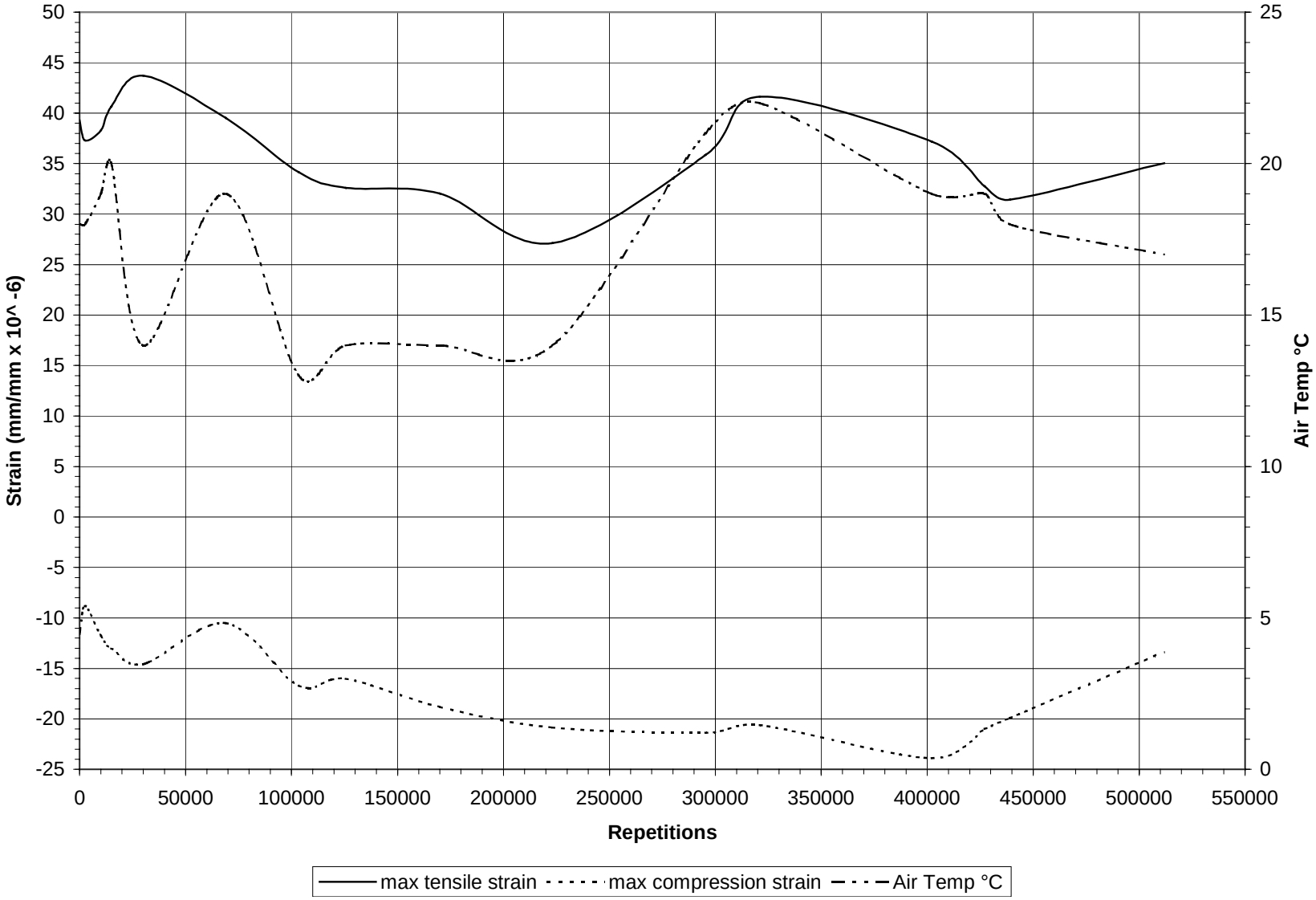

Figure 27. Dynamic strain data from Section 516CT under 60kN load. Dynatest PAST-2PCC strain gage located at the bottom of the pavement near the middle slab edge, oriented parallel to slab edge.

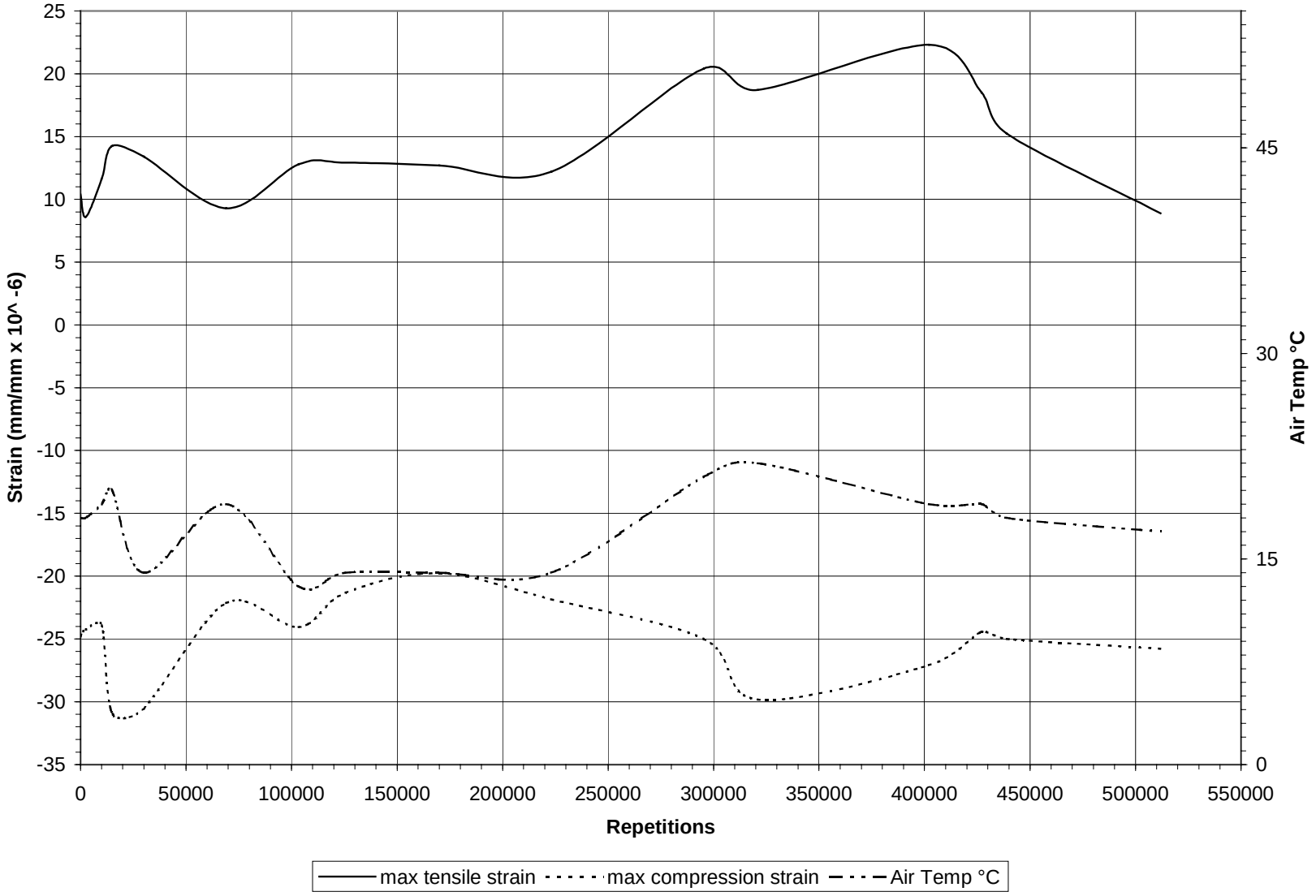

Figure 28. Dynamic strain data from Section 516CT under 60kN load. Tokyo Sokki PMR-60-6L strain gage located near the surface of the pavement near the middle slab edge, oriented parallel to slab edge.

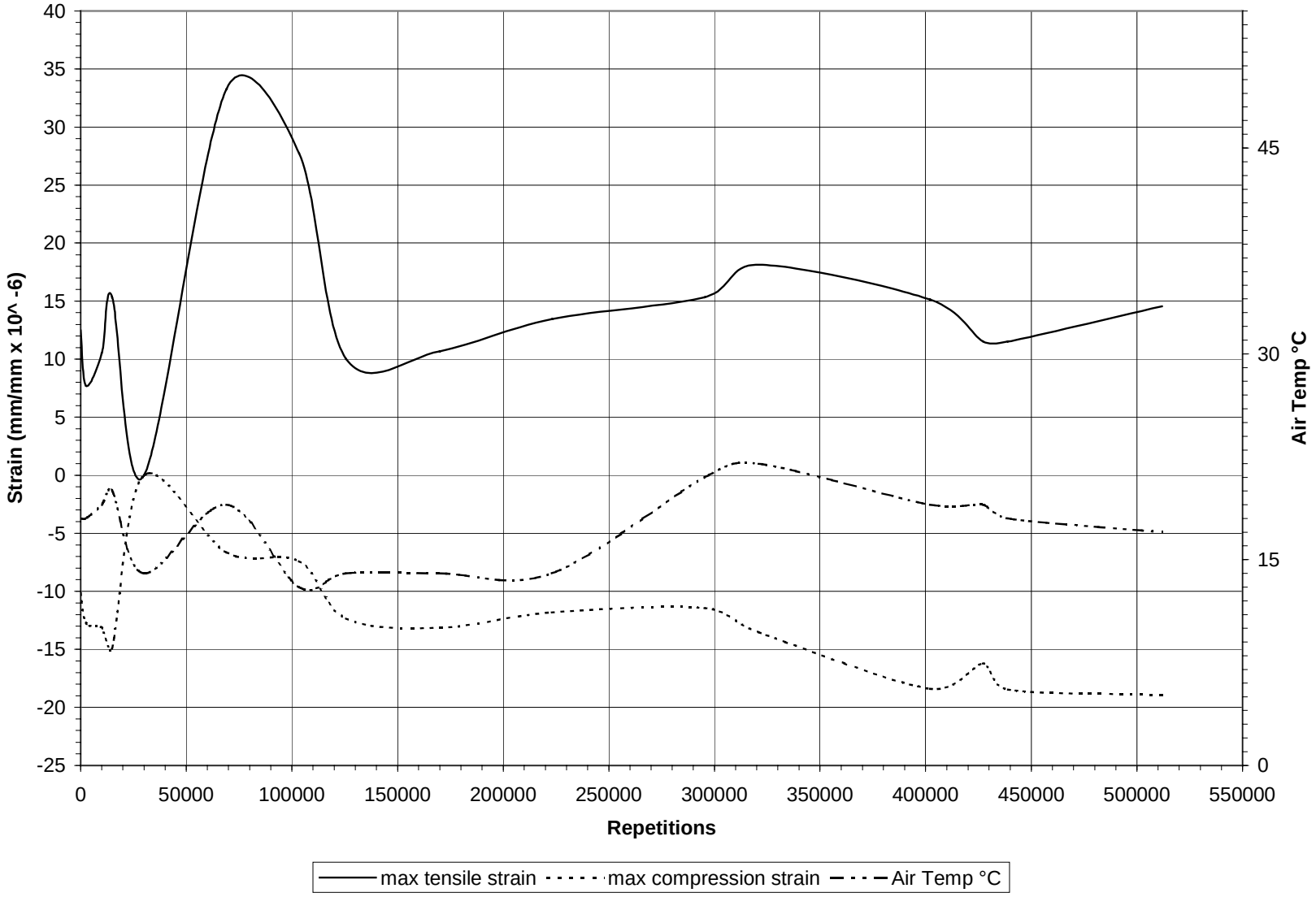

Figure 29. Dynamic strain data from Section 516CT under 60kN load. Tokyo Sokki PMR-60-6L strain sage located near the surface of the pavement, near the middle slab edge, oriented perpendicular to slab edge.

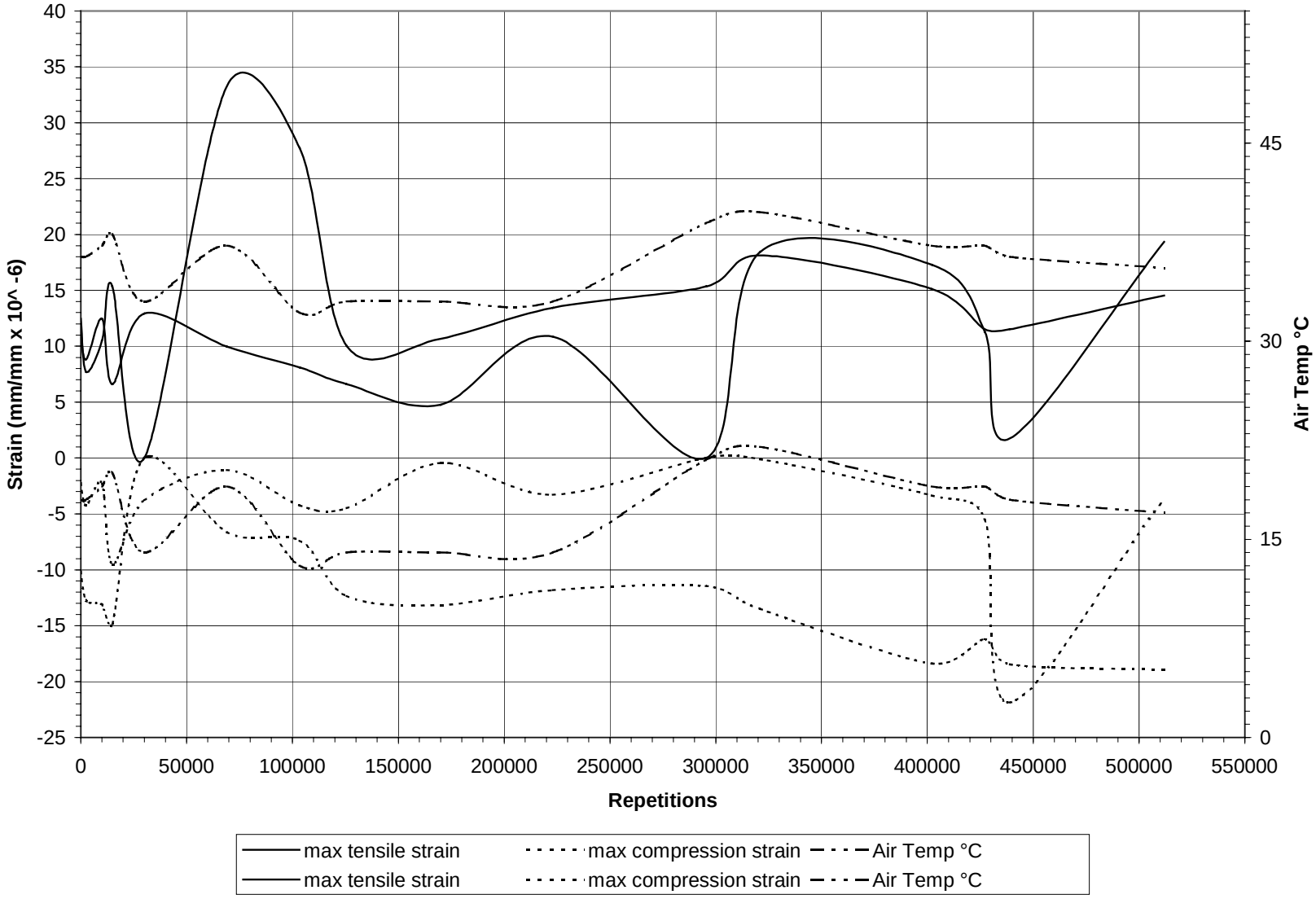

Figure 30. Dynamic strain data from Section 516CT under 60kN load. Strain gage located near the surface of the pavement, near the middle slab edge, oriented at +45-degree angle to slab edge.

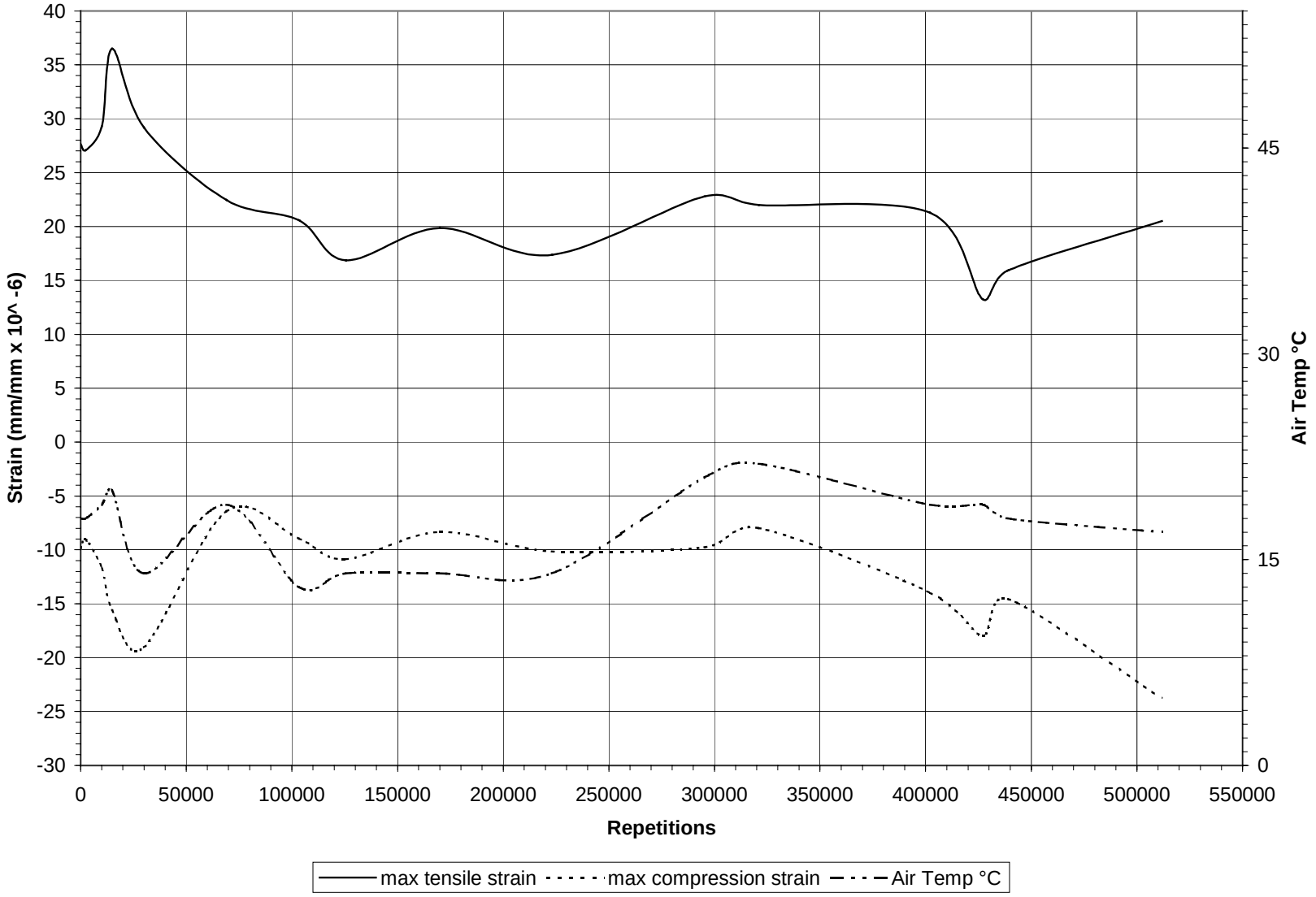

Figure 31. Dynamic strain data from Section 516CT under 60kN load. Dynatest PAST-2PCC strain gage located near the bottom of the pavement, 0.3 m from Joint 1, oriented parallel to slab edge.

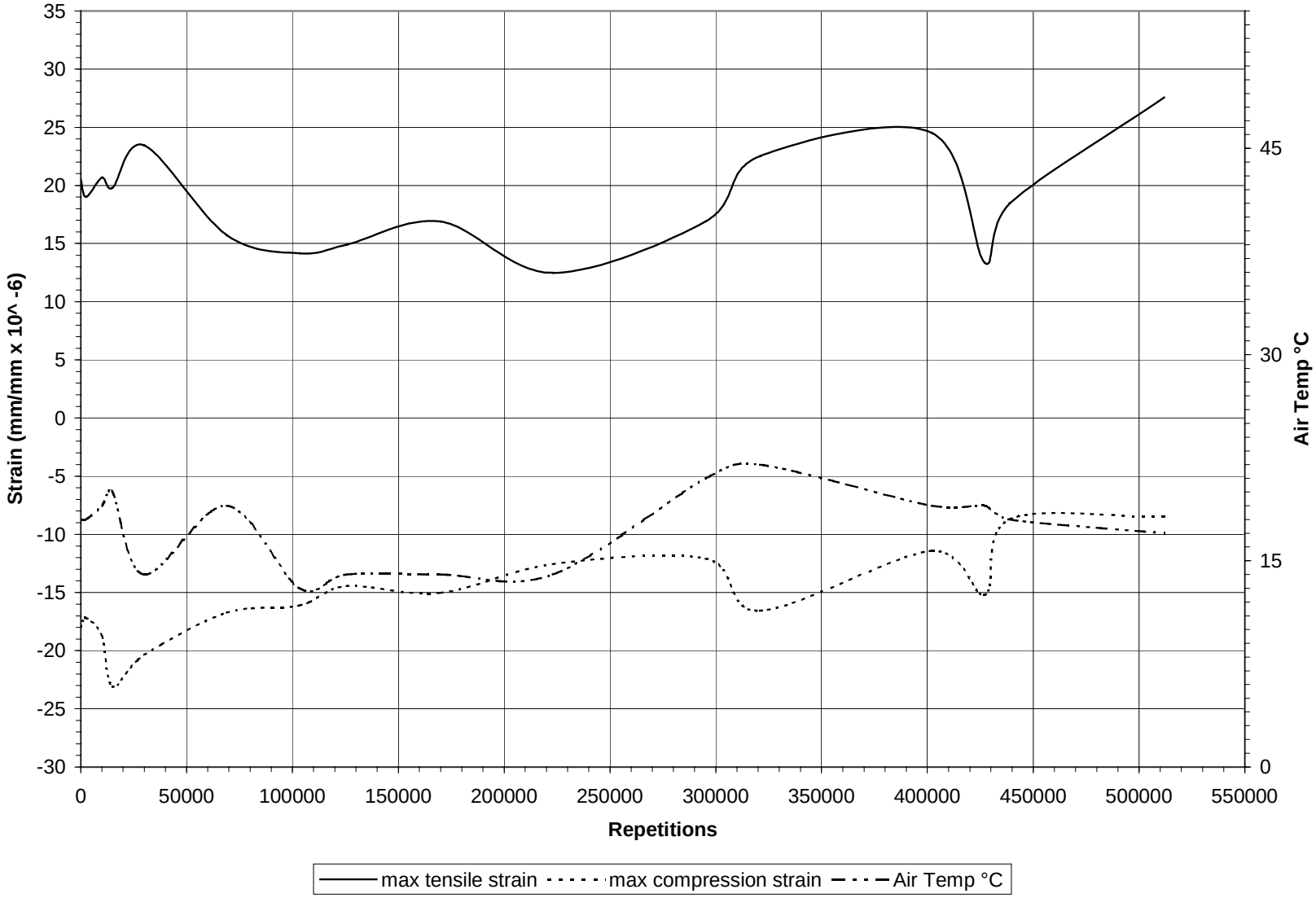

Figure 32. Dynamic strain data from Section 516CT under 60kN load. PMR-60-6L strain gage located near the surface of the pavement, 0.3 m from Joint 1, oriented parallel to slab edge.

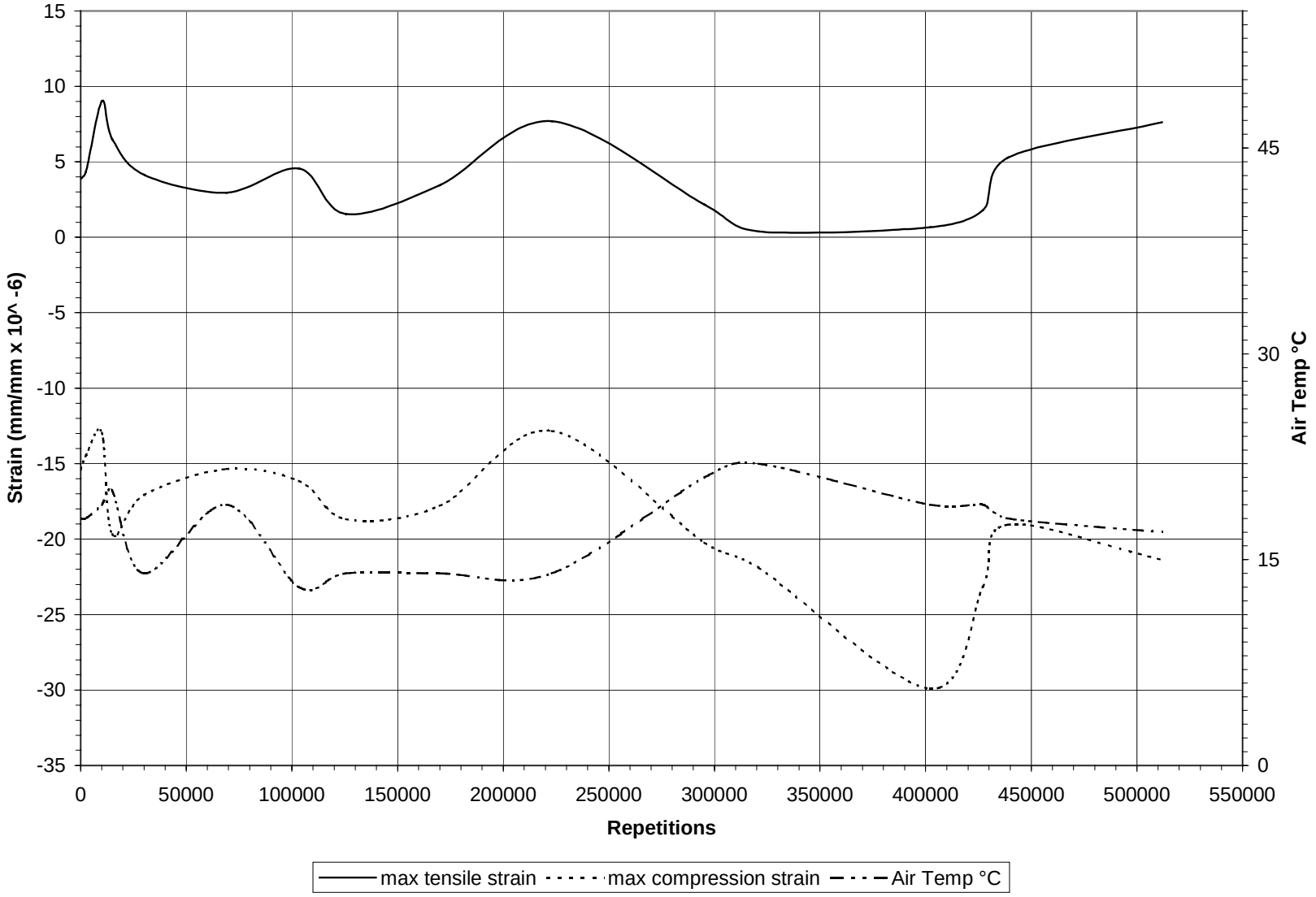

Figure 33. Dynamic strain data from Section 516CT under 60kN load. Strain gage located near the surface of the pavement, 0.3 m from Joint 1, oriented at +45-degree angle to slab edge.

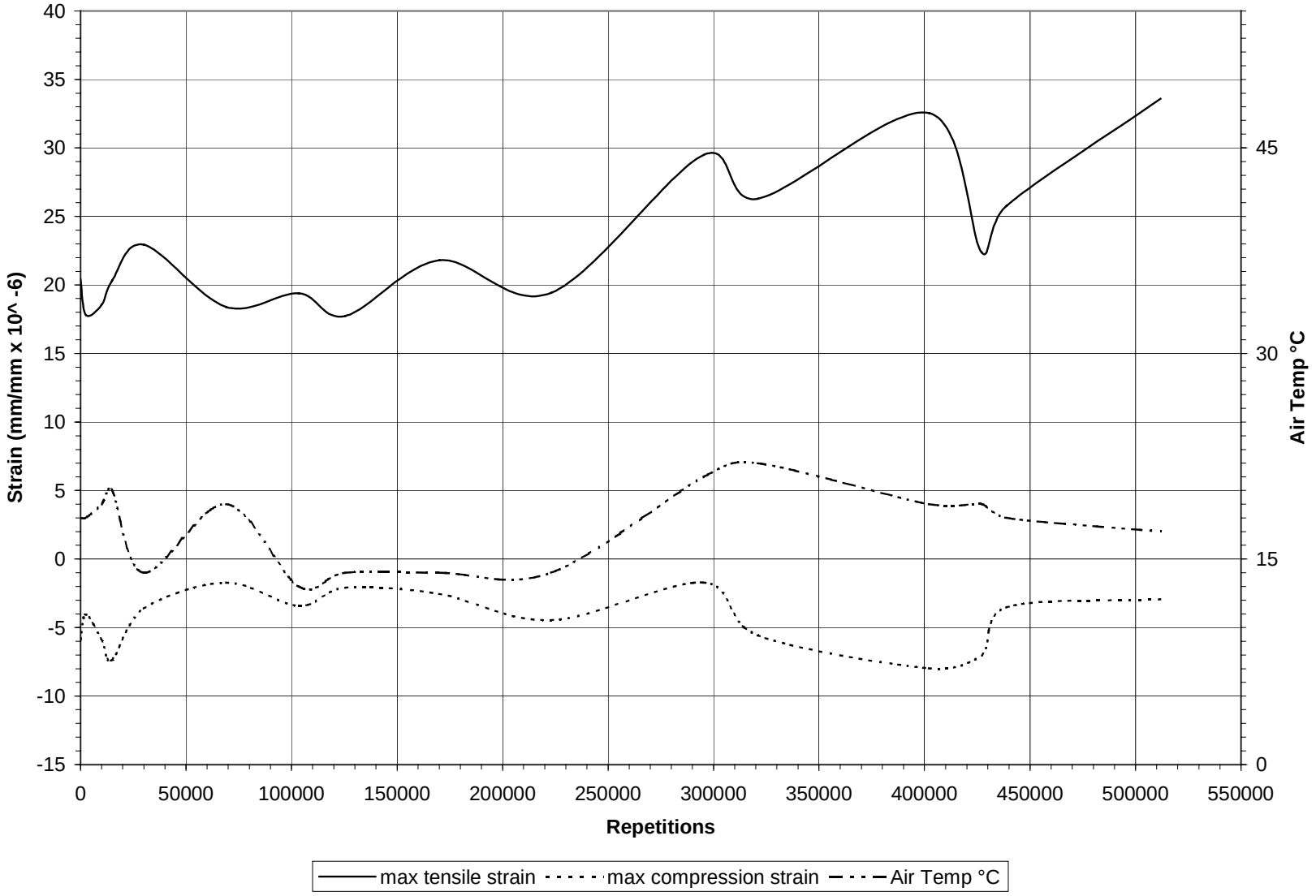

Figure 34. Dynamic strain data from Section 516CT under 60kN load. Strain gage located near the surface of the pavement, 0.3 m from Joint 1, oriented at -45-degree angle to slab edge.

middle slab gage, which explains why the compressive strain decreased and the tensile strain increased. The majority of the slab in this area was now acting like a cantilever.

Figure 31 shows the strain versus time for the bottom gage located 0.3 m from Joint 1 (see Figure 14). The strains were not high because the gage was placed perpendicular to the joint, close to the joint. At this gage location, the strain parallel to the joint is more critical. Figures 32 shows strain values for the PMR gage oriented parallel to the slab edge, and Figures 33 and 34 shows the strain value for the PMR gage oriented at ±45 degrees from the joint.

7.2.3 Crack Activity Meter results

CAM measurements were used for two purposes:

- to measure the joint movement between the middle slab and the two adjacent slabs, and
- to measure activity of any cracks that developed as a result of loading.

Figure 35 shows the locations for the CAM. At the beginning of the test, little movement between joints was detected because aggregate interlock provided shear transfer across the joint. After 430,000 repetitions, a corner crack developed in the middle slab from one of the joints as shown in Figure 35. CAM measurements were taken on either side of the crack. The CAM measures the relative vertical and horizontal movement between two slabs. If the crack face has 100 percent deflection transfer, then the vertical CAM reads zero. Likewise if the crack does not open or close, then the horizontal CAM measurement reads zero.

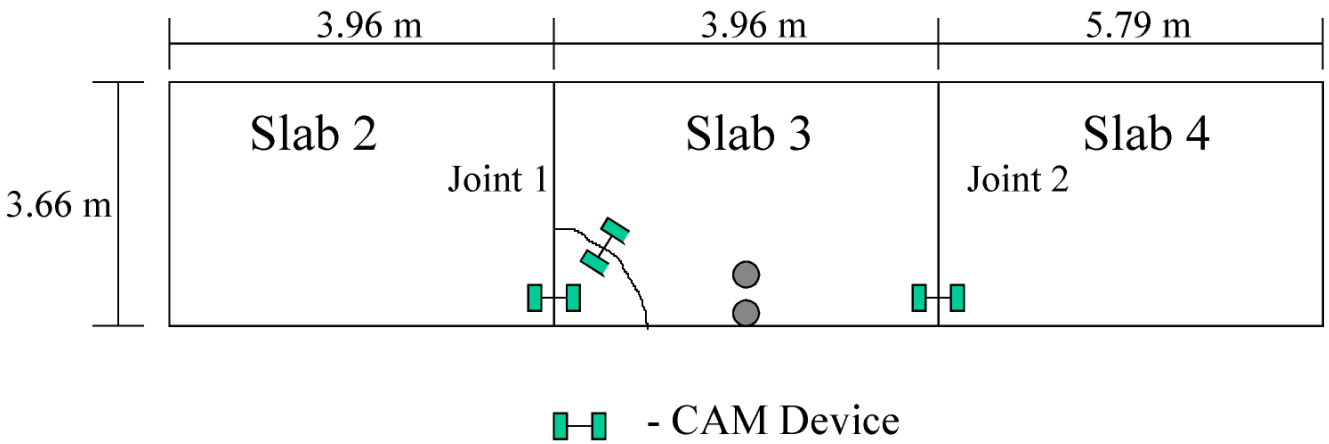

Figure 35. Location and orientation of CAM device and corner crack on Section 516CT.

The sign conventions of CAM movement with respect to Figure 35 is as follows:

- vertical positive movements are when the left hand side of a joint/crack is moving up relative to the right hand side and negative when the left hand side of a joint/crack is moving down relative to the right hand side
- horizontal positive movement indicates that the gap created by the crack is closing; horizontal negative movement indicates that the gap created by the crack is opening.

In this report, the CAM movements at both sawed joints (Figure 35) are presented after 427,709 HVS repetitions. The joint movement of the left-hand joint (Joint 1) can be seen in Figure 36 and the right hand joint (Joint 2) in Figure 37, respectively. On both graphs, the horizontal as well as the vertical movement can be seen. The average maximum positive and negative CAM movement after 427,709 load applications can be seen in Table 13

Table 13 CAM Measurements Across the Concrete Slab Joints.

	Vertical movement ($m \times 10^{-6}$)		**Horizontal movement ($m \times 10^{-6}$)**	
	Positive	Negative	Closing	Opening
Joint 1 (left slab)	815	652	282	7
Joint 2 (right slab)	517	958	197	43

Table 13 demonstrates the movement at the joints is not symmetric, especially at Joint 2. Given the vertical CAM movements were not symmetric, one could conclude that one side of the joint received more load as the wheel moved across it. Therefore the load transferred across the joint was different depending on the direction the test wheel was traveling. The vertical CAM movements can be used to estimate the load transfer

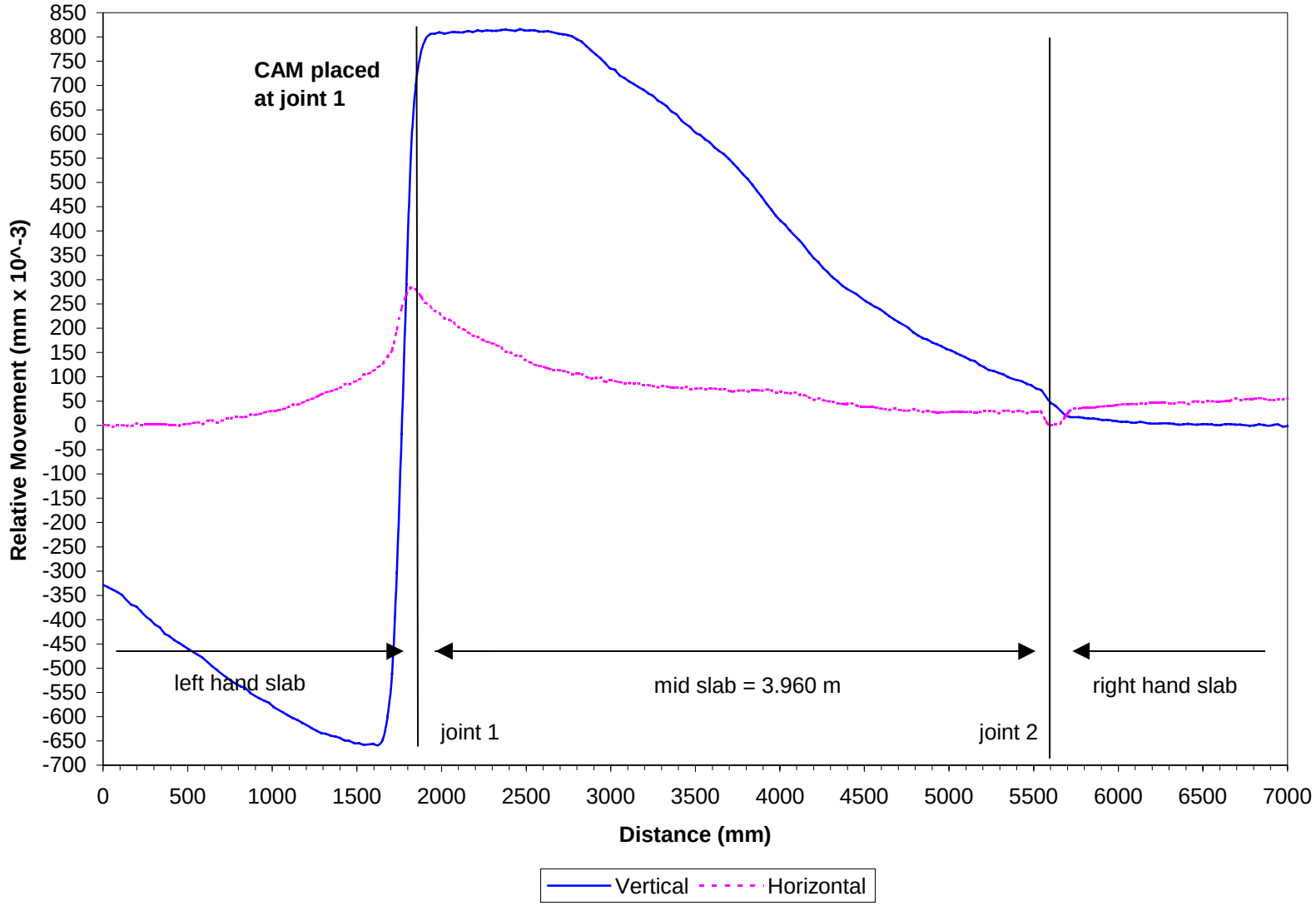

Figure 36. CAM response at Joint 1 After 427,709 load repetitions.

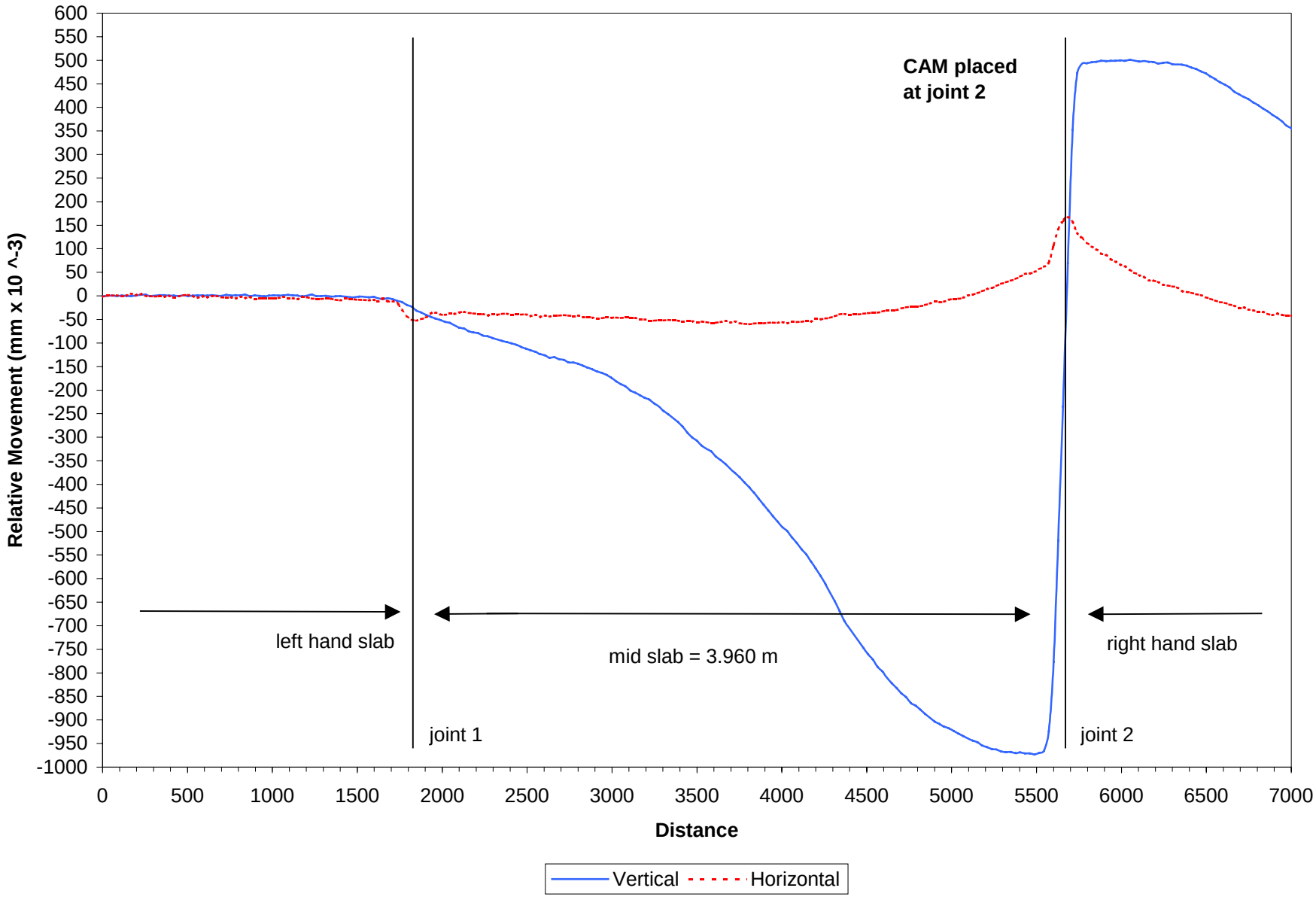

Figure 37. CAM response at Joint 2 After 427,709 load repetitions.

across the joints, as is explained in greater detail in Section 7.4.

The CAM was also utilized to investigate the activity of the first visual crack. The first crack appeared at Joint 1 after 430,000 load applications about 1 m from the edge. The crack was in the middle slab and grew towards the edge to form a classic corner crack. CAM measurements were taken across this crack at 439,022; 476,207; and 511,719 load applications. The CAM data for the crack can be seen in Figures 38 and 39 for the horizontal and vertical movement, respectively.

As the crack grew in length (see Figures 40a and 40b), the horizontal movement increased as displayed in Figure 38. The vertical crack movement also increased, but to a lesser degree than the horizontal, as shown in Figure 39. The most probable reason for the horizontal movement being greater than the vertical was the cantilever effect and the CAM location. The CAM location, shown in Figure 35, was the point where the crack face tended to open horizontally and rotate rather than move vertically relative to the HVS wheel position. If the CAM were placed across the crack directly beneath the test wheel, then the vertical movement would likely have been greater than the horizontal.

7.3 Thermocouple Temperature Results

Thermocouple data was collected every 30 minutes, 24 hours per day for the duration of the HVS test. Each thermocouple location had five sensors recording temperature at the surface, and 50 mm, 100 mm, 150 mm, and 200mm from the surface of the pavement. For the exact location of the four sets of thermocouples, see Figure 14.

An example of the raw data is presented in Figure 41. The figure shows daily

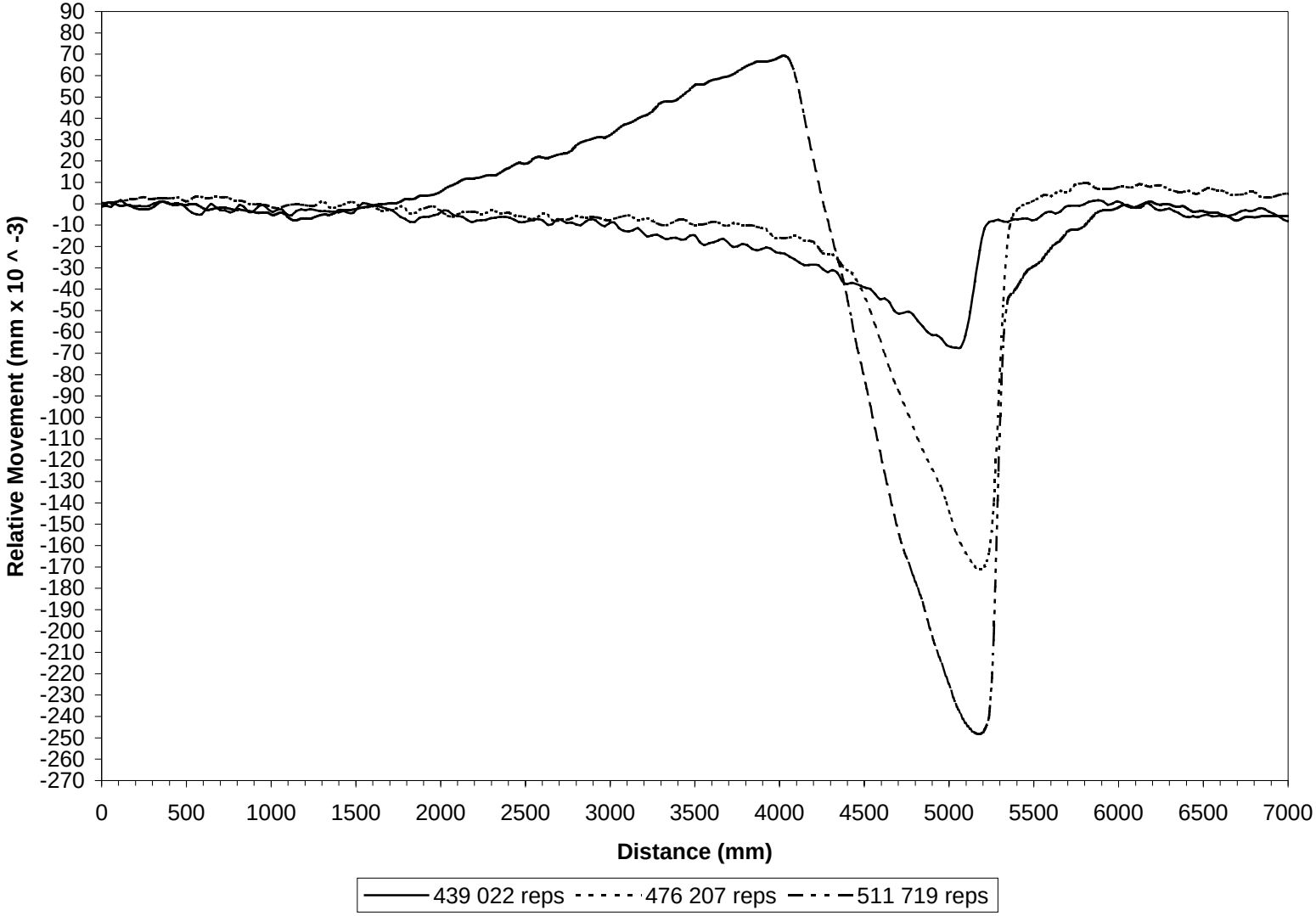

Figure 38. CAM horizontal response at first visually detected crack on Section 516CT.

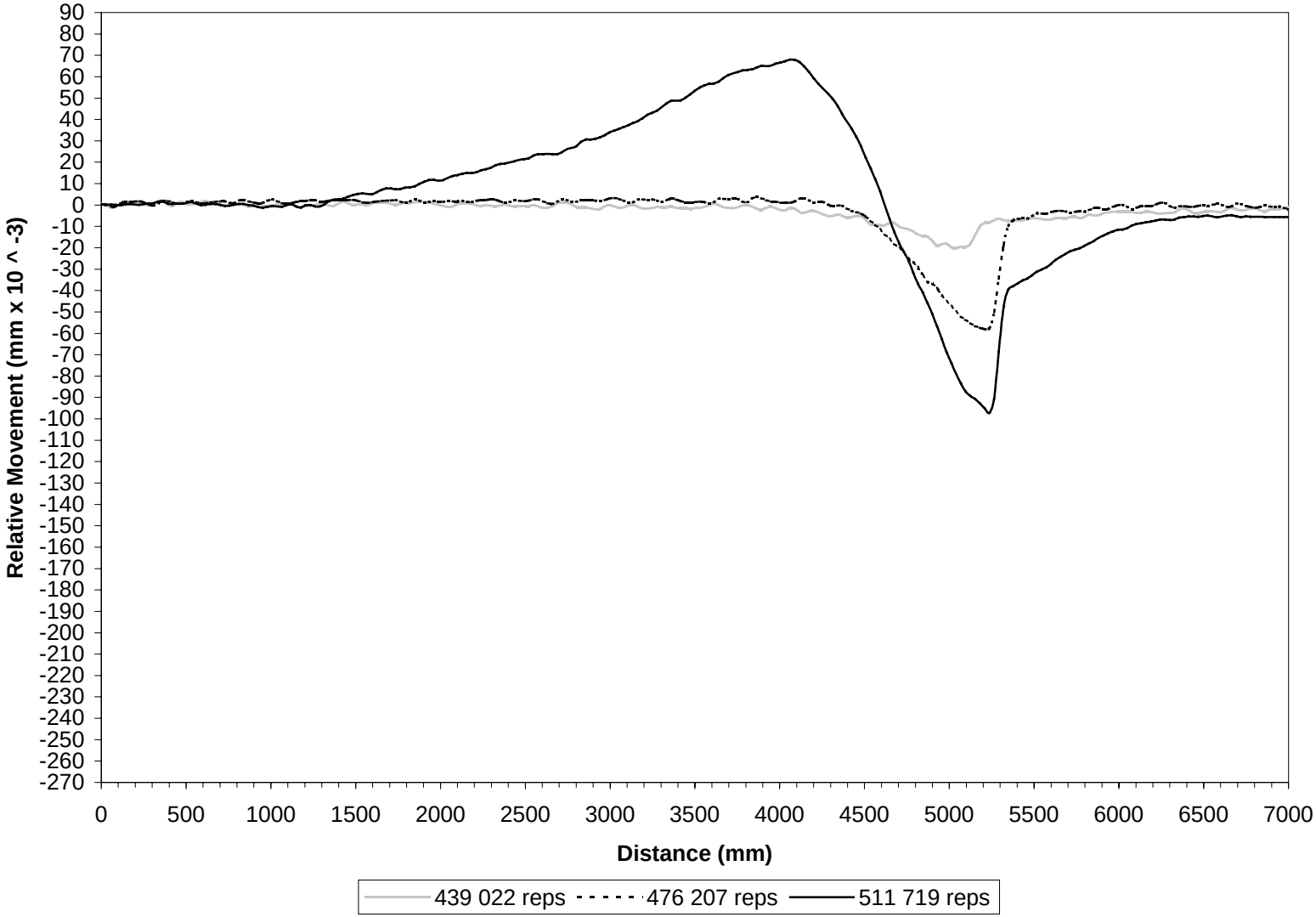

Figure 39. CAM vertical response at first visually detected crack on Section 516CT.

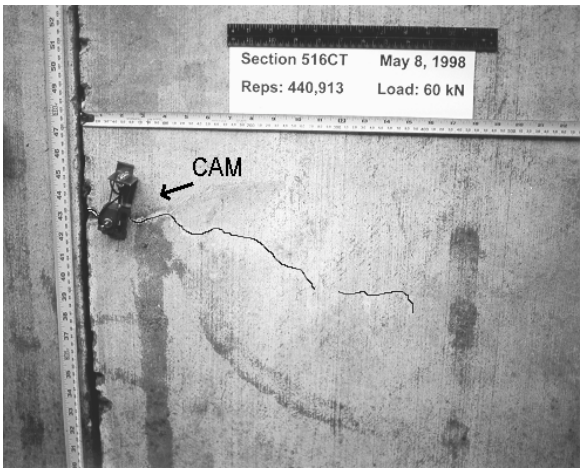

Figure 40a. Crack growth on 516CT at 440,913 repetitions. (Crack line has been enhanced for easier viewing.)

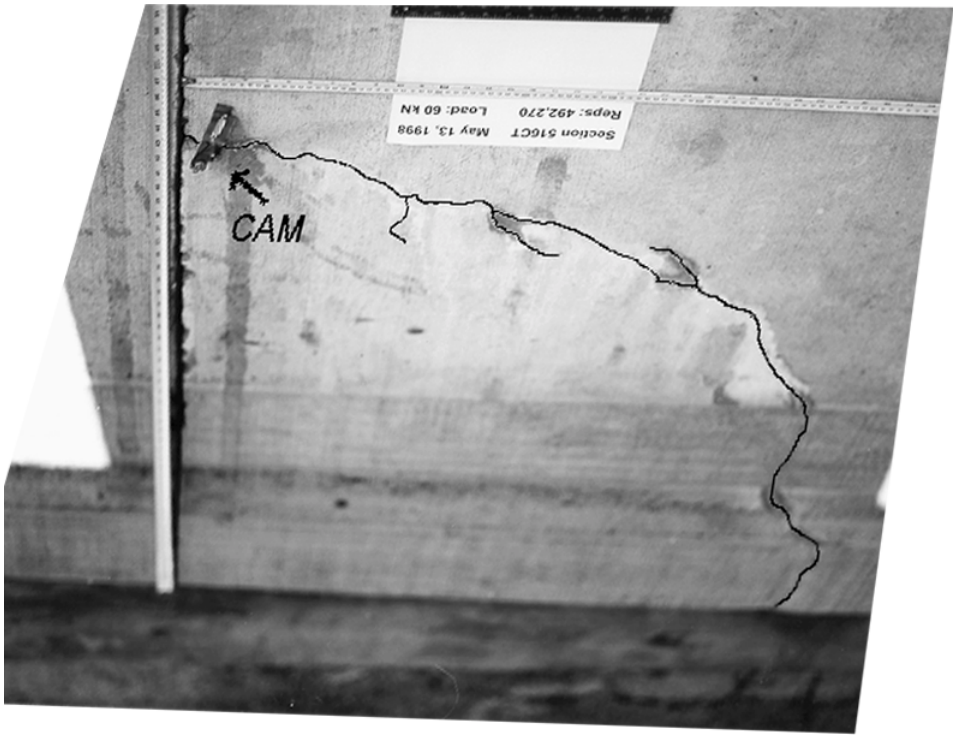

Figure 40b. Crack growth on 516CT at 492,270 repetitions. (Crack line has been enhanced for easier viewing; image has been skewed to remove camera perspective and show relationship to Figure 40a.)

temperature fluctuation of Thermocouple #4 for the 72-hour period of February 28 to March 2, 1998. From this data, various types of analysis are possible, of which the following are important:

- the maximum and minimum pavement temperature,
- the temperature gradient through the slab thickness, and
- the temperature frequency distribution during HVS testing.

The temperature gradient in the slab fluctuated between the day and night causing curling. During the day, the upper part of the pavement was hotter than the lower part, causing the pavement to curl downwards. This process was reversed at night when the lower part of the pavement was hotter than the top, and the pavement curled upward. Figure 42 presents the difference between the top and bottom temperature measurements for all four thermocouples. The time period is similar to that shown in Figure 41 (March 28 to April 2, 1998), and the graph shows the bottom (at 200 mm in-depth) subtracted from the surface temperature. Positive values indicate a positive gradient (hotter at the surface than at 200 mm in-depth) while negative values indicate a negative gradient. The largest positive gradients occurred in the middle of the day, the largest negative gradients occurred at 6 a.m.

Figures 43 and 44 show the maximum positive and negative temperature gradient recorded during HVS testing. Figure 43 shows the maximum positive temperature gradient was nonlinear and depended on the location of the thermocouple. This maximum occurred on April 4, 1998 at 14:00. Similarly, Figure 44 shows the maximum negative temperature gradient, which occurred on March 27, 1998 at 3:00 a.m. The

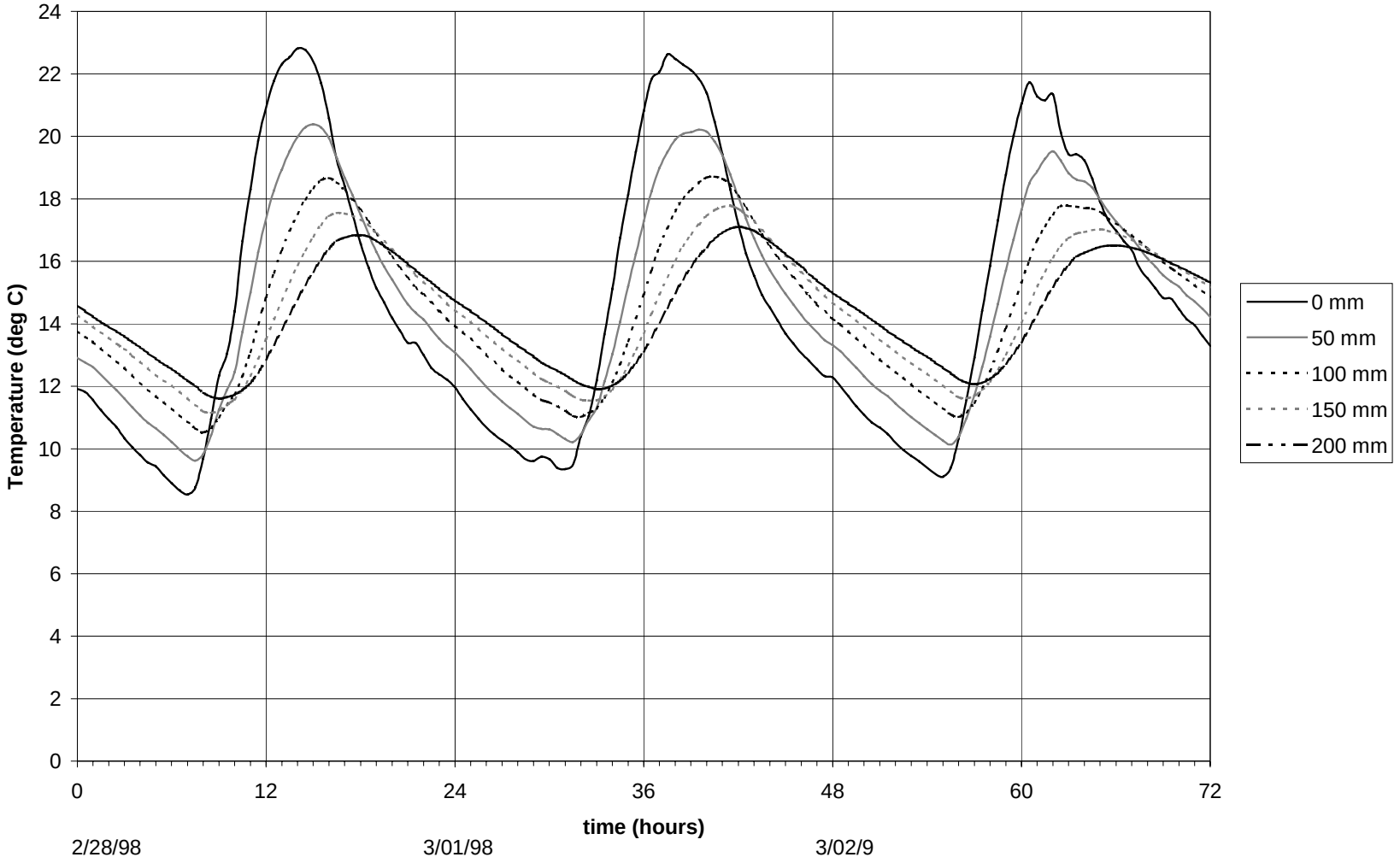

Figure 41. Raw thermocouple data from Thermocouple #4 for the 72-hour period of February 28, 1998 to March 2, 1998.

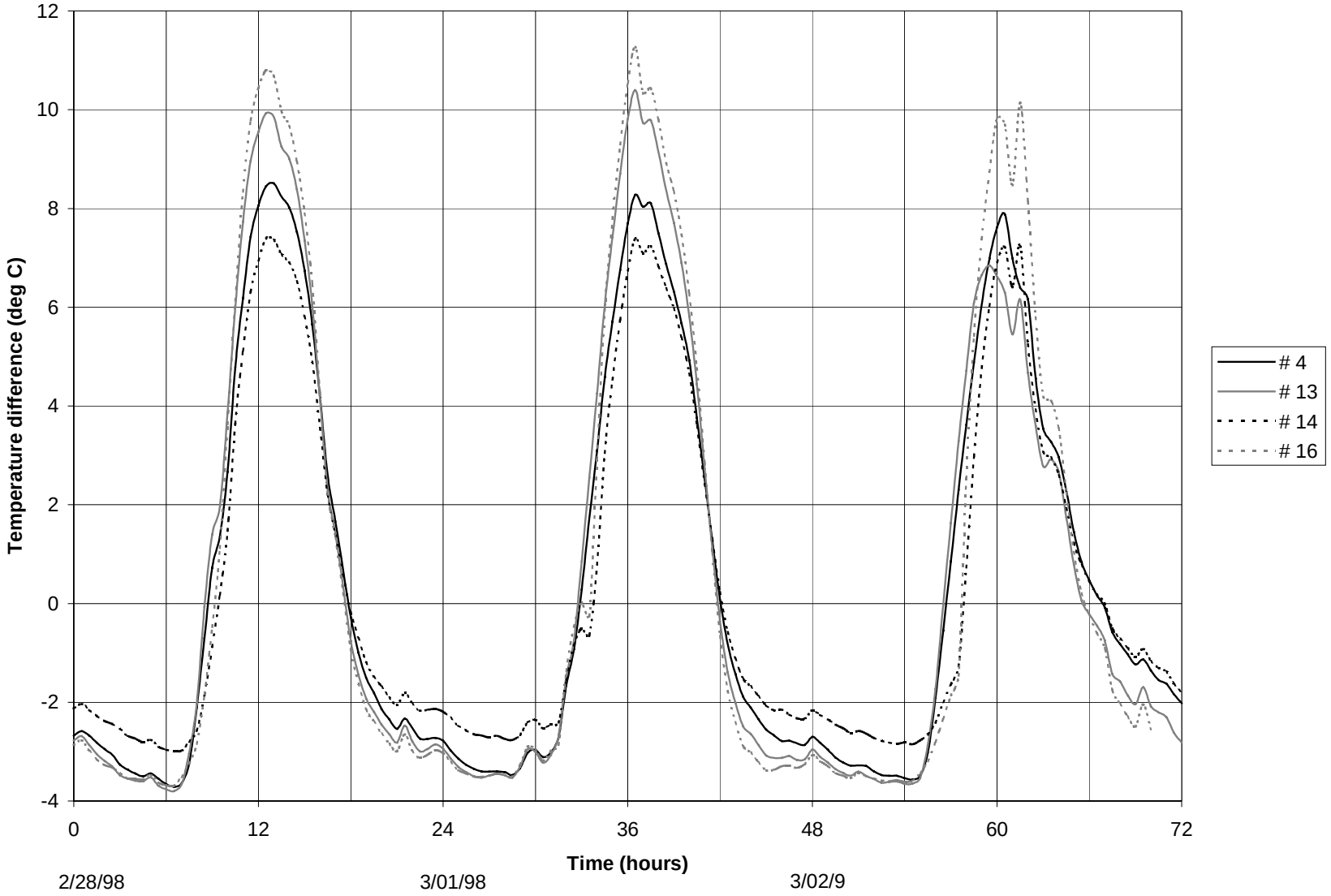

Figure 42. Chart of the difference between the top and bottom temperature measurement for all four thermocouples on Section 516CT.

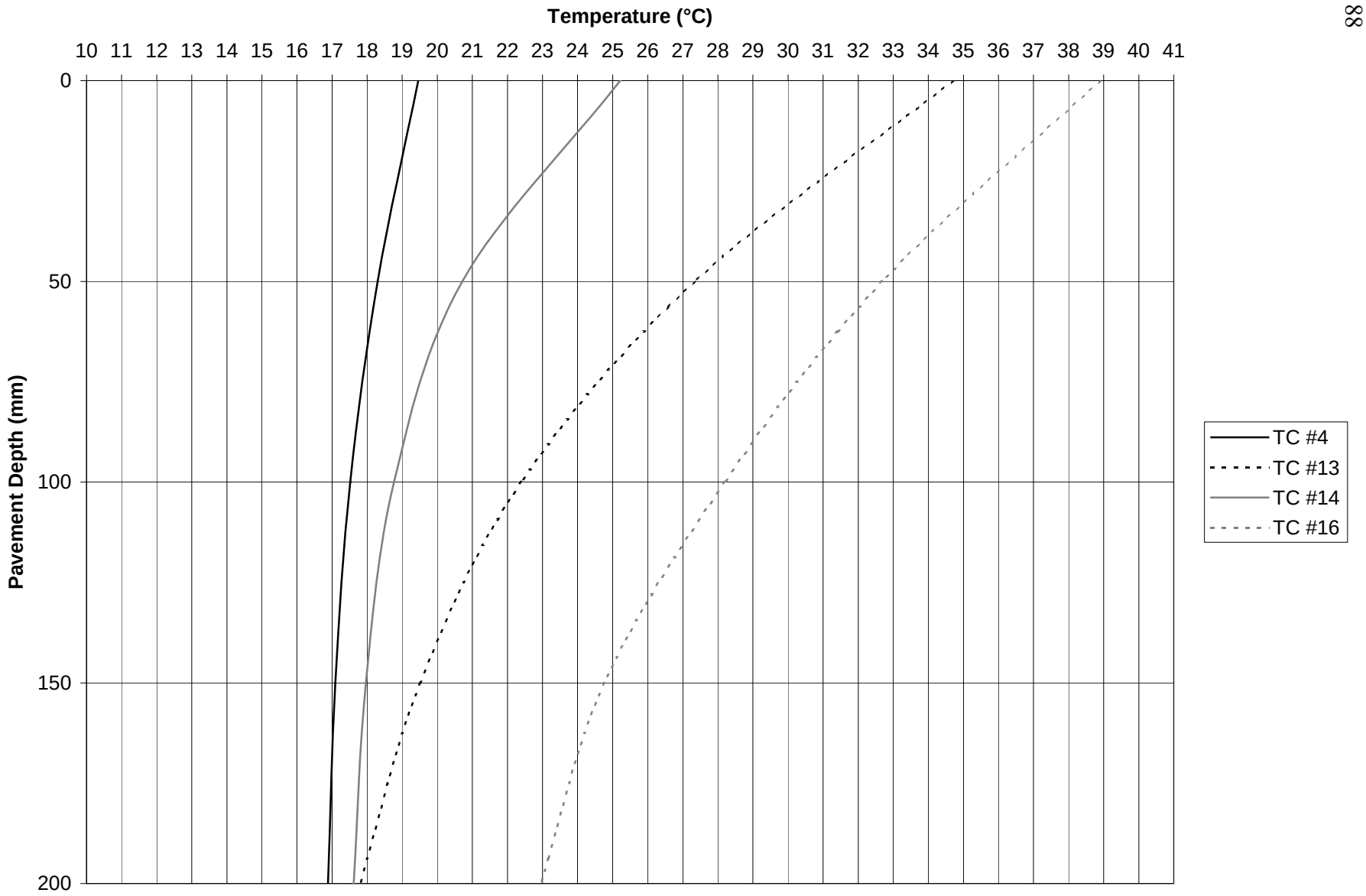

Figure 43. Maximum positive temperature gradient recorded during HVS testing on Section 516CT.

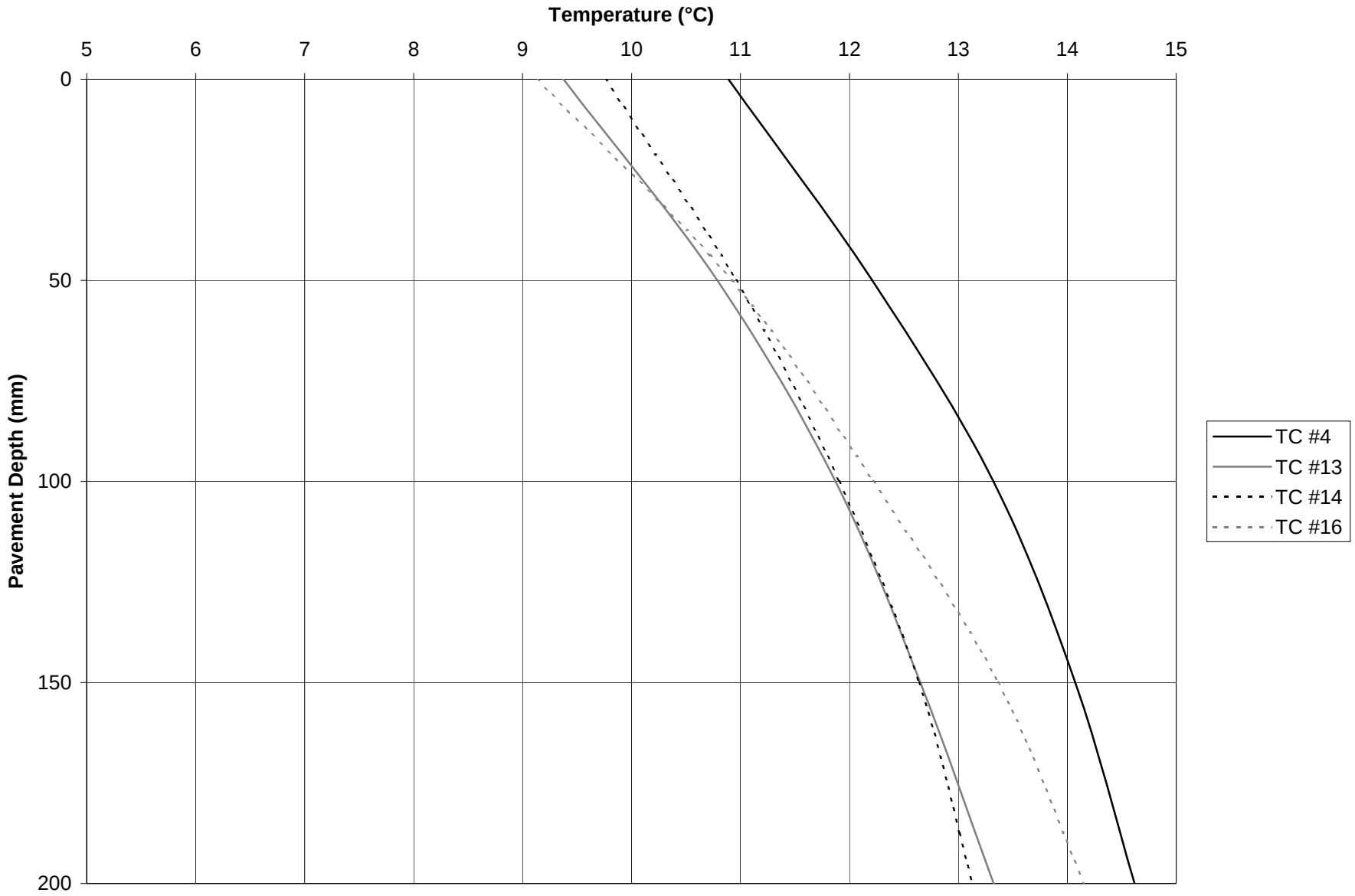

Figure 44. Maximum negative temperature gradient recorded during HVS testing on Section 516CT.

maximum negative temperature gradient in the slab was also nonlinear but was not as dependent on location of the measurement. The maximum positive and negative temperature differentials in the pavement for the days shown in Figures 43 and 44 is summarized in Table 14.

Table 14 Maximum Positive and Negative Temperature Differentials between the Slab Surface and Bottom.

Thermocouple Number	Temperature difference between surface and bottom (°C)	
	Positive Gradient(at 14:00)	Negative Gradient(at 3:00)
Thermocouple 4	2.6	-3.7
Thermocouple 13	16.9	-3.9
Thermocouple 14	7.6	-3.4
Thermocouple 16	16.0	-5.0

The influence the shade of the HVS had on the daytime pavement temperatures is clearly visible from Figures 43 and 44 and Table 14. Thermocouples 4 and 14 were shaded by the HVS during the hottest time of day (11:00 - 15:00), and thus a small temperature differential between the surface and the bottom were observed at these locations. In contrast, Thermocouples 13 and 16 were not shaded by the HVS and had significant temperature differences between the slab surface and bottom. During the night, the shade of the HVS played no role and subsequently the measured temperature differences were similar among all thermocouples.

The last method of presenting temperature data is the frequency distribution of the concrete pavement temperature differential, shown in Figure 45, and the cumulative frequency distribution, shown in Figure 46. Over 3,000 temperature readings were used to create the temperature differential distribution figures.

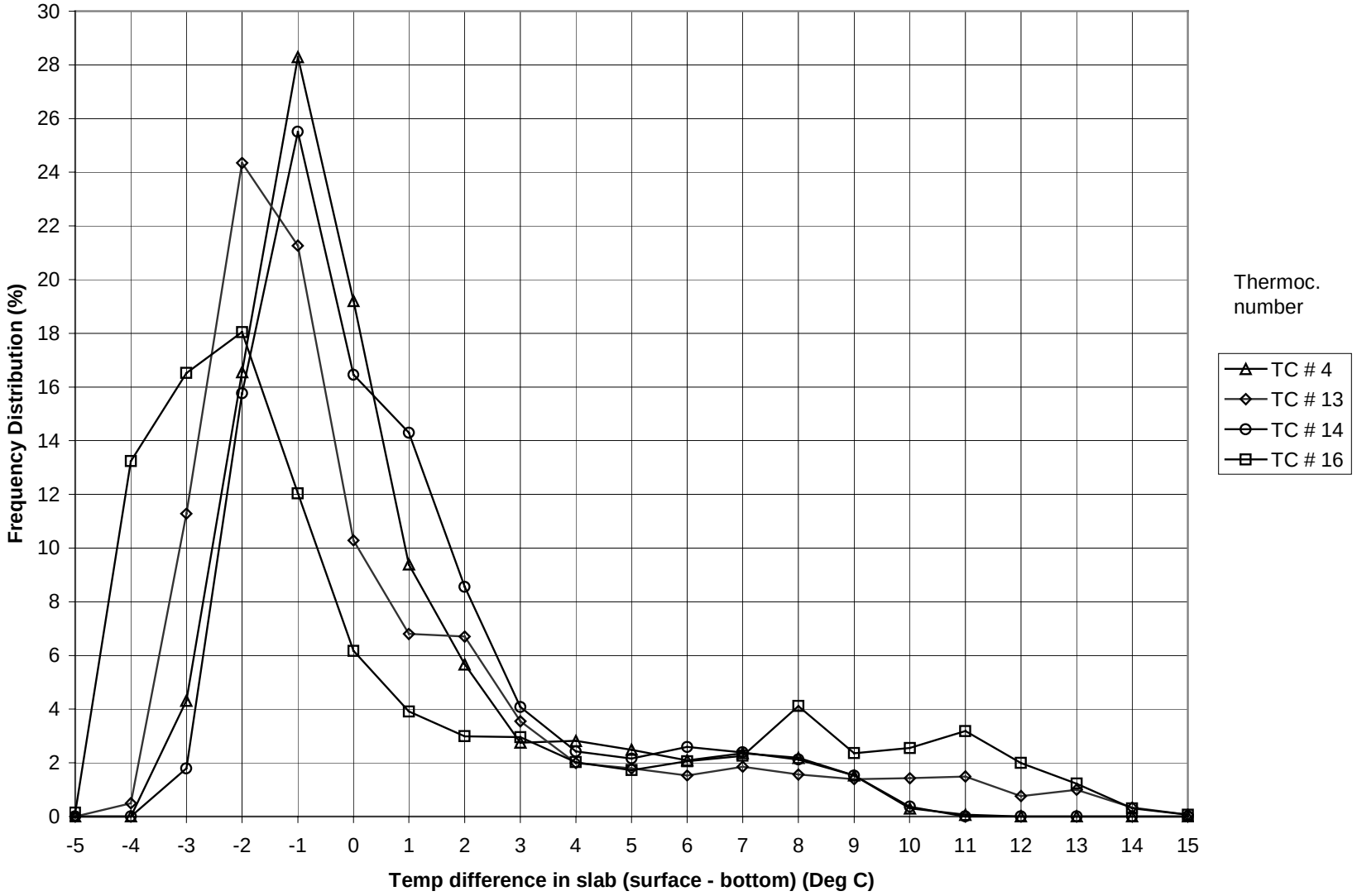

Figure 45. Frequency distribution of the concrete pavement temperature differential in Section 516CT.

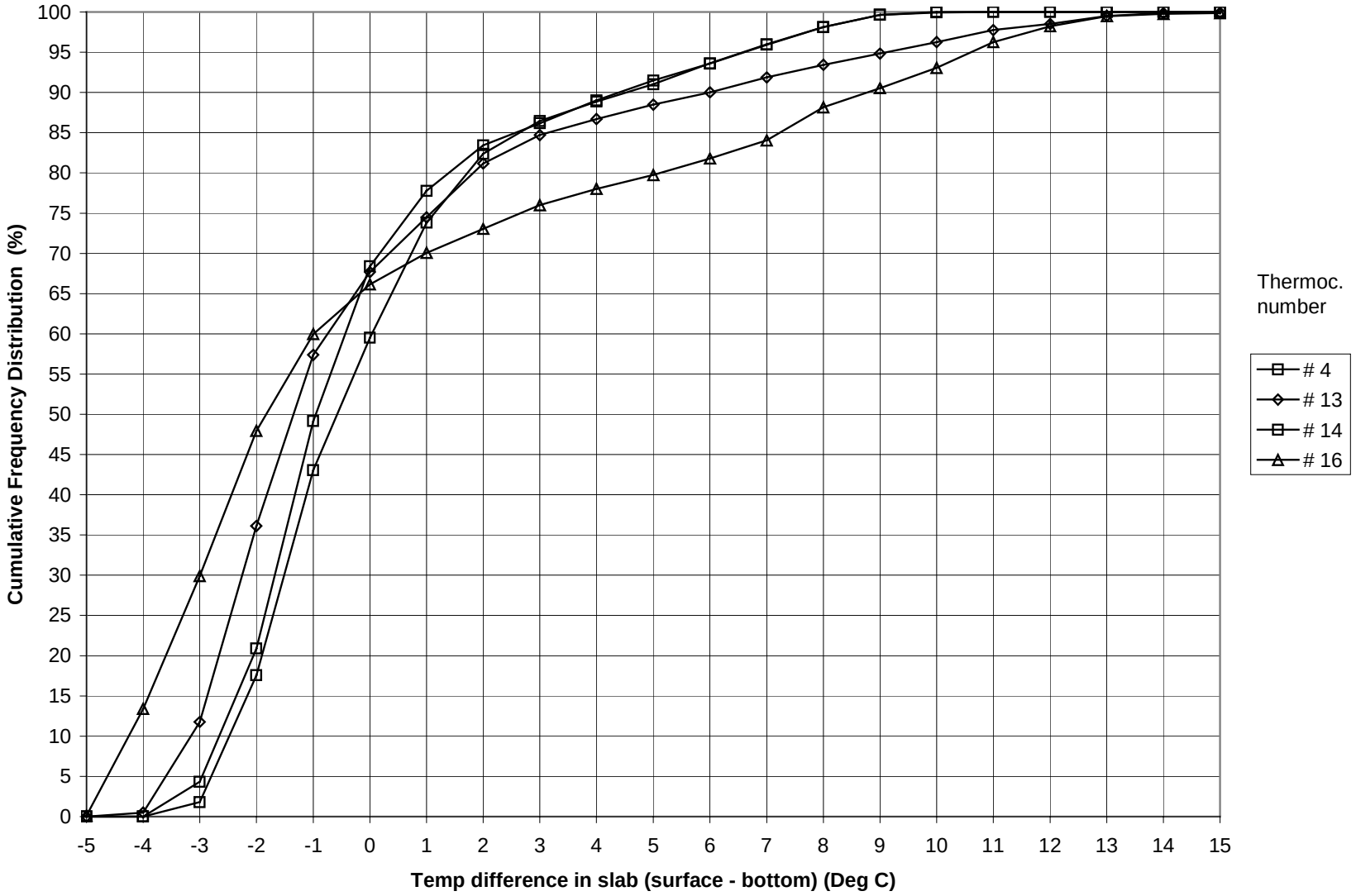

Figure 46. Cumulative frequency distribution for the temperature data from Section 516CT.

Some important observations to make from these graphs are:

- For most of the time, the pavement temperature differential was less than 4 degrees.
- The pavement was hotter at the bottom than at the surface 60 percent of the time.
- For less than 10 percent of the time, the temperature difference was between 2.5°C and 5.0°C.
- For less than 13 percent of the time, the temperature differential was greater than 5.0°C, with the exception of Thermocouple 16.
- The shade created by the HVS has an effect on the test pavement temperature gradient.

These observations mean that pavement curling due to a high temperature differential between the surface and the bottom of the pavement only took place for a relatively short period during the HVS test. For most of the test duration, the temperature differentials were small, resulting in low curling stresses in the slab.

7.4 Joint Load Transfer Efficiency (LTE)

It is possible to determine the deflection transfer across the joints from the RSD data at both joints and the CAM measurements at the joints. The first attempt was made after 427,709 load applications. At this point, the large deflections at the joints were visually evident. Figure 47 is an enhanced photograph of the joint crack from the saw-cut to the bottom of the slab in Joint 1 and 2. The joint crack at the left-hand joint (the joint between the left-hand slab and the middle slab)—Joint 1—was almost vertical with the

crack lightly skewed towards Slab 3. The joint crack at Joint 2 was skewed towards Slab 4.

The amount of load transfer efficiency of a joint is defined as the deflection at the unloaded area (on one side of the joint) expressed as a percentage of the deflection at the loaded area (on the other side of the joint). This percentage is expressed as a number between 0 and 100 percent and is called the joint Load Transfer Efficiency (LTE).

The joint Load Transfer Efficiency was determined as follows:

$$DTE = \frac{\delta y}{\delta x} \times 100$$

where: x and y are two points on either side of the joint, and

δx is the deflection at the loaded side of the joint (point x) and

δy is the deflection at the unloaded area on the opposite side of the joint (point y).

With the aid of the RSD and the CAM, δx and δy were determined at both joints with the loaded HVS wheel running from Slab 2 to Slab 4 and from Slab 4 to Slab 2. By running the HVS wheel in both directions, it was possible to determine the joint Load Transfer Efficiency for either direction of wheel travel.

First, the average RSD measurements at the two joints after 427,709 load applications are required. These values were extracted from Figure 26 and represent δx and are summarized in Table 15.

Figure 47a: Photo of Joint 1. Joint crack is enhanced for easier viewing.

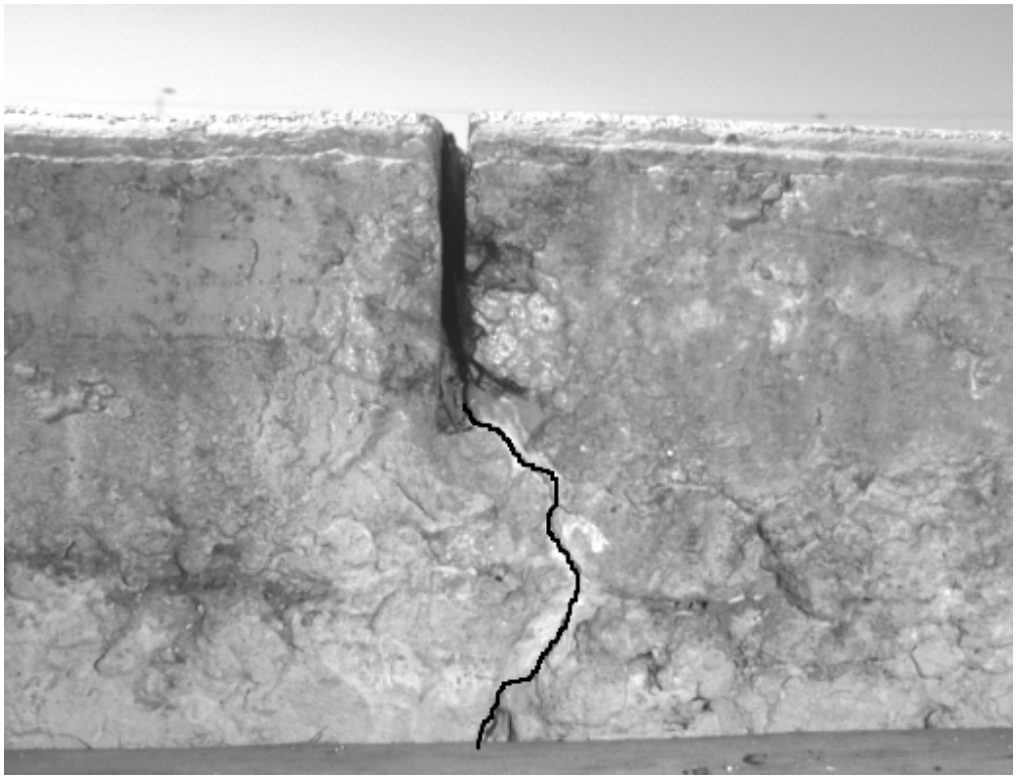

Figure 47b: Photo of Joint 2. Joint crack is enhanced for easier viewing.

Table 15 Average RSD Deflections at the Joints after 427,709 Repetitions.

Location		Ave RSD Deflection (μm)
Joint 1	Slab 2: RSD point 1	1155.5
	Slab 3: RSD point 2	1491.5
Joint 2	Slab 3: RSD point 4	1189.5
	Slab 4: RSD point 5	986.0

Second, CAM data is required for relative vertical movement at the joints for the traffic wheel approaching from Slab 2 to Slab 4 and from Slab 4 to Slab 2. The data is shown in Table 16.

Table 16 CAM Measurements Across the Concrete Slab Joints after 427,709 Repetitions.

	Maximum Relative Vertical movement (δx – δy)	
	Wheel running from Slab 4 to Slab 2	Wheel running from Slab 2 to Slab 4
Joint 1	817 μm	666 μm
Joint 2	535 μm	975 μm

From the RSD data, δx was determined. The CAM measurements determine δx - δy which can be used to solve for δy. With δx and δy known, the joint Load Transfer Efficiency was then determined by dividing δy by δx and multiplying by 100 percent. The results are shown in Table 17.

Table 17 Determination of LTE After 427,709 Repetitions.

	Vertical movement ($m \times 10^{-6}$)	
	Wheel running from Slab 4 to Slab 2	Wheel running from Slab 2 to Slab 4
Joint 1 (between Slab 2 and 3)	δx = 1492 δy = 675 **LTE = 45 percent**	δx = 1156 δy = 490 **LTE = 42 percent**
Joint 2 (between Slab 3 and 4)	δx = 986 δy = 451 **LTE = 46 percent**	δx = 1190 δy = 214 **LTE = 18 percent**

These results correspond well to the visual observation made earlier about the vertical cracks at the joints. At Joint 1, the LTE is almost the same with the loaded wheel

approaching from either direction (LTE = 45 and 42 percent). This suggests the crack at Joint 1 was closer to vertical and equal deflection transfer took place with the wheel load approaching the joint from either side.

At Joint 2, a different observation was made. The crack starting from the bottom of the saw cut was more skewed towards Slab 4. When the loaded wheel approached Joint 2 from Slab 4, the unloaded slab (Slab 3) provided some support to the loaded slab (Slab 4) and the LTE (42 percent) was similar to Joint 1. However, when the wheel approached Joint 2 from the Slab 3, Slab 4 provided little support due to the angle of the crack (see Figure 47), and very little deflection was transferred to Slab 4 across Joint 2 (LTE = 18 percent). The crack at the slab edge may not be indicative of the crack pattern all the way across the joint, and coring at the joint is needed to confirm the amount of skew in the joint crack.

8.0 ANALYSES OF CONCRETE PAVEMENT STRUCTURE AT RICHMOND FIELD STATION

The HVS loaded the concrete test section at RFS at the edge to accelerate damage and to force the slab to fail in fatigue. In order to quantify the performance of the concrete pavement structure mechanistically, a stress-based analysis technique was employed. Stresses can be forward-calculated using the applied load, the physical properties of the concrete, and the geometry of the concrete slabs. The applied stress can also be backcalculated from measured deflections (FWD or RSD testing) and strains (output of dynamic concrete strain gages).

One common way to calculate stresses in concrete pavements is finite element analysis. Closed-form solutions such as Westergaard's can be used, but have limited applicability to small slab sizes. ILLI-SLAB is one type of finite element analysis tool used to evaluate the stresses, strains, and deflections in concrete pavements. (4, 5) Other finite element programs, such as EverFE (6), KENSLABS (7) J-SLAB (8), FEACON (9), can be used to analyze rigid pavements. ILLI-SLAB was used in this study because of the authors' familiarity with it, its extensive validation with field data, and its widespread acceptance among the pavement engineering community. For further details of ILLI-SLAB capabilities and underlying finite element assumptions, the following references should be consulted: Tabatabaie, 1977 (4); Ioannides, 1984 (10); Korovesis, 1990 (11); Khazanovich, 1994 (12).

8.1 Load Stress Analysis of Test Section 516CT

The load stress analysis for the RFS test section 516CT was done using ILLI-SLAB with measured pavement layer properties and the slab geometry. Figure 1 shows

the slab geometry and pavement features for section 516CT. Although the design thickness of the slab was 200 mm, several cores taken from the slab edge had an average thickness of 228 mm.

Figure 48 shows the ILLI-SLAB model and location of the dual wheel configuration at the slab edge. The slab edge, midway between the two joints, is the location of maximum tensile bending stress for this slab configuration. Figures 49 and 50 show the distribution of stress and deflection along the middle slab edge. The maximum edge stress is approximately 2.5 MPa (360 psi) with a maximum edge deflection at the same location of 0.53 mm (0.021 in.). The slab temperature gradient was not accounted for in this analysis, but is discussed in Section 8.4. This type of load stress analysis is what is ultimately used in a mechanistic-based pavement design. At the pavement design stage, all that is known is the approximate wheel loads, the proposed pavement geometry, and the estimated pavement properties, along with the approximate environmental conditions. The load stress calculated above can now be input into a fatigue-based analysis program to determine the allowable number of load applications to failure.

8.2 Deflection-based Stress Analysis of Section 516CT

The measured dynamic deflections, taken from the RSD at regular intervals, can be used to backcalculate the approximate bending stresses in the concrete slab over time.

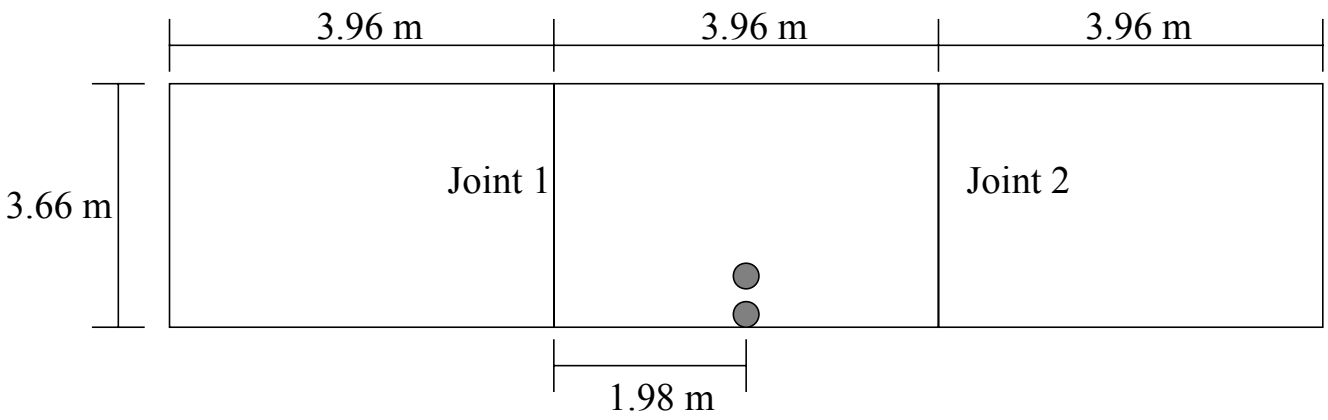

Pavement Properties:

H_{PCC} = 228 mm

E_{PCC} = 28 Gpa

Poisson's Ratio = 0.15

Joint LTE = 100%

Load Parameters:

Load = 60 kN

Pressure = 690 kPa

Dual Spacing = 356 mm

Edge Loading Condition

Figure 48. ILLI-SLAB model of concrete Section 516CT.

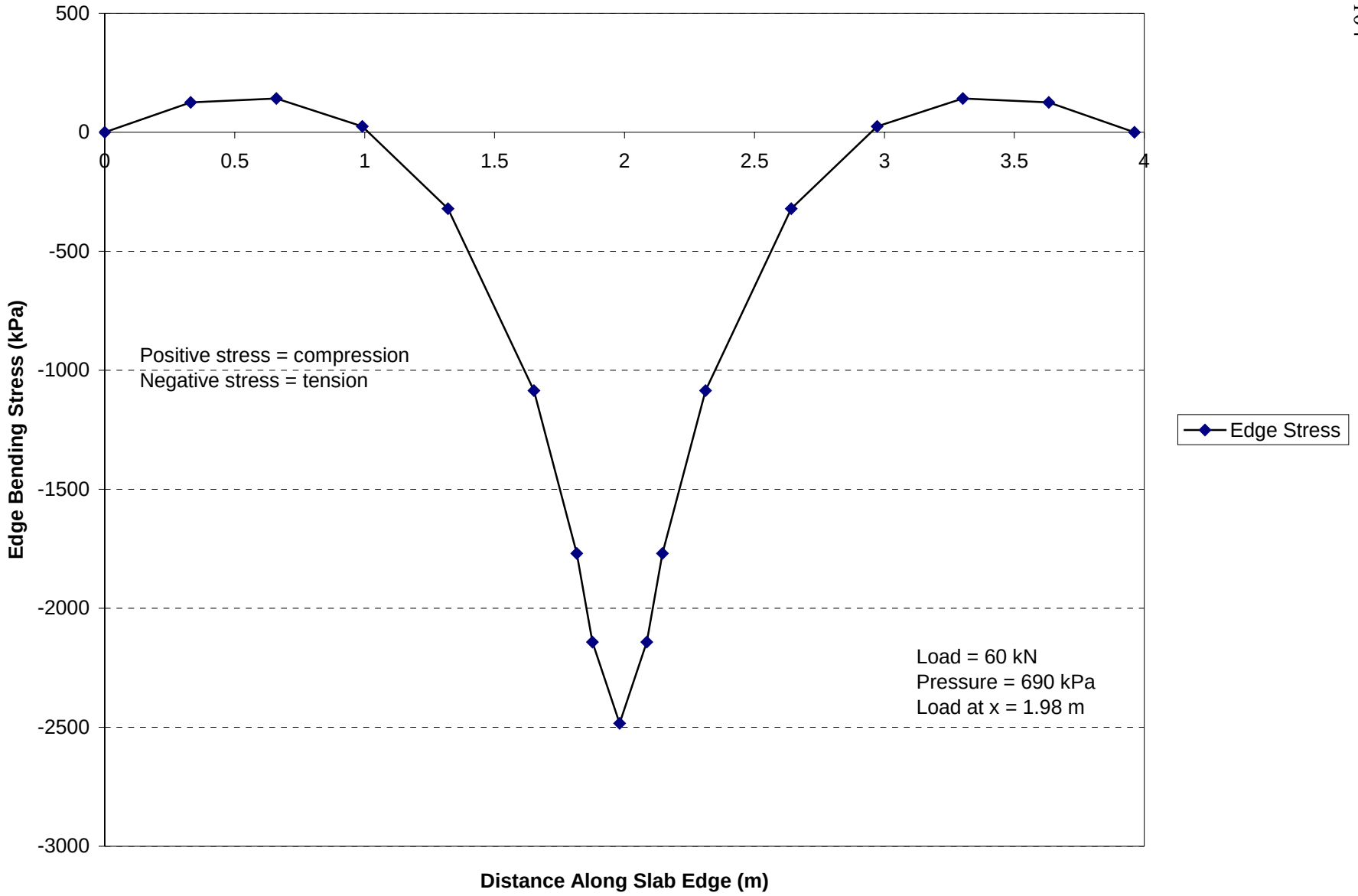

Figure 49. Critical bending stress along middle slab edge.

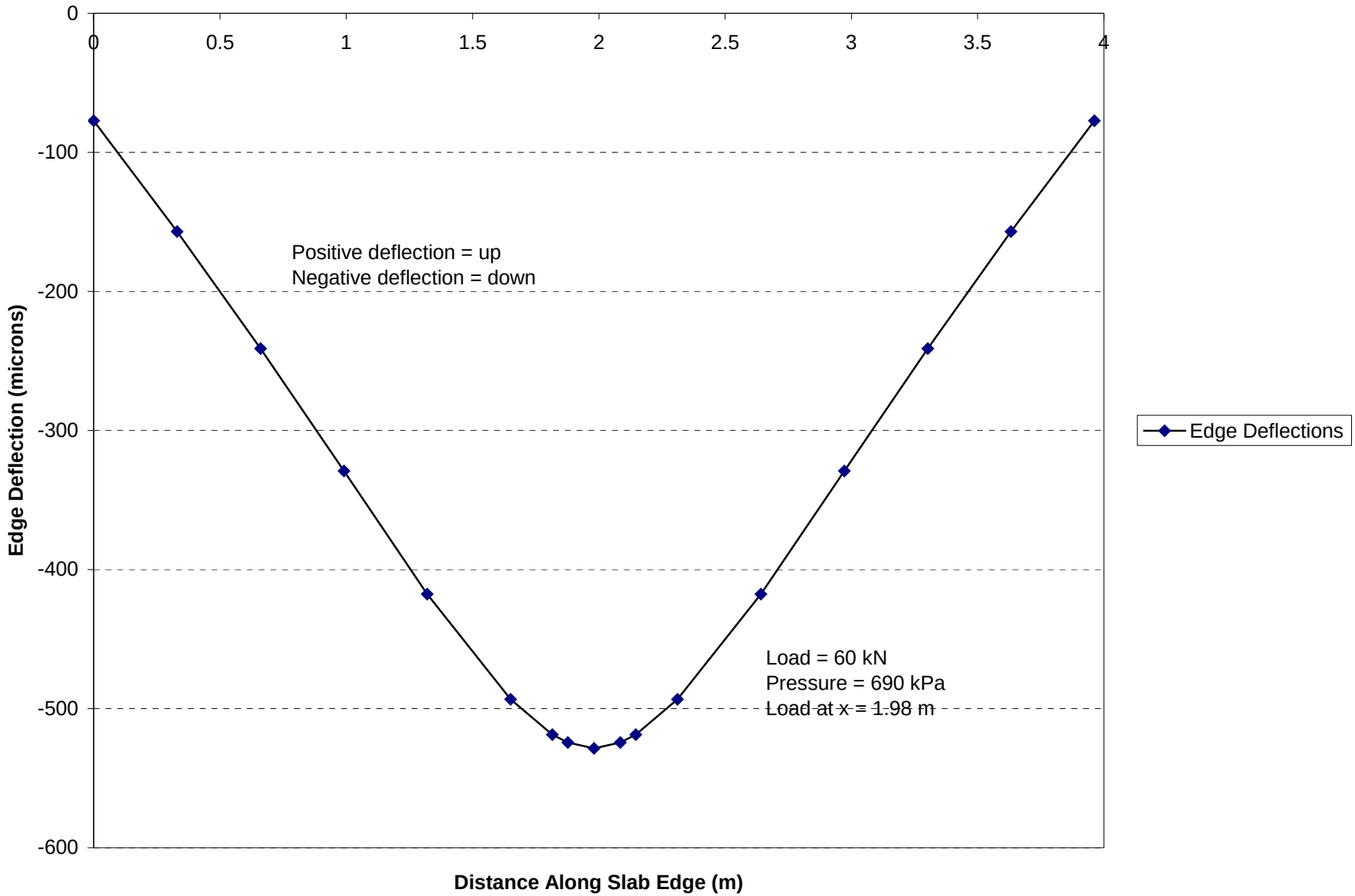

Figure 50. Critical deflections along middle slab edge.

This procedure was simple to perform in ILLI-SLAB by matching the maximum measured deflection (RSD) with the calculated deflection. However, most RSD measured deflections had a significant error included in them due to the daily temperature fluctuations in the test slab. As shown in Figure 51, the measured deflections had a high variability within one day, which had to be associated with whether the slab was curling up or down when measurements were taken. Figure 26 shows that the deflection over time varied greatly for different locations in the slab.

However, a backcalculated edge stress from the measured slab deflection (RSD point 3) can be estimated. Figure 20 shows the middle slab edge deflection was first measured 300 mm from the edge. An average deflection at this point was approximately 0.4 mm. The corresponding slab edge stress for this deflection was 2.4 MPa. The RSD edge deflection was matched by changing the support value (modulus of subgrade reaction) in ILLI-SLAB. The backcalculated edge stress was within 4 percent of the load calculated edge stress, as discussed in Section 8.1.

Towards the end of HVS2 testing, a new methodology was used to measure deflection with the RSD. To eliminate the effects of slab deflection on the RSD reference feet, the RSD was positioned perpendicular to the slab edge, as shown in Figure 20. The dual wheel had to be moved 55 mm from the slab edge to accommodate the RSD. Unfortunately, variation in the slab deflection throughout the day was still experienced with this configuration.

The backcalculated edge stress using the new RSD measuring technique was 2.26 MPa for a measured deflection of 0.6 mm. By moving the dual wheel 55 mm away from

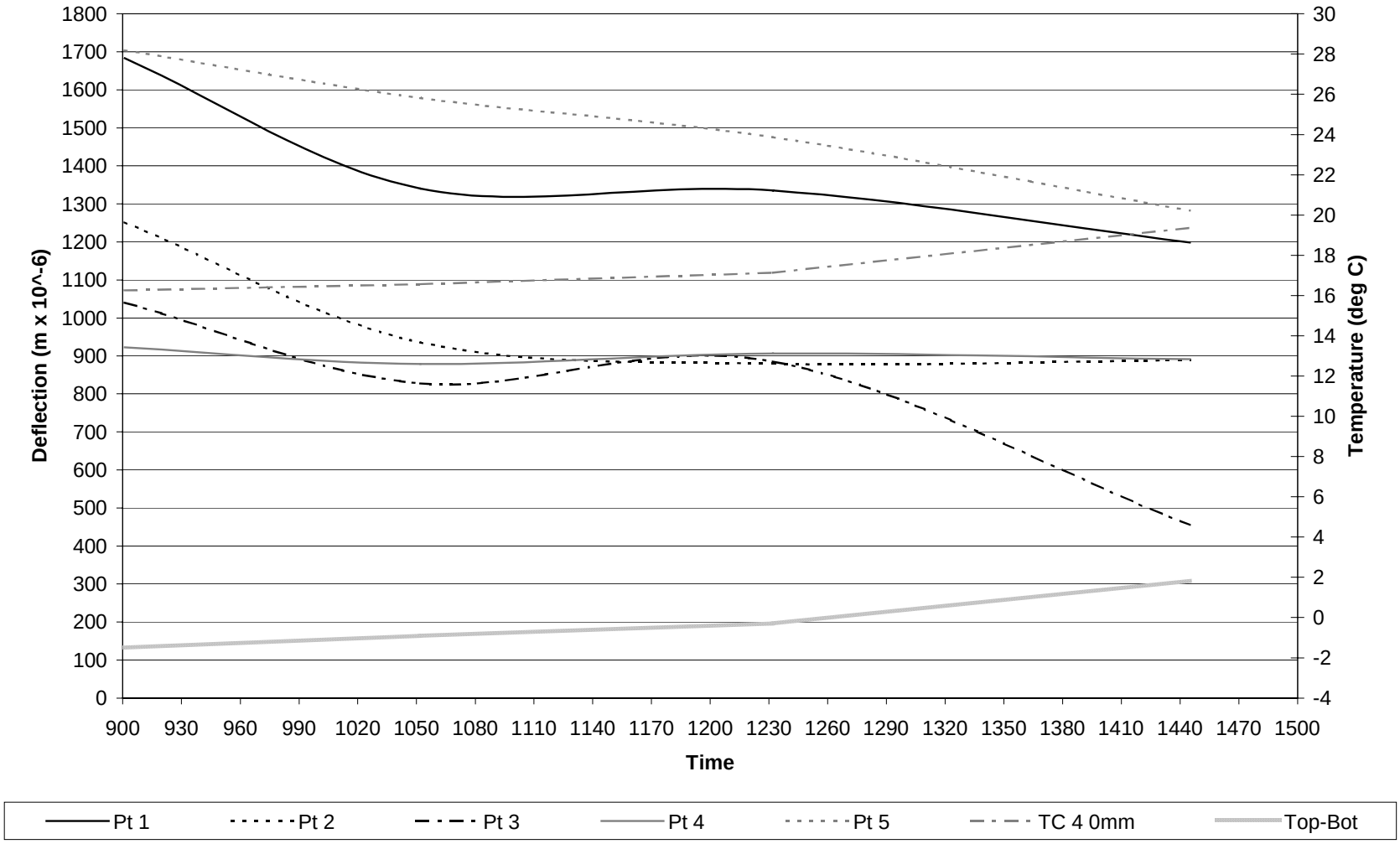

Figure 51. RSD deflections for Section 516CT plotted with temperature.

the edge, the edge stress was reduced by 10 percent. The problem with the RSD measurement technique was that the actual bending stress applied during repetitive loading was not applied during data acquisition measurements. The first RSD methodology was found to be preferable to the second methodology because the first method gave more realistic backcalculated edge stress.

The deflection testing at the Palmdale test site will eliminate the RSD and utilize LVDTs at the edge of the slab. Figure 52 shows the proposed schematic of LVDTs to be used on the Palmdale test section. The set of LVDTs at the joints will measure deflection load transfer efficiency (LTE) and the LVDT at the slab edge will be used to backcalculate the pavement's bending stress with time.

8.3 Strain-based Stress Analysis of Section 516CT

Figure 14 shows the location of two dynamic gages situated in the wheel path of the HVS. Given that the dynamic strain gages were placed with the primary concern of constructability, their location was not ideal for measuring maximum bending strain in the slab. The data from the dynamic strain gage in the middle slab (Slab 3) can be used to backcalculate the approximate stress in the slab at the gage location. This stress can be obtained by multiplying the measured strain by the concrete modulus of elasticity. The Dynatest strain gage had an average tensile bending strain of 38 microstrain under the influence of the 60 kN wheel load. This bending strain was measured at 38 mm from the bottom of the slab. Extrapolation of the strain to the bottom concrete fiber resulted in an

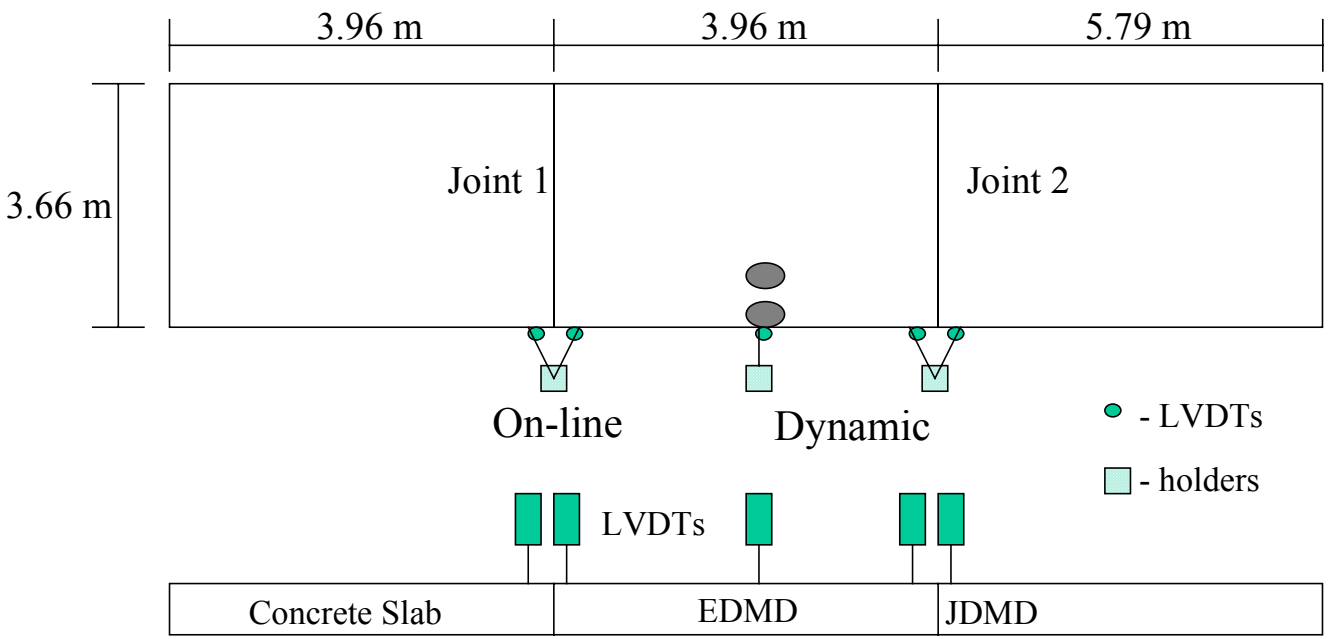

Figure 52. Proposed positioning of displacement measuring devices.

average bending strain (tensile) of 61 microstrain. The average concrete stress at the gage location was 1.7 MPa.

The measured strains can be compared to the calculated stresses and strains from ILLI-SLAB. ILLI-SLAB was run for the properties and load shown in Figure 48. The calculated bending strain, output from ILLI-SLAB at the same place as the measured strain, was 61 microstrain. The ILLI-SLAB and the average measured dynamic strains were identical. The main reason for their similarity was that the loading was in the elastic regime of the concrete. The stress ratio in the slab was less than 50 percent, which was in the concrete's linear elastic range. Roesler found that strain gages produced good agreement with load calculated strains when the slab stress was less than 70 percent of the concrete modulus of rupture. (13)

Given that the calculated and measured bending strain in the slab were similar at one location, it can be assumed the calculated strain in another slab location was also correct. This suggests that the ILLI-SLAB maximum edge stress (2.5 MPa) for this configuration gave the approximate applied stress occurring in the slab.

8.4 Expected Fatigue Performance

The load test plan for section 516CT was designed to fail the pavement in bending fatigue. The load-based stresses were used to estimate the fatigue life of the pavement section using mechanistic analysis techniques. To account for the curling stresses in the pavement due to temperature differentials in the slab, thermocouple data presented in section 7.3 was used. The pavement analysis program ILLICON (14) was utilized to incrementally calculate the load plus temperature damage in the pavement.

The ILLICON program was used to calculate the total edge stresses, load plus curl stresses, for a given set of pavement features. ILLICON was developed as a pavement analysis supplement for the Illinois Department of Transportation (IDOT) mechanistic rigid pavement design procedure. (15) ILLICON uses algorithms derived from a factorial of ILLI-SLAB runs for various pavement parameters. ILLICON allows the user to answer a variety of "what if?" questions regarding changes in the material properties, environmental conditions, and pavement conditions. A laboratory beam fatigue model was used to relate the total stress ratio in the pavement to the number of allowable repetitions at a given stress level. The beam fatigue model used in ILLICON was taken from Darter and Barenberg and is the following:

$$\text{Log } N = 17.61 - 17.61(\sigma/M_R)$$

where N is the number of allowable repetitions at a given stress ratio, σ is the applied stress, and M_R is the concrete modulus of rupture. (16) The actual number of 60 kN axle passes was included in the fatigue analysis. This type of traffic analysis is called load spectra. An ESALs-based fatigue analysis was also completed and compared to the load spectra analysis.

The AASHTO load equivalency factor for the 60 kN dual wheel configuration was 5.645 ESALs per pass. This load equivalency factor was selected for a 200 mm pavement with a terminal serviceability index of 2.0. The ESALs for one pass of the HVS test wheel assumed that the HVS wheel loading occurred approximately 300 to 450 mm from the edge of the slab. This is the typical mean distance from the edge of the pavement to the edge of the vehicle tire for highway traffic. (16)

Given that the HVS was loading at the slab edge, the ESALs per pass had to be magnified due to the channelization of the traffic. Zollinger and Barenberg used the concept of equivalent damage ratio (EDR) to quantify the difference in damage between trucks loading at the edge versus the mean lateral distance from the edge (300 to 450 mm). (15) Zollinger and Barenberg found for mean wheel paths located 450 mm from the edge, the EDR for a 200 mm concrete pavement was 0.05. (15) This means only five percent of the total truck traffic at the edge does the equivalent damage of 100 percent of the trucks located 450 mm from the edge. Their results were similar to the results used in the PCA concrete thickness design guide. (17)

The channelization of the HVS loading at the edge has magnified the ESALs per pass from 5.645 to 112.9 (5.645 × 1/0.05). This means every HVS dual wheel pass was equivalent to 113 ESALs. Figure 52 shows the number of HVS repetitions versus time. Figure 54 shows the accumulation of ESALs versus time for test section 516CT. In Figure 54, the Caltrans required pavement thickness for a given number of ESALs are shown. Before the first distress appeared, the 228 mm pavement at RFS took four times more traffic than would be required for a 260 mm Caltrans concrete pavement design.

The fatigue failure in ILLICON is quantified by the percentage of slabs experiencing transverse cracks. In ILLICON, a pavement that has 20 percent of its slabs cracked is considered failed. This percentage of slabs cracked corresponds to 50 percent reliability. Although only one full slab was tested at RFS, failure was still defined as 20

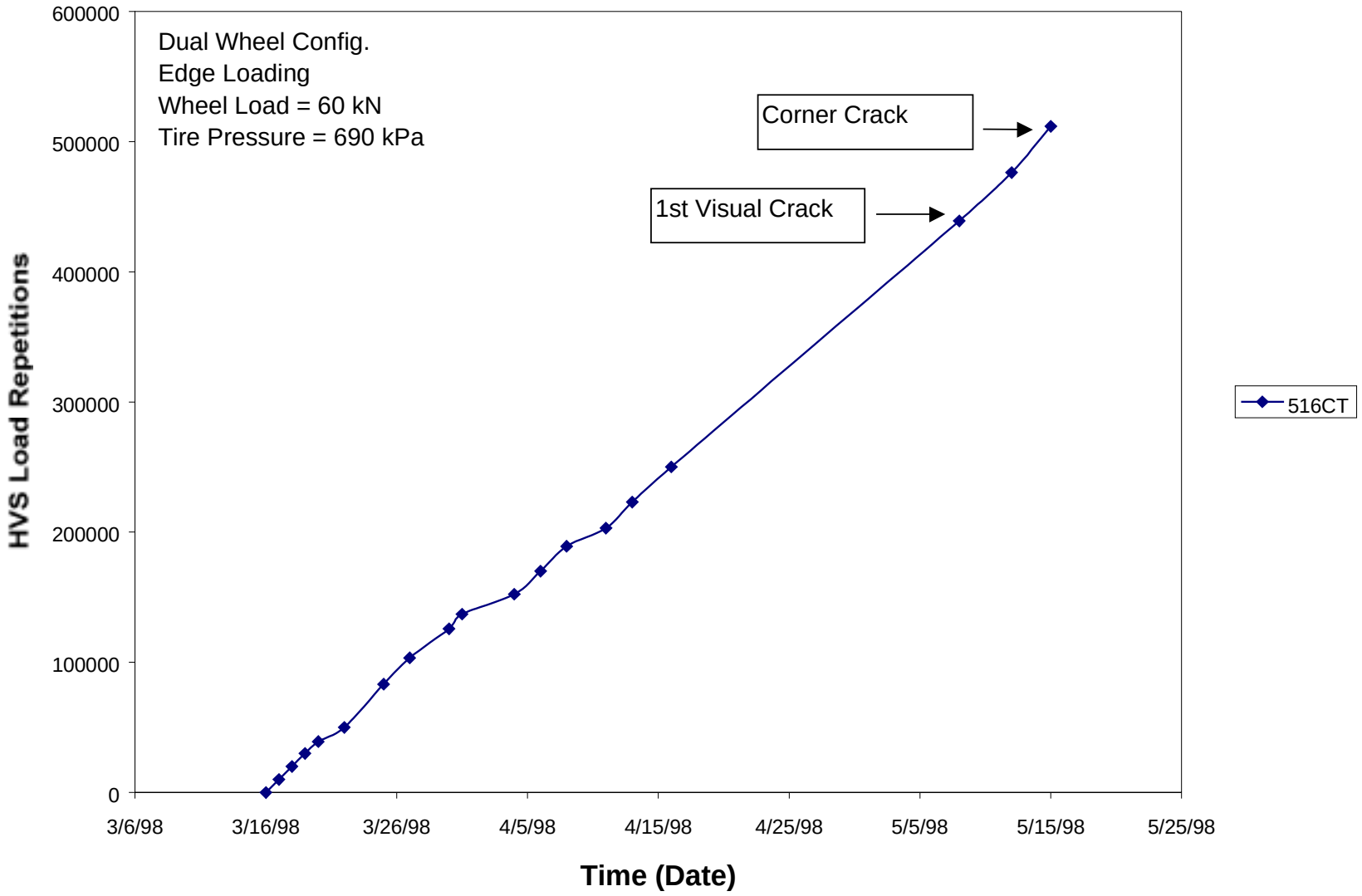

Figure 53. Richmond Field Station concrete test Section 516CT load repetitions versus time.

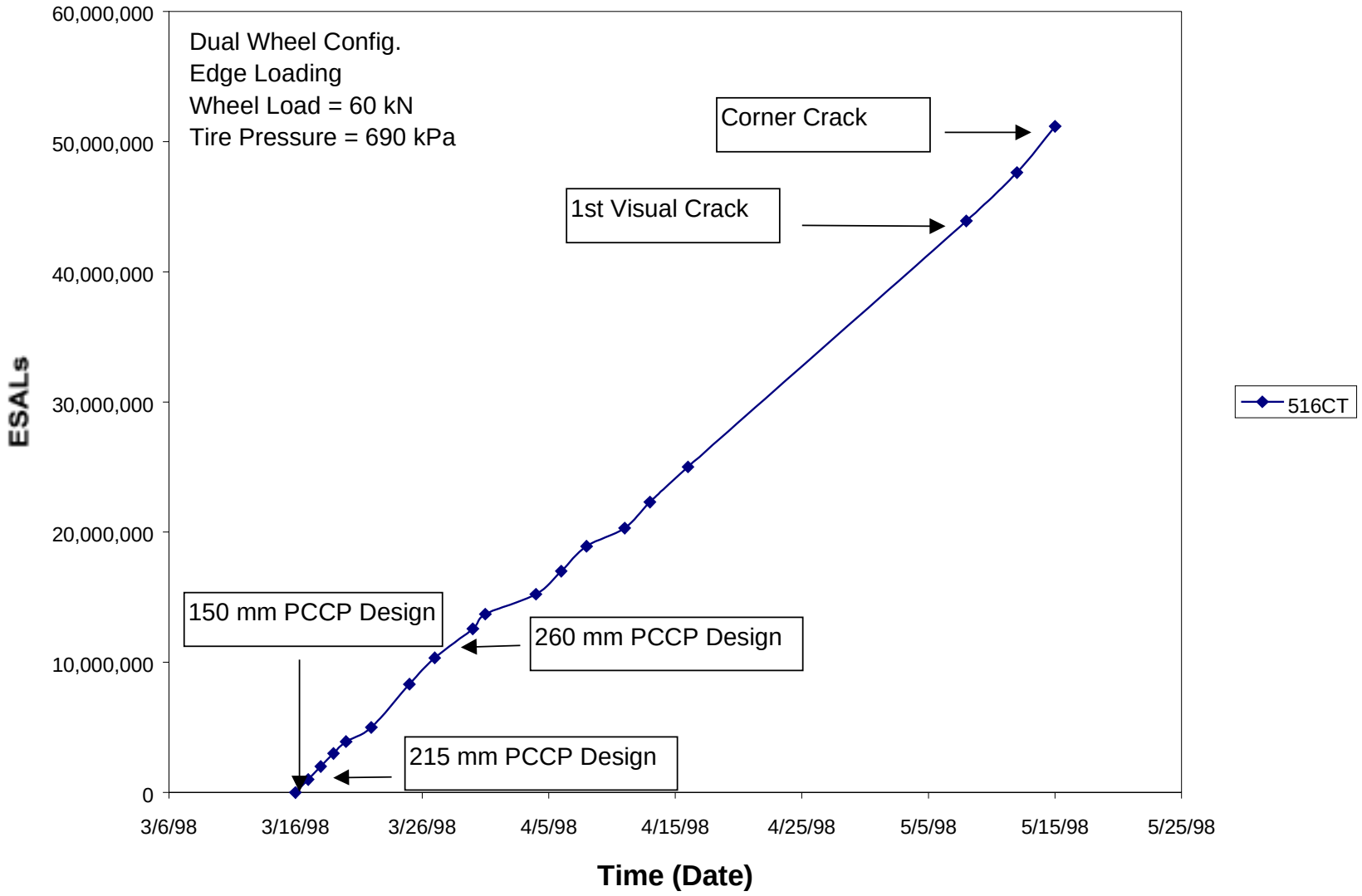

Figure 54. Richmond Field Station concrete test Section 516CT ESALs versus time.

percent of the slabs cracked in ILLICON. Some states, such as Illinois, use the 20 percent slabs cracked as a failure criterion for concrete pavements.

ILLICON fatigue analysis found over three hundred million ESALs still would not have resulted in fatigue failure (transverse cracking) of the concrete test section at RFS. This allowable number of repetitions to failure indicates the slab will not fail in fatigue, rather it will fail in another mode during its service life

The load spectra analysis for the test section found that greater than one billion HVS repetitions would most likely not cause fatigue failure of the concrete slab. Three reasons why the ESALs and load spectra analyses came up with such high numbers of repetitions to failure are the following: concrete slab length was 3.96 m which greatly reduces the slab curling stress, small temperature differentials in the slab were experienced during most of the testing, and the 98 day concrete flexural strength was 5.9 MPa which was more than two times larger than the applied load stress. The ILLICON analyses demonstrated the importance of shorter joint spacing, small slab temperature differentials, and higher long-term concrete strength with respect to fatigue life.

The average stress during loading with the HVS was approximately 2.5 MPa. The average applied stress ratio to the concrete slab was 0.43. Stress ratios around 0.50 have close to an infinite fatigue life. Another factor not accounted for in the analyses was the increased strength concrete slabs have over concrete laboratory beams. Roesler found concrete slabs could have 10 to 100 times higher fatigue life as compared to concrete beams tested in the laboratory. (13) This research suggests that concrete pavements will last even longer than predicted by a beam fatigue model. The added factor of safety from

using laboratory beam fatigue test results over slabs is not exactly known because the results are dependent on specimen size and loading configuration.

8.5 Actual Performance of Section 516CT

The fatigue failure of section 516CT would be indicated by a transverse crack across the slab starting at the middle slab edge halfway between Joints 1 and 2. As discussed in Section 8.4, the slab was not expected to fail in fatigue mode over the test life. The slab did fail at approximately 439,000 repetitions. The structural failure was a corner break, which took only several days to propagate across the slab corner and completely fracture the corner wedge through the entire thickness of the pavement. The corner break occurred because of the high amount of rainfall (1.1 m) since its construction, the high water table of surrounding soil, the presence of a pumpable base, and high deflections at the joints. Furthermore, the joints had no dowels, so load transfer across the joints deteriorated quickly.

Similar performance results were obtained from the AASHO Road Test for undoweled jointed plain concrete slabs. Pumping and corner cracks were prevalent at this road test. Corner cracks are seen on Caltrans pavements, but probably are a result of other factors such as erosion of the CTB, nighttime temperature curling, and overloaded axles. However, the corner crack on section 516CT and corner cracks on Caltrans pavements can be reduced if dowels are used to keep the joints aligned during repetitive loading. Properly aligned joints will ensure adequate load transfer between adjacent slabs.

9.0 SIGNIFICANT FINDINGS AND RECOMMENDATIONS FROM HVS TEST 516CT

Reducing the maximum stresses at the edge by increased concrete strength, greater concrete thickness, and shorter joint spacing resulted in a concrete pavement with close to an infinite fatigue life. The concrete strength was approximately 55 percent higher than the minimum strength required by Caltrans for opening concrete pavements to traffic. The concrete thickness was also an average of 28 mm thicker than the design thickness. When the fatigue life of a slab approaches infinite, other failure modes become prevalent such as corner breaks, pumping, and joint distress. In order to extend the life of the pavement, these distress types must also be addressed through the use of non-erodible base materials, good load transfer across the joints (dowels), and positive pavement drainage systems (edge drains).

The concrete test sections constructed at RFS demonstrated that instrumentation could be successfully embedded in the concrete. The methodologies used to place the instruments were adequate as evidenced by the fact that all gages functioned properly throughout the entire test program. It was found the Road Surface Deflectometer (RSD) would not accurately measure slab deflection due to the slab deflection basin affecting the RSD reference feet. A new method for measuring joint and edge deflections was developed to more accurately and efficiently measure the slab behavior over time.

Thermocouples placed under the HVS were shaded and did not give the same thermal gradients in the slab as other non-shaded thermocouples. It was also discovered that the slab's measured deflections were variable depending on the time of day. The air temperature greatly affected the deflection results making it necessary to employ a temperature control box encompassing the HVS loading area in the future.

The deflection transfer efficiency across the slab joints was found to be dependent on the direction of wheel travel across the joint and the orientation of the joint crack. The joint with the closest to vertical joint crack transferred more deflection across the joint then the joint with the skewed joint crack. By the end of HVS testing (430,000 repetitions) both joints were found to have approximately 45 percent deflection transfer efficiency (DTE). This low DTE suggests the use of dowels is necessary in order to maintain high DTE and minimize faulting, pumping, and corner breaks.

Deflection backcalculated edge stresses agreed with load calculated stresses. Dynamic strain gages were successfully utilized to backcalculate bending stresses in the slab. However, the measured strains were in the concrete's linear elastic region and this calculation of bending stresses may not work in the future if the applied bending stress exceeds 70 percent of the concrete's flexural strength. Fatigue analyses using existing mechanistic procedures predicted the concrete test section 516CT would never fail in fatigue with a 60 kN wheel load. Concrete test section 516CT ultimately failed after 430,000 HVS repetitions at 60 kN due to a corner break from excessive rainfall and pumping at the pavement edge and joint.

10.0 REFERENCES:

1. Barker, W. R. 1981. Introduction to a Rigid Pavement Design Procedure. *Proceedings, 2nd International Conference on Concrete Pavement Design,* 135-48. Purdue University, West Lafayette, Indiana.

2. CAL/APT Contract Team. 1988. Test Plan for CAL/APT Goal LLPRS—Rigid Phase III. *Report prepared for California Department of Transportation* (April).

3. Harvey, J. *et al.* 1996. Initial CAL/APT Program: Site Information, Test Pavements Construction, Pavement Materials Characterizations, Initial CAL/HVS Test Results, and Performance Estimates. *Interim Report for Caltrans*. Institute of Transportation Studies, University of California, Berkeley.

4. Tabatabaie-Raissi, A. M. 1977. *Structural Analysis of Concrete Pavement Joints.* Ph.D. Thesis, University of Illinois, Urbana-Champaign, IL.

5. Tabatabaie, A. M. and Barenberg, E. J. 1980. Structural Analysis of Concrete Pavement Systems. *Transportation Engineering Journal*, ASCE, Vol. 106, no. TE5:493-506.

6. Davids, W. G., Turkiyyah, G. M., and Mahoney, J. M. 1998. EverFE – a Rigid Pavement 3D Finite Element Analysis Tool. *Transportation Research Board*, Paper no. 360.

7. Huang, Y. H. and Wang, S. T. 1974. Finite-Element Analysis of Rigid Pavements with Partial Subgrade Contact. *Transportation Research Record* 485:39-54, Transportation Research Board, National Research Council, Washington D.C.

8. Tayabji, S. D. and Colley, B. E. 1983. Improved Pavement Joints. *Transportation Research Record* 930:69-78, Transportation Research Board, National Research Council, Washington, D.C.

9. Tia, M., Armaghani, J. M., Wu, C. L., Lei, S., and Toye, K. L. 1987. FEACONS III Computer Program for an Analysis of Jointed Concrete Pavements. *Transportation Research Record* 1136:12-22, Transportation Research Board, National Research Council, Washington, D.C.

10. Ioannides, A. M. 1984. *Analysis of Slabs-on-Grade for a Variety of Loading and Support Conditions.* Ph.D. Thesis, University of Illinois, Urbana-Champaign, IL.

11. Korovesis, G. T. 1990. *Analysis of Slab-on-Grade Pavement Systems Subjected to Wheel and Temperature Loadings.* Ph.D. Thesis, University of Illinois, Urbana-Champaign, IL.

12. Khazanovich, L. 1994. *Structural Analysis of Multi-Layered Concrete Pavement Systems.* Ph.D. Thesis, University of Illinois, Urbana-Champaign, IL.

13. Roesler, J. R. 1998. *Fatigue of Concrete Beams and Slabs.* Ph.D. Thesis, University of Illinois, Urbana-Champaign, IL.

14. Salsilli Murua, R. A. 1991. *Calibrated Mechanistic Design Procedure for Jointed Plain Concrete Pavements.* Ph.D. Thesis, University of Illinois, Urbana-Champaign, IL.

15. Zollinger, D. G. and Barenberg, E. J. 1989. Proposed Mechanistic Based Design Procedure for Jointed Concrete Pavements. *Illinois Cooperative Highway Research Program - 518*, Urbana: University of Illinois.

16. Darter, M. I. and Barenberg, E. J. 1977. Design of Zero-Maintenance Plain Jointed Concrete Pavement, Volume 1: Development of Design Procedures. *Federal Highway Administration Report* no. FHWA-RD-77-III.

17. Packard, R. G. 1984. *Thickness Design for Concrete Highway and Street Pavements*, Portland Cement Association, p. 46.

18. Harvey, J., Roesler, J., Farver, J., and Liang, L. 1998. Preliminary Evaluation of Proposed LLPRS Rigid Pavement Structures and Design Inputs. Report prepared for the California Department of Transportation. University of California, Berkeley Institute of Transportation Studies Pavement Research Center. April.

19. Kurtis, K. E. and Monteiro, P. 1999. Analysis of Durability of Advanced Cementitious Materials for Rigid Pavement Construction in California. Report prepared for the California Department of Transportation. University of California, Berkeley Institute of Transportation Studies Pavement Research Center. April.

20. Roesler, J. R., du Plessis, L., Hung, D., Bush, D., Harvey, J. T. 1999. CAL/APT Goal LLPRS – Rigid Phase III: Concrete Test Section 516CT Report. Report prepared for the California Department of Transportation. University of California, Berkeley Institute of Transportation Studies Pavement Research Center. April.